CHALMERS
UNIVERSITY OF TECHNOLOGY

Development of a computer vision system for ensuring quality of Fetal Spiral Electrodes

Master's thesis in Production Engineering and Biomedical Engineering

Matilda Dahlin
Linnea Johansson

DEPARTMENT OF INDUSTRIAL AND MATERIALS SCIENCE
CHALMERS UNIVERSITY OF TECHNOLOGY
Gothenburg, Sweden 2023
www.chalmers.se

Master's thesis 2023

Development of a computer vision system for ensuring quality of Fetal Spiral Electrodes

MATILDA DAHLIN
LINNEA JOHANSSON

CHALMERS
UNIVERSITY OF TECHNOLOGY

Department of Industrial and Materials Science
Division of Production Systems
Chalmers University of Technology
Gothenburg, Sweden 2023

Development of a computer vision system for ensuring quality of Fetal Spiral Electrodes
MATILDA DAHLIN
LINNEA JOHANSSON

Supervisor: Hao Wang, Department of Industrial and Materials Science
Examiner: Björn Johansson, Department of Industrial and Materials Science

Master's Thesis 2023
Department of Industrial and Materials Science
Division of Production Systems
Chalmers University of Technology
SE-412 96 Gothenburg
Telephone +46 31 772 1000

Cover: Goldtrace Fetal Spiral Electrode.

Typeset in LaTeX
Printed by Chalmers Reproservice
Gothenburg, Sweden 2023

Development of a computer vision system for ensuring quality of Fetal Spiral Electrodes
Matilda Dahlin & Linnea Johansson
Department of Industrial and Materials Science
Chalmers University of Technology

Abstract

Computer vision systems are becoming increasingly common in industrial applications. One of the areas where they are being used more and more is in quality control, as they can provide both increased efficiency and effectiveness. This thesis aims to develop a computer vision system that can quality control the dimensions of a fetal spiral electrode. The electrode is used to monitor the fetal heart rate during childbirth, by inserting the spiral electrode into the scalp of the fetus. The wrong dimensions can cause the creation of a wound on the baby's head, and thereby potentially cause an infection. This new computer vision system is needed because the current manual measuring solution lacks precision and there is a lot of room for human errors to occur, which can affect the measuring results.

Four different parts were conducted, forming a project consisting of knowledge acquisition, concept development, system development, and evaluation of the system. These resulted in a prototype performing height measurement and tip angle measurement of the spiral. This is done by binarizing the image by thresholding and then processing and evaluating the contour to find important points, shapes, and changes in the image. It was also done by creating a fixture that holds the electrode in position and optimizes the external conditions. The evaluation shows that the developed computer vision system performs with higher precision and accuracy compared to the currently used system.

Keywords: Production, Quality control, Inspection, Computer vision, Machine vision, Image processing, Image thresholding, Fetal spiral electrode

Acknowledgements

We would like to express our sincere gratitude to Together Tech and Niclas Gustafsson for providing us with the opportunity to work on this project. We are immensely thankful to our supervisors, Anna Rydén and Mattias Alnervik, whose guidance, expertise, and incredible support have been invaluable throughout our journey. Furthermore, we are very grateful to our supervisor at Chalmers, Hao Wang, for his guidance and expertise, which has been important in shaping the direction of this research. Also, we express our appreciation to our examiner, Björn Johansson, for his role in evaluating this thesis. Special thanks to the people at Neoventa, for their cooperation, constructive feedback, and amazing support. Working with Neoventa has been a rewarding experience, and their input has enriched our understanding of the project. Finally, we would also like to extend our thanks to the entire team at Together Tech for their kindness, encouragement, and for showing interest in our project. It has truly made a difference and has been very appreciated.

Matilda Dahlin, Linnea Johansson, Gothenburg, May 2023

List of Acronyms

Below is the list of acronyms that have been used throughout this thesis listed in alphabetical order:

2D	2 Two-dimensional
3D	Three-dimensional
AQL	Acceptance Quality Limit
CAD	Computer-aided design
CCD	Charge Coupled Device
CMOS	Complementary Metal Oxide Semiconductor
ECG	Electrode cardiogram
FSE	Fetal Spiral Electrode
FOV	Field of view
FPS	Frames per second
LED	Light-emitting diode
MDR	Medical device regulation
QMS	Quality Management System
UTF-8	Unicode Transformation Format – 8-bit

Contents

List of Figures

List of Tables

1

Introduction

1.1 Background

Fetal monitoring is crucial in childbirth, and it is a way to ensure the safety of the fetus, which can be done by both internal and external monitoring, that is, monitoring from inside of the abdomen or outside the abdomen [1]. Internal monitoring is often used in childbirths of high-risk pregnancies and it means that a spiral wire electrode is placed on the fetus's head to measure the Electrode Cardiogram (ECG) of the baby [2]. This gives a more accurate measurement of the fetus's heart rate since external noise, such as movements, does not affect it. The electrode is called Fetal Spiral Electrode (FSE) and is invasive, because it penetrates the baby's skin. Goldtrace FSE, produced by Neoventa Medical AB, is an FSE that is developed to perform ST analysis over time, which requires an accurate signal [3]. The ST analysis means that part of the ECG curve is analyzed, and it helps clinicians detect signs of hypoxia and demonstrates how the fetus handles stress during childbirth.

Incorrect dimensions of the spiral in the invasive electrode can pose a risk of injuries to the fetus. Such injuries may result in wounds that could potentially lead to infections, necessitating the baby to take antibiotics [4], [5]. Due to the small dimensions of the spiral, ensuring accurate quality control becomes challenging. Currently, the control of the spiral involves a manual height measurement. This measurement is conducted using a measuring tool that is greatly affected by human errors. It can also impact the shape of the electrodes which results in an incorrect measurement. The inspection is carried out in both the production site, where all electrodes are measured, and in Gothenburg upon the electrodes' arrival after production. However, only a sample of the electrodes is measured in Gothenburg. The sampled electrodes are selected randomly according to the statistical method Acceptance Quality Limit (AQL) [6], to guarantee the quality of the electrodes.

Ways to measure small objects include using for example calipers or a micrometer screw gauge. This kind of manual measuring tool is currently used in the quality control, and it has shown limitations as it requires physical contact with the measuring object, posing a risk of compressing the FSE spiral. Therefore, computer vision is being explored in this project as it does not require contact with the measuring object.

Computer vision systems aim to make computers perceive and understand objects in the real-world through image analysis, and the technology is used in all kinds of applications [7]. Machine vision is an application of computer vision in the industrial environment, where the system focuses on using image processing in a controlled environment with pre-determined parameters to output a decision [8], [9]. These machine vision systems use digital sensors and cameras to inspect and interpret the object data to automatically calculate a conclusion on whether the object parameters, such as size or color, are according to specification. Hence, machine vision has become very useful for tasks such as robotic guidance, process monitoring and automatically performed inspections [9]. This subset of computer vision has become widely used for implementing automated inspections and quality controls in industries as it provides reliable high-speed inspections with economic and productivity benefits [7]. The implementation of machine vision in industries has been one of the important digital technologies during the necessary transition into Industry 4.0. Partially owing to the possibilities of implementing the machine vision to do the quality assurance with higher accuracy, lowering the risk for human errors and mistakes [9].

This thesis will focus on improving the quality control of the FSE by applying an automated computer vision system to replace the current manual quality testing that is performed in the production.

1.2 Aim

The aim of this thesis is to improve the quality control of the Goldtrace FSE by making it more accurate and more efficient to ensure high-quality standards of the FSE. This will be done by creating an automatic computer vision system that quality controls the spiral needle of the FSE. This thesis also targets proposing an implementation of the system and presenting an effectiveness analysis regarding time efficiency and performance of accuracy and precision.

1.3 Delimitations

- Due to time limitations, the finished product will be limited to a prototype. Further necessary work to transform the prototype into a finished product that can be introduced in the actual production chain is out of the scope. Although, future improvements will be discussed and suggested.

- The focus of the project will be the software, and a fixture will be built to support the creation of the software. The fixture will be developed with support from the mechanical department at Together Tech who will CAD and 3D print necessary parts.

- The lack of existing data limits the development of the prototype to traditional image processing techniques for the quality insurance without considering usage of learning-based solutions. The prototype will neither include

consideration to other mechanical solutions, such as integrating calipers into a system.

- Due to time limitations, the computer vision system will be built on pictures captured from solely one camera, and therefore the system will be built on analyzing images from only one view.

- The evaluation of the prototype will be limited to the fact that only a prototype is created, and an exact estimation of accuracy, precision and efficiency will therefore not be possible to perform.

1.4 Research questions

- How can a computer vision system be designed and used to ensure high-quality fetal scalp electrodes?

- How effective and efficient would a computer vision system be as a quality inspection system in the production?

2

Theory

This chapter contain an introduction to the regulations concerning the FSE and the quality control of it. In addition, related work and the Goldtrace FSE are introduced. Also relevant theory regarding image processing, imaging and cameras and other important mathematical theory for the project is introduced.

2.1 Regulations for quality testing medical devices

Medical device regulation (MDR) controls medical devices in European countries [10]. The objective of this regulation is to facilitate the manufacturing process by implementing consistent laws throughout the entire European Union, thereby providing clarity on the required manufacturing standards for medical products. Among its various provisions, the regulation oversees aspects such as development, design, verification, marking, production, documentation, traceability, release, and supply of products. Compliance with the regulatory framework is indicated by the presence of a CE marking [10]. MDR defines what qualifies as a medical device, and one of its definitions is as follows, among others:

> *[...]any instrument, apparatur intended by the manufacturer to be used, alone or in combination, for human beings, for the purpose of diagnosis, prevention, monitoring, prediction, prognosis, treatment or alleviation of disease* [11].

This definition of a medical device includes the Goldtrace FSE. Furthermore, MDR categorizes medical devices into different risk classifications, which determine the level of risk associated with their use and the corresponding documentation requirements from manufacturers. Neoventa's Goldtrace FSE falls under the classification of class IIa medical devices as per Rule 7 in MDR annex VIII chapter III. This classification indicates that it is:

> *Surgically invasive devices intended for short-term use* [11].

Producing a class IIa medical device means that the production is required to contain defined processes to get a CE marking [12]. A notified body also has to approve the

documents and the devices. One necessary application is the Quality Management System(QMS). Among other things should the application, following MDR appendix IX chapter 1, section 2.1, include an adequate description of:

> *- the verification and quality assurance techniques at the manufacturing stage and in particular the processes and procedures which are to be used, particularly as regards sterilisation and the relevant documents; and*
> *- the appropriate tests and trials which are to be carried out before, during and after manufacture, the frequency with which they are to take place, and the test equipment to be used; it shall be possible to trace back adequately the calibration of that test equipment [11] .*

This implies that if there is a modification in the quality control procedures for a class IIa device, it would be necessary to update the QMS. Moreover, the quality control system developed as part of this study must be included into the QMS.

2.2 Related work

Constant advancements in computer vision technology have led to the development of various applications, including its use as a measuring system in different contexts. This potential is exemplified in the two following articles, which are studies concerning vision-based measuring.

2.2.1 Study of temperature automatic verification system based on computer vision measuring

A study presents an automated temperature verification system done with high accuracy with the use of computer vision measuring, controlling techniques, and digital image processing [13]. It is based on a first-class standard mercury thermometer as a measuring source, which is much more accurate than a digital thermometer according to the study. A digital camera photographs the thermometer and by using imaging techniques such as enhancement, filtering, binarization and edge detection, straight lines are approximated to the image. The lines are then processed considering the amount, thickness and color of the lines to determine the accurate temperature in the room.

2.2.2 Vision-based measurement for quality control inspection in the context of Industry 4.0: a comprehensive review and design challenges

An article discusses the development of systems performing vision-based measurements and how to integrate them into diverse manufacturing systems who request autonomous quality control systems with high accuracy and precision [14]. It analyzes computer vision techniques, setup, calibration and tailored 2D and 3D algorithms related to enabling the integration of autonomous vision-based measurement

quality controls. Furthermore, the article present ongoing research efforts and the challenges of designing and constructing an autonomous vision-based control.

2.3 Goldtrace Fetal Spiral Electrode

Neoventa's Goldtrace FSE is shown in Figure 2.1, displaying its components. The FSE spiral needle protrudes from the hub, which is a plastic cylinder, and the spiral has approximately 1.5 turns till the tip. In addition, it consists of several other components, one being an additional electrode called the reference plate. Both electrodes consist of gold-plated stainless steel. The purpose of the reference plate is to obtain a reference signal of the mother's ECG so that it can be filtered out, retrieving a final signal consisting of only the signal from the fetus. The two electrodes are welded to one wire each, the spiral to a gray and the reference electrode to a white wire. The spiral needle and the reference plate are then molded together into the hub. The spiral is attached to the top of the hub and the reference plate is placed to the bottom of the hub, as seen in Figure 2.1. The reference plate acts as a stop to prevent the drive tube from rotating freely, thanks to the grooves in the drive tube where the plate is positioned. The drive tube is a hollow cylinder enclosing the wires and it goes from the hub to the attached drive tube grip. The drive tube grip is made from plastic, and the grip fixates the wires, preventing the drive tube from loosening from the hub. On the drive tube grip there is a tab that helps holding the additional guide tube in place. The guide tube is also a hollow cylinder that encloses the drive tube and the hub. The tab can be positioned in two different ways. Firstly, it can be placed in a position that ensures the guide tube encloses the spiral needle, thereby facilitating safe insertion. Alternatively, the tab can be positioned in a manner that leaves the spiral needle free, allowing for potential attachment to the fetus illustrated in Figure 2.1. In addition to these components, there is a connector that is attached to the end of the wires. This connector allows for the electrode to be connected to a signal-measuring machine.

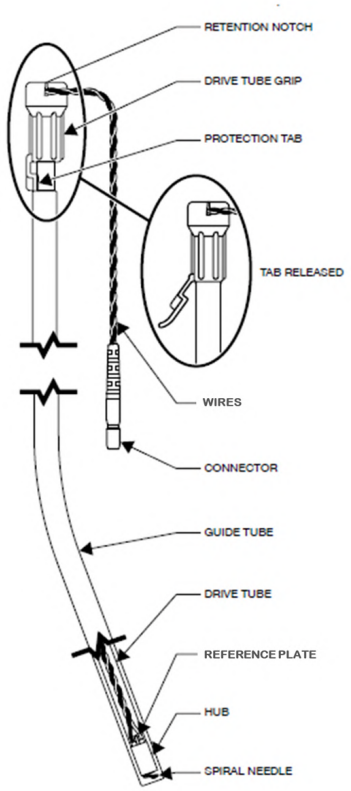

Figure 2.1: The different components of the electrode. (Courtesy of Neoventa Medical AB)

2.4 Image Processing

RGB images consist of three different matrices representing each color where each element in the matrix represents one pixel [15]. The element in each matrix represents which ratio of each color the pixel should consist of. When grayscaling an image the mean of the RGB pixels is taken to create one grayscaled pixel [15]. The maximum value of a pixel is different for different formats, one common is the Unicode Tranformation Format 8-bit (UTF-8). Each pixel in the imaging format used for this project is composed of 8 bits, allowing for a maximum value of 255 for each pixel [15]. A pixel value of 255 represents white, while a value of 0 corresponds to black. In image processing are many filtering operations performed by a convolution of the image and a kernel [15]. This is done to extract information from the picture, for example extract edges or reduce noise. Kernels are square matrices that are around 3x3 in size. When using convolution, the kernel slide over the image and each pixel of the kernel is multiplied with the same pixel in the image and then added together [15]. This is visualised in Figure 2.2 and Equation 2.1.

$$(-1)\cdot 4 + 0\cdot 0 + 0\cdot 0 + 0\cdot 0 + 1\cdot 1 + 1\cdot 0 + 0\cdot 0 + 1\cdot 0 + 2\cdot 1 = (-1) \qquad (2.1)$$

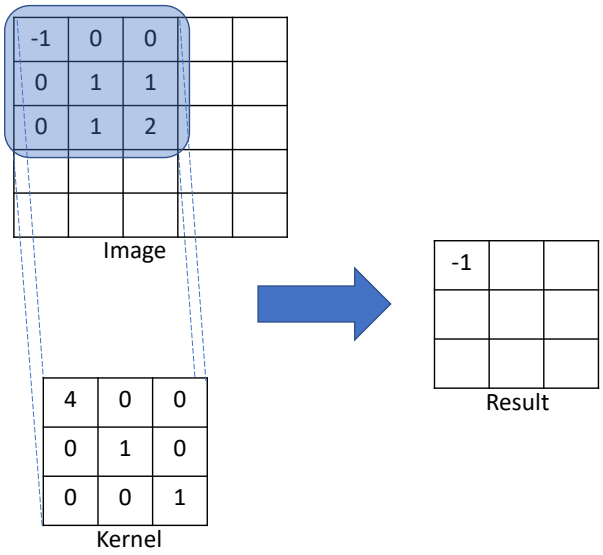

Figure 2.2: A kernel is convoluted with an image at one out of nine different possible positions of the kernel. The result is calculated by Equation 2.1.

2.4.1 Image segmentation

The following sections describe the various image processing techniques utilized in this project.

2.4.1.1 Laplacian edge detection

Laplacian is a 2D measure of the 2nd spatial derivative of the image and it is used to detect edges in an image [16]. It strengthens the regions in the image with rapid intensity change, which corresponds to being an edge. The method works best if the image is smoothed first, for example by a Gaussian filter. The reason for needing a smoothed image is that the second derivative is sensitive to noise. The filter removes rapid changes due to noise but keeps the changes due to objects in the image. Two kernels that are used to find the second derivative are stated in Equation 2.4.1.1.

$$\begin{bmatrix} 0 & -1 & 0 \\ -1 & 4 & -1 \\ 0 & -1 & 0 \end{bmatrix}, \quad \begin{bmatrix} -1 & -1 & -1 \\ -1 & 8 & -1 \\ -1 & -1 & -1 \end{bmatrix}$$

2.4.1.2 Sobel edge detection

The Sobel edge detection is another edge detection technique and it measures the gradients in the image to decide if it is an edge or not [17]. The method uses two kernels as described in Equation 2.2 and the kernels are designed to respond maximally to horizontal lines (G_x) and vertical lines (G_y).

$$G_x = \begin{bmatrix} -1 & 0 & 1 \\ -2 & 0 & 2 \\ -1 & 0 & 1 \end{bmatrix}, \quad G_y = \begin{bmatrix} 1 & 2 & 1 \\ 0 & 0 & 0 \\ -1 & -2 & -1 \end{bmatrix} \tag{2.2}$$

The kernels are applied to the image separately by convolution to find the gradients and the combined gradient magnitude is given by Equation 2.3 [17].

$$|G| = \sqrt{Gx^2 + Gy^2} \tag{2.3}$$

After the magnitude is calculated is the angle of the edge conducted. Meaning the perpendicular direction from the line and it is done as described in Equation 2.4.

$$\Theta = arctan(G_y/Gx) \tag{2.4}$$

2.4.1.3 Canny edge detection

Canny edge detection is an operator that uses a multi-stage algorithm with five different steps [18]. The steps are the following:

1. Noise reduction
2. Gradient calculation
3. Non-maximum Suppression
4. Double threshold
5. Edge tracking by Hysteresis

The noise reduction is performed since Canny, similar to Laplacian, is sensitive to noise in the image [18]. The noise is removed by a Gaussian filter with different kernel sizes depending on the desired performance. A large kernel size makes the edge detection less sensitive to edges and a smaller size makes it more sensitive. The gradient finding is done by using the same technique as the Sobel gradient edge detection. The non-maximum suppression is used since the result of the Sobel edge detection has often thick lines where the edges are. The non-maximum suppression makes the line thin, containing only one pixel, by finding the pixel with the maximum value in the edge direction [18]. The edge direction is the perpendicular direction towards the lines found by the Sobel edge detection Equation 2.4. The double threshold step categorizes all the pixels into three different categories: strong pixels, weak pixels and non-relevant pixels [18]. This is done by setting an upper threshold, where all pixels higher than the threshold are set to strong pixels. A lower threshold is also determined, and all pixels under it are considered non-relevant. The pixels in between the thresholds are considered weak pixels. The fifth step, Edge tracking by Hysteresis, determines if the weak pixels are strong or non-relevant. A pixel is then classified as strong if one or more of the eight surrounding pixels are strong.

2.4.1.4 Threshold and contour

Another way to find edges and objects in an image is by performing a threshold over the image [19]. This means that the pixels in the image are categorized into two different categories, black or white. The categorization is done by setting a value which separates the pixels. If the pixel value is higher than the threshold, the pixel is set to white, otherwise black. This method can be combined with adding a contour to find edges. That means that lines are surrounding all the white areas in the image. The threshold technique is simpler than the other presented edge detection methods and therefore has lower computations and performs faster in a real time environment [19].

2.4.2 Hough line transform

The Hough line transform finds straight lines in an edge detected image [20]. It is based on lines expressed in polar coordinates that is illustrated in Figure 2.3.

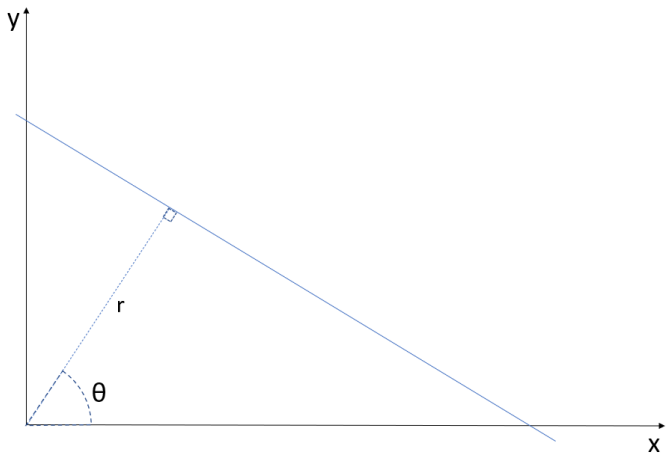

Figure 2.3: The polar coordinate system for Hugh line transform.

The equation for the line can then be written as Equation 2.5.

$$r_\Theta = x_0 \cdot cos(\Theta) + y_0 \cdot sin(\Theta) \tag{2.5}$$

If the values of x_0 and y_0 are fixed and all the representations of lines (r_Θ, Θ) passing through that point are plotted, the resulting plot resembles a sinusoid [20]. This means that a line in the image space is a point in the Hough space and a point in image space is a sinusoid in Hough space. If multiple points on a straight line in the image space are represented as sinusoids individually in Hough space, there will be an intersection point where all of the sinusoids intersect. This intersection point in Hough space corresponds to the parameters (r_Θ, Θ). This is the basics of how Hough line transform operates [20]. The method takes all the pixels detected

as an edge and represents them in Hough space. If there is a point where many curves intersect, it means that there is a line at that point. When configuring a Hough line transform, a threshold is determined to establish the minimum number of intersections required to classify a line.

2.5 Principles of Imaging and Cameras

The two most important components of a camera are the lens and the sensor. The lens collects the light and projects it toward the sensor. The sensor consists of photosites that convert the light into a signal [21]. There are two different kinds of camera sensors, Charge Coupled Device (CCD) and Complementary Metal Oxide Semiconductor (CMOS) [22]. Traditionally, CCD cameras were regarded as having superior image quality compared to CMOS sensors. However, advancements in CMOS sensor technology have narrowed the gap, and the image quality of CMOS sensors is now approaching that of CCD sensors. Additionally, CMOS sensors offer certain advantages over CCD sensors, such as higher speed and faster readout capabilities. The sensor can be either monochrome meaning that it captures a black and white image, or it can be a color sensor. The color sensor works by arranging the photosites in the sensor into an alternating pattern where some of the photosites capture red light, some capture blue light and some capture green light [22]. In a digital image, this means that the image is arranged into three different channels containing the red value respectively blue and green. In comparison, the monochrome camera captures all the light in every photosite and then only uses one channel. CMOS cameras can be divided into two categories, area scan and line scan [23]. Line scan cameras capture one single row of pixels at a time and are therefore suitable when the camera is moving over an object, or an object is moving under the camera. An area scan camera takes an image of a fixed area and transfers it to a pre-determined number of pixels. CMOS cameras are built on two additionally different techniques, rolling shutter or global shutter [24]. A rolling shutter captures the image frame in a sequential row-by-row manner while a global shutter captures the entire frame at the same time. This means that global shutter cameras are better to use when capturing an object in movement, no capturing of stretching or wobbling. This can be seen in Figure 2.4.

(a) An image of a stationary electrode captured by a camera with global shutter.

(b) An image of a moving electrode captured by a camera with global shutter.

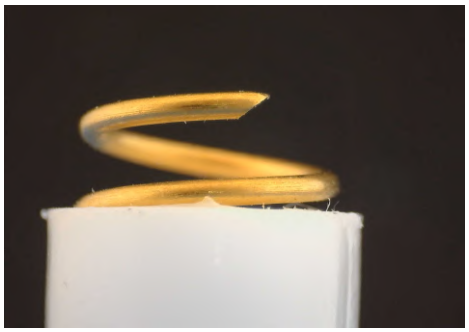

(c) An image of a stationary electrode captured by a camera with rolling shutter.

(d) An image of a moving electrode captured by a camera with rolling shutter.

Figure 2.4: Examples showing how global and rolling shutter affects an image captured in motion. A less blurry image is obtained in motion with the global shutter camera than with the rolling shutter camera.

Another important parameter regarding capturing objects in motion is the frame rate measured in frames per second (FPS) [25]. It determines how many frames that will be captured every second, which is relevant when considering how fast the object is moving and is most relevant for not obtaining a discontinuous video.

The resolution of the camera affects the pixel size and thereby the size of the object that the camera can detect. The pixel size depends however not only on the resolution but also the field of view (FOV), the size of the image, as seen in Equation 2.6 [26].

$$Pixel\ size\ in\ one\ dimension = \frac{Size\ of\ field\ of\ view\ in\ that\ dimension}{Pixel\ count\ in\ that\ dimension} \tag{2.6}$$

The FOV is influenced by various factors, including the depth of field. The depth of field is affected by how close to the object the picture is taken and thereby how large the FOV is. If the camera is located near the object it focuses on, the depth

of field is shorter and the pixel size is smaller. Conversely, if the camera is further away from the object, the depth of field increases, leading to larger pixel size.

An additional camera feature is the aperture [27]. The aperture determines how much light that should pass the opening of the lens and enter the camera sensor. This is done by shrinking or enlarging the opening of the lens. If a photo is taken in a darker environment, it is beneficial to have a larger aperture in order to not get a too dark image [27]. The aperture affects not only the brightness of the image but also the depth of field. While a larger aperture means that the image is brighter it also means that the depth of field is smaller. The aperture is determined by a f-number of the camera and is often expressed as f/"f-number" [27]. This means that a large aperture has a low f-value. Every lens has a specified interval of the f-values possible, which means that it is important to consider the f-value before deciding on a camera. Often a high f-value as f/11-f/16 is used by lenses that are focused on landscape photographing. Small f value as f/0.95-f/1.4 is often used for dark environments such as photographing the night sky.

2.6 Mathematical tools used during development

During the system development, mathematical equations and relationships are utilized, particularly equations concerning distances and angles in 2D space, as well as linear regression. These mathematical tools will be employed in the upcoming section.

Minimal distance between line and point

The minimal distance between a line expressed as Equation 2.7 and a point in the 2D space is described in Equation 2.8 [28].

$$ax + by + c = 0 \tag{2.7}$$

$$distance = \frac{|ax + by + c|}{\sqrt{a^2 + b^2}} \tag{2.8}$$

Linear regression

In scientific investigation, the result of a system is often believed to be a certain shape, such as a line [29]. One way to do a line approximation is to use the method least square where k and m are chosen to minimize the total distance from the points to the line. This is done by fitting the points into Equation 2.9 and 2.10 and approximate the line from the given answers [29].

$$k = \frac{n(\sum_{i=1}^{n} x_i y_i) - (\sum_{i=1}^{n} x_i)(\sum_{i=1}^{n} y_i)}{n(\sum_{i=1}^{n} x_i^2) - (\sum_{i=1}^{n} x_i)^2} \tag{2.9}$$

$$m = \frac{(\sum_{i=1}^{n} x_i^2)(\sum_{i=1}^{n} y_i) - (\sum_{i=1}^{n} x_i)(\sum_{i=1}^{n} x_i y_i)}{n(\sum_{i=1}^{n} x_i^2) - (\sum_{i=1}^{n} x_i)} \tag{2.10}$$

Angle between lines

The angle between two straight lines is calculated as in Equation 2.11 where M1 and M2 are the slopes of each line [30].

$$tan(\alpha) = \left| \frac{M2 - M1}{1 + M1 \cdot M2} \right| \tag{2.11}$$

3

Methods

This project has consisted of four parts presented in Figure 3.1. The project began with Knowledge acquisition, where the focus was acquiring the information needed from the customer regarding the current measuring system used in the quality control and also acquiring information about the future aim. It also included a literature study to gather background theory for the project. The project continued with Concept development to perform initial brainstorming and idea generation which culminated in the creation of detailed development plans. The next step of the project was to initialize the System development, to create both the software system and the fixture that integrated into a final prototype. The final part of the project was the Evaluation of the system which had a focus on both the precision and accuracy performance and also the efficiency performance of the new system. It was compared to the system currently used by the customer.

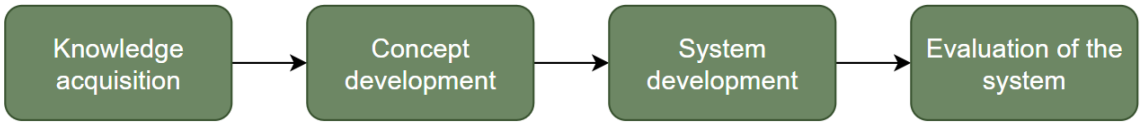

Figure 3.1: Process tree for the project methodology.

3.1 Knowledge Acquisition

The knowledge acquisition process was divided into three parts, initial study, customer needs study, and observation and time study of the current system. The conduction of these methods is presented in the following sections.

3.1.1 Initial study

The initial study focused firstly on gathering information on computer vision systems applied in quality controls, to collect background and theory that could lay the foundation of the project. This was performed by going through mainly scientific papers from databases such as Scopus, Google Scholar, ScienceDirect and Chalmers Library. The study was performed by various search strings as *Computer vision*, *Machine vision*, *vision*, *Industry 4.0*, *Production*, *Automation*, *Quality inspection*, *Quality assurance*, *Quality control*, *Measuring AND Computer vision*, and *Image*

processing AND segmentation. In addition, also the Google search engine was used to get an understanding of the subject and gain initial knowledge.

Secondly, information about the product, value chain, and the current quality test solution was gathered to understand and define the problem formulation. This was done by having an interview with the stakeholders Together Tech AB and Neoventa Medical AB. There are three different kinds of interviews: unstructured-, semi-structured- and structured interviews [31]. An unstructured interview was done with Neoventa and Together Tech on February 1st, 2023, to get a good overview of the product and the current situation. The participants were three representatives from Neoventa that together have much knowledge of the Goldtrace FSE and its quality: Laura Goethals (Quality Coordinator), Anna Ragnerius (Software Engineer), and Johan Sundberg (Chief Technology Officer) together with the supervisors from Together Tech. The answers were noted after the interview was conducted and the questions asked are found in Appendix A.1.

3.1.2 Customer needs study

The customer needs study was performed to find out the needs of the project, and to set the aim and requirement specification. The study was primarily performed by analyzing and discussing the answers from the initial study interview and setting requirement specifications from that. It was also established on provided documents from Neoventa regarding the current situation. Thereafter, the development of the needs of the system started, and these were developed during the entire development phase through discussions with Neoventa and Together Tech.

March 23rd, 2023, a second interview with Neoventa was conducted. This interview primarily focused on more specific questions regarding the implementation of the prototype into the current workflow and discussing the findings that had already emerged during the project. This was performed both by asking prepared questions and also by having a discussion with Neoventa. It was therefore a semi-structured interview [31]. Attending the interview was Laura Goethals (Quality Coordinator) and the answers were noted during the interview. The questions that were asked can be seen in Appendix A.2.

3.1.3 Observation and time study on current quality control system

An observation and time study was planned and performed to retrieve comparable data from the current quality test process. The aim of the observation was to make a time study of the measuring test and to analyze the risks and problems presented by Neoventa, furthermore, identify more risks and problems of the process.

The time study focused on retrieving time parameters that would be comparable with the new developed system so that an efficiency analysis could be performed during the evaluation stage of the project. Furthermore, the study also focused

on finding method improvements that could be considered during the development phase.

The study was prepared by creating a time study form for a repetitive task. It is most common to do 10 observations on a repetitive time study and therefore, 10 observations and time recordings were planned for this project [32]. An electronic stopwatch with a digital display was used since these tend to provide the most accurate results, owing to the numbers being frozen while recording the values [32]. The clock had a cumulative mode which made it easy to also retrieve the accurate total testing time per observed electrode. The quality test was performed by the operator who normally performs the quality test on the samples from the delivered batches that arrives approximately two times a month to Neoventa. The choice of the observed operator is an important factor since time studies should be performed on qualified operators that can operate at the normal performance level [32]. The study began with dividing the quality inspection into work tasks that could be measured and analyzed separately, which gave the opportunity to more easily find nonproductive work that preferably would be eliminated in the new system [32].

3.2 Concept Development

3.2.1 Initial brainstorming

Brainstorming is one of the important factors when creating new ideas involving the collaboration of individuals within a group to generate new ideas by combining their existing knowledge. [33]. An initial brainstorming was performed to understand the problem and the important parameters to consider during the upcoming development. This brainstorming was based on the initial study, which involved acquiring knowledge about the product, value chain, and quality testing. During this initial brainstorming, an available camera was used to further understand the capturing of the electrode and existing difficulties that would have to be considered when generating solution ideas. The used camera model was a Dino-Lite Edge Digital Microscope AM4815ZTL [34]. During this brainstorming session, different software was considered and investigated to make a decision on which software would be used in this project. The questions that were discussed and answered were the following:

- What camera view will be used in the system?
- How should the electrode be placed and fastened?
- What programming language and programming libraries would be suitable to use?

3.2.2 Idea generation

When the initial brainstorming was completed, more details were set in an idea generation phase. The details were refined by discussing and testing different concepts and ideas, as well as by gathering information on important camera parameters.

The camera information was collected by searching websites on how to choose the right camera for a computer vision system, what different parameters meant, and what effect those parameters would have on the final camera image. When the information regarding parameters was finalized, a requirement specifications list for the camera was conducted. From that, different concepts were discussed regarding what systems and setups could be used for different cameras. This was partly done by testing and comparing with the given camera from Together Tech, Dino-Lite. The camera was also used to get an idea of how the system could be built, both regarding the fixture and the software. When an idea was set, sketches were made to simplify discussions with Neoventa and Together Tech. The importance of decreasing the human impact and thereby decreasing the margin of error [35] was one of the main things considered and discussed during the idea generation phase.

3.2.3 Detailed development plan

After the idea generation was performed, a final concept idea was decided on and from that, a detailed development plan was created. The plan included deciding in which order everything would be performed and how to combine the physical fixture and the software development. The plan also contained two more detailed separate plans, one for the software and one for the fixture.

3.3 System Development

When the detailed development plan had been established, it was time to enter the system development phase of the project. The two separate plans for software and fixture were performed simultaneously and were then integrated to test and evaluate the combined system, visualized in the process tree in Figure 3.2. This development, integration, testing and reevaluation were iterated many times and thus the software development and fixture development were updated and changed a lot throughout the whole development phase to get the most optimal final prototype. The following two sections focus on explaining in further detail the processes of the software and fixture developments and the iteration that has been done in those specific parts of the system development, marked in Figure 3.2.

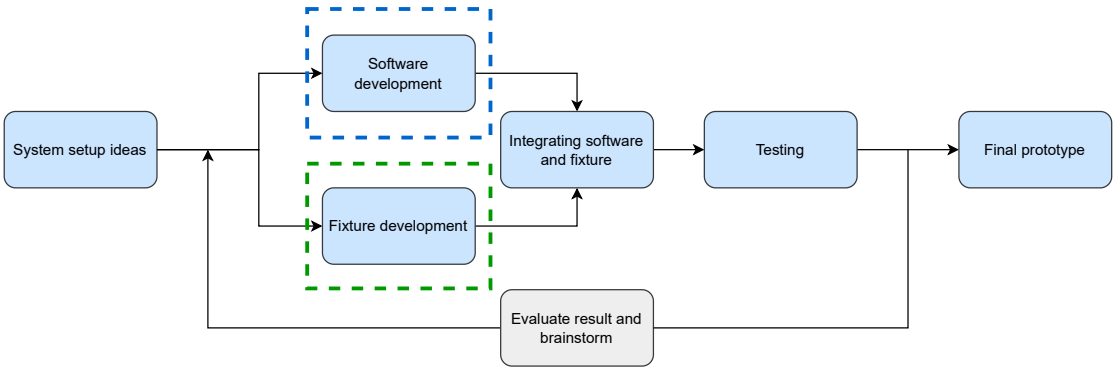

Figure 3.2: Process tree for the System development.

3.3.1 Software development

This section explains further how the process of the software development has been executed and it is visualized in more detail in Figure 3.3. The development started with an idea generation based on the Software setup plan, which then exceeded into starting the development of the detection system. The first step was to develop the detection of the hub and the spiral to be able to later base the measurements on the detection. All small progress within this detection development was evaluated and improved throughout the entire development. Also, when the whole detection system was considered done, the result was evaluated and improved again before developing the measuring system. The same approach was implemented when developing the measuring system, which aimed at performing measurements with the smallest variation and highest accuracy possible. All smaller progress was evaluated and improved separately, and a final evaluation and improvements of the measuring system performance were done over and over. The next part of the process consisted of evaluating the detection and measuring processes in combination before the system was ready for integration with the fixture. It was then time to test, evaluate and improve the whole integrated system, as was visualized in Figure 3.2.

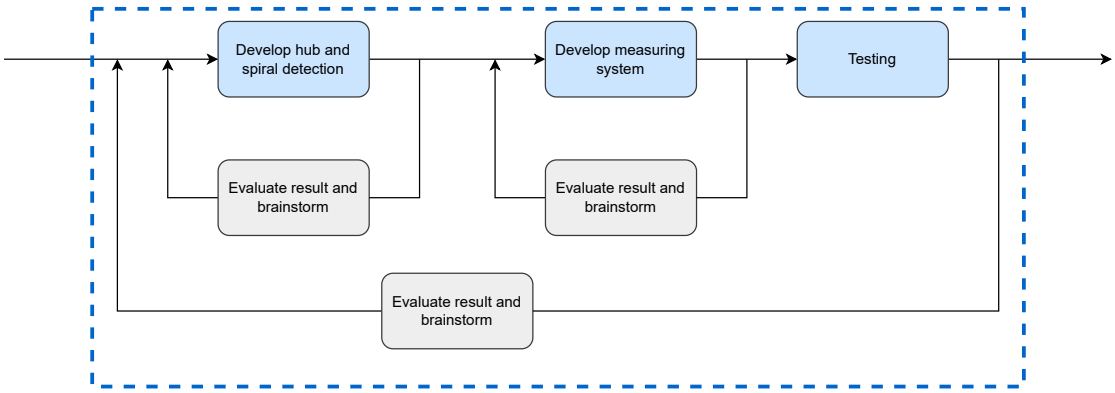

Figure 3.3: Process tree for the Software development.

3.3.2 Fixture development

This section explains the fixture development execution in further detail, and it is visualized as a process tree in Figure 3.4. Such as in the software development, the development of the fixture started with generating ideas from the Fixture setup plan. The development then continued by creating the first, preliminary fixture and then later in the project creating the second, final fixture.

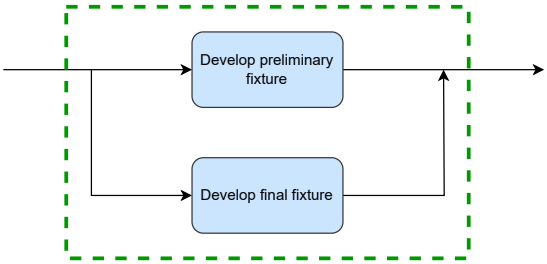

Figure 3.4: Process tree for the Fixture development.

The purpose of the first fixture was to enable adjustments and modifications to test different settings to find what worked best for the system. This fixture was used to assist the development of the system and it was continuously changed to optimize the conditions for the software, such as adding more lightning in the box and trying different materials to hold the electrode in place. To enable this continuous improvement and adaptation to the software system, the preliminary fixture was integrated with the software many times to try how the improvements worked in combination. So, as it was visualized in Figure 3.2 the integrated system was evaluated and then new ideas and improvements were implemented again.

Toward the end of the project, the preliminary fixture was evaluated and replaced with a final fixture that was meant to provide the important parameters and settings that had been stated by experimenting with the first, preliminary fixture. This fixture could then be used to evaluate the developed system and compare it to the current quality testing solution in the production of the FSE. The final fixture was done by finding and producing metal parts that could provide more stability and consistency for the final prototype compared to the preliminary. It was also done by having the mechanical department at Together Tech design two CAD parts and 3D print them for the fixture. The CAD models were performed from supplied sketches and meetings where the fixture was discussed and planned.

3.3.2.1 Camera selection

The Dino-Lite Edge Digital Microscope AM4815ZTL [34] camera was used to get an understanding of the camera needs. When the detection of the hub and spiral was finalized, the Dino-Lite camera was evaluated. Testing was conducted to determine the optimal measurement method and identify the requirements that the camera would need to fulfill, which were not met by the Dino-Lite. Additionally, the specifications of the Dino-Lite that were necessary for the project were identified. Once the requirements were established, an evaluation was conducted to determine which camera could meet those requirements. Once a suitable camera was identified, it was ordered to serve as the final camera for the system. Subsequently, the camera was implemented into the already-developed software, and the program was adjusted accordingly to accommodate the new camera.

3.4 Evaluation of the system

An evaluation of the system was done based on the system's performance, regarding precision, accuracy, and time efficiency. The way the evaluations were conducted is described in the following sections.

3.4.1 Precision and accuracy performance

To evaluate how well the detection of the hub and the tip lines work, all the available electrodes were tested in the detection system. It was noted how many electrodes that got a hub detection that would mean that the height measurement would be less accurate as well as how many tip lines detection that were placed wrong, resulting in an incorrect angle measurement. There were 140 tested electrodes and those that were considered to have an incorrect detection were photographed.

3.4.1.1 Calibration system

Two people performed the testing of the calibration system and the test consisted of carrying through the calibration 10 times each. The calibration ruler and the rest of the system were left unchanged during the 10 tests to exclude other parameters, and to investigate how much the result could vary depending on how a person chooses to carry through the test, and also how much the result could vary between different persons.

3.4.1.2 Height measurement

The evaluation of the developed height-measuring system was done in three steps. The first step aimed to find the precision of both the developed and the current system and to compare these two. The second step aimed to determine the precision of the developed system by comparing iterative tests on the developed system. The third step aimed to determine the accuracy of the developed system by comparing it with two other measuring systems.

The first step consisted of repeating the measurement 10 times on three electrodes for both systems. This was carried through by four users, users A and B, who were very experienced with the developed system, performed tests on both systems. User C who was very experienced with the current system only performed tests on the current system, and user D who was experienced in neither system performed tests only on the developed system. In this way, data was collected for both experienced and inexperienced users on both systems. For each user and each electrode, the maximum and minimum acquired height values from the 10 repetitions were extracted and the difference was calculated between the two. This difference could then show how high precision the two systems had and which system was better in this aspect.

The second and third part of the height evaluation was to measure 25 electrodes in the developed system, in the current system, and also with the Dino-Lite camera

that was used in the earlier stage of the project. The measurements on the developed system were performed by two users, users A and B, two times each, in order to analyze how much the measurements varied within the system, hence finding out what precision the developed system has. In order to estimate the uncertainty, half of the maximum variation was calculated, as it was assumed that the accurate value lies exactly in between the minimum and maximum of the obtained values. The measurements with the Dino-Lite were obtained in the software for the camera, Dino-Capture, which allows the user to calibrate and manually place two lines in the picture to retrieve a distance, seen in Figure 3.5. The measurements for each electrode could then be compared between the systems to analyze how they varied and correlated to each other, thereby analyzing the accuracy of the developed system.

To obtain an overview, the 25 differences between the different systems and tests were calculated, the absolute value was determined and the mean, maximum, and minimum values were then computed and stated.

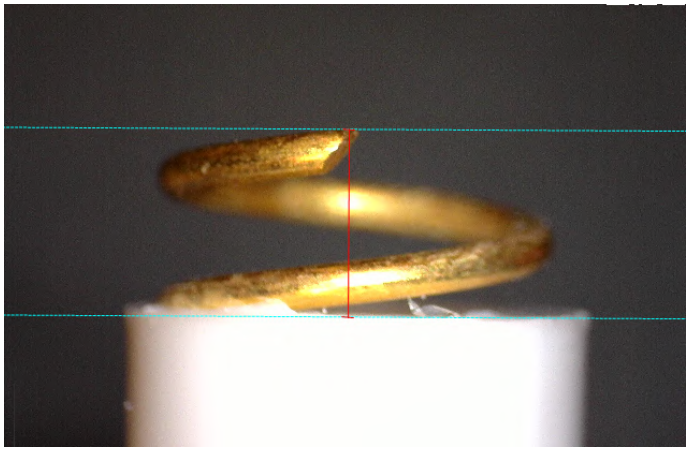

Figure 3.5: Measuring performed on an electrode in Dino-Capture.

3.4.1.3 Angle measurement

The evaluation of the angle measurement was done in three different tests. The first one was a test where four different users with different experiences of the system measured five different electrodes 10 times each. The inexperienced users got the instruction that they should place the electrode in the position where they found the optimal measuring, and also a quick illustration of how the electrode should be placed. The difference in the tests and between users was then examined to get an understanding of whether different users perform differently or not. The second test was an evaluation where two experienced users tested 25 different electrodes each. The difference between the user's performance was then analyzed to get an understanding of the deviation of the system. The third test was built on the idea of testing the system with another measuring technique. The Dino-Lite software, Dino-Capture, has built-in measuring functions and therefore this software was used together with the Dino-Lite camera. The user placed the electrode in front of the camera in a position that was considered the correct position and placed lines on the

image. The program then calculated the result. The same user did the measurements with the developed system but on a different occasion. The result was evaluated to see if the systems performed similarly.

3.4.2 Efficiency performance and observations

An observation and time study was planned and performed on the developed system in order to retrieve data comparable to the current system. This study was performed in the same way as the study performed on the currently used system, described in Section 3.1.3. Equivalently, the observation and time recording were done when the system was operated by a qualified person who knew how to use the system and who has done so a lot during the development of the system. Time recordings were done on 10 electrodes and observations and discussions were done to evaluate the performance of the system. The time recordings retrieved were then compared to the values from the current measuring system by analyzing mean time consumption for tasks that were equivalent and comparing the time consumption for the whole measuring process of one electrode.

4

Knowledge Acquisition

This chapter presents the outcomes of the initial knowledge acquisition process, which includes a customer needs study as well as an observation and time study of the existing measuring system used in quality control.

4.1 Customer Needs Study

The customer needs study is divided into two different sections, first, the current situation and current measuring system is explained, and then the future need and future system requirements are stated and explained.

4.1.1 Current quality control system

In the production site, the measurement is done on every electrode to certain the dimensions are within the tolerances. The spiral height measurement is performed with an instrument using a micrometer screw gauge, which can be seen in Figure 4.1. The electrode is inserted according to Figure 4.2, marked part 1 in Figure 4.1. The system uses the idea of manually screwing an electrically charged measuring cylinder, part 3 in Figure 4.1, towards the electrode that is in contact with a copper plate, part 2 in Figure 4.1. When the measuring device touches the electrode a Light-emitting diode (LED), part 4 in Figure 4.1, turns on, indicating that the measurement can be taken by pressing a button on the tool. For this measurement, the drive tube and guide tube are not yet mounted to the electrode. After the production is done, the electrodes are sent to Neoventa in Gothenburg where they are measured again. Only a part of the batch is remeasured in order to certain that the controls done at the production site are correct. Two tests are done in Gothenburg, measuring the spiral height and measuring the thickness of the drive tube. The same instrument is used to measure the spiral height in Gothenburg as in the production site. However, the measurement of the drive tube thickness necessitates that the drive tube is split and therefore the electrodes that are tested in Gothenburg cannot be sold and used. The electrodes that are not tested are then sent for packaging and sterilization by an outsourced company.

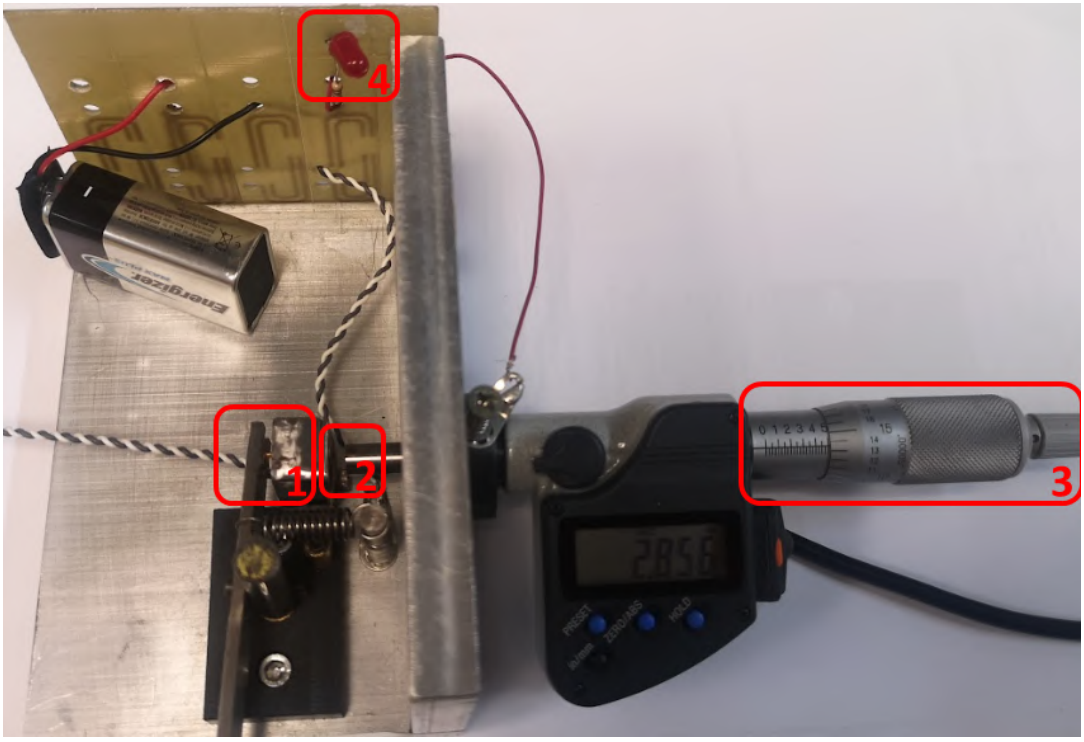

Figure 4.1: The current measuring system used by Neoventa to measure the height of the electrodes in the quality control.

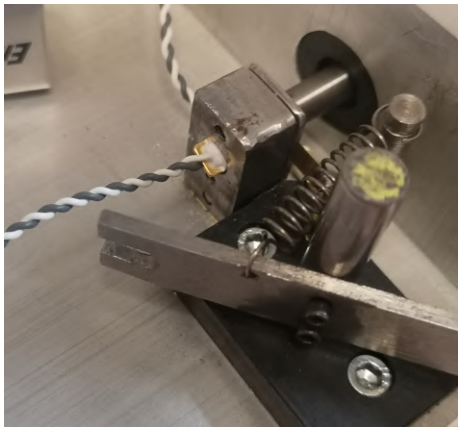

Figure 4.2: The insertion of the electrode in the current measuring system.

4.1.2 Desired quality control system

Neoventa aims to have a height-measuring system that is more reliable than the one used today. That means that it should be easier to use as well as more accurate. In addition, they wish that the system should be used both on the production site and at Neoventa. Neoventa would also like a system that not only measures the height of the spiral but also the angle of the spiral tip. In Gothenburg, it would be beneficial if the drive tube could still be attached during the measurement since the electrodes arrive mounted with the drive tube and thereby Neoventa will not need

to spend time on separating them. Meanwhile, in the production site it is currently better with only the hub and no tubes mounted, then no tubes would be discarded if the electrode failed to meet the measurement dimension criteria.

The required accuracy of the final measuring system is calculated by looking at the tolerances of the height and the angle. The height tolerance is stated to be $y \pm x$ inches by Neoventa. That interval is illustrated in Figure 4.3 as the yellow arrows. There are values that are greater or smaller than the given interval but are still considered correct. This is because the numbers are rounded. The value of how much greater the electrode can be than the tolerance and still be measured as an approved electrode is represented with an ϵ in Figure 4.3 and the orange interval. Because of this, the desired required accuracy of the height measuring system is set to the value ϵ, defined as ϵ_{height}. The same method was used when finding the desired accuracy of the angle measurement, called ϵ_{angle}. An example of ϵ values in relation to the tolerance x is presented in Table 4.1.

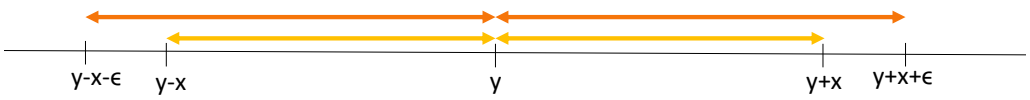

Figure 4.3: The height measurement value y and the tolerance ± x. The value ϵ represents the error in which electrodes are rounded to be in the correct height.

Table 4.1: Examples on possible given tolerances from the company and what measuring uncertainty that would correspond to.

The measuring tolerance, x	The maximum uncertainty of measurement, ϵ
1	0.5
0.1	0.05
0.5	0.05
0.01	0.005
0.05	0.005
0.001	0.0005

The aim from Neoventa along with the determined accuracies are converted into the preferable system requirements in Table 4.2.

Table 4.2: Preferable system requirements formulated from the customer needs study.

Number	System requirements
1	The system should measure the height of the spiral
1.1	The height is the distance between the hub and the highest point of the spiral
1.2	The measuring accuracy should be less than ϵ_{height}
2	The system should measure the angle of the spiral tip
2.1	The measuring accuracy should be less than ϵ_{angle}
3	The system should be as robust against human and external factors as possible.
3.1	One electrode should have the same measurement on several tests made by different users
3.2	One electrode should have the same measurement even if the system is moved to a different place
4	The system should be as efficient as possible.
4.1	It should be faster to use than the current system.

4.2 Observation and time study on current quality control system

Observations are made on the usage of the current spiral height measuring device used in the quality control, described in Section 4.1.1 and shown in Figure 4.1. The measuring process is divided into four work tasks. The four work tasks are described in Table 4.3. The time study is performed on these four tasks on 10 electrodes, and the result is presented in Table 4.4.

Table 4.3: Work tasks and observations of the measuring process of the current quality inspection.

Task	Work task	Comment
1	Separate electrode from drive tube	
2	Attach hub to the measuring tool	Have to reattach electrode ca. one out of five tests
3	Screw the measuring cylinder toward the electrode spiral	LED indicator not distinct
4	Collect measurement value and detach electrode from tool	Important to screw out the measuring cylinder

Table 4.4: Time study of 10 electrodes E1-E10, tests performed by the operator at Neoventa.

	Task 1 (s)	Task 2 (s)	Task 3 (s)	Task 4 (s)	Total time (s)	Comment/deviation
E1	9.7	6.2	6.3	4.8	26.9	
E2	8.1	6.1	10.2	3.4	27.8	
E3	6.8	7.2	6.4	4.6	24.9	
E4	7.4	12.9	9.2	5.2	34.8	
E5	8.9	9.3	31.9	5.0	55.2	Had to reattach and remeasure the electrode
E6	9.6	10.4	7.9	2.3	30.2	
E7	7.4	7.7	5.7	4.5	25.2	
E8	8.0	8.3	9.9	4.3	30.6	
E9	8.7	7.3	5.1	5.8	26.8	
E10	7.7	7.3	4.6	4.4	24.0	
Mean	**8.2**	**8.3**	**9.8**	**4.3**	**30.6**	

Task 1, separating the electrode from the drive tube, is performed almost entirely without difficulties both according to the observations and the operator's assessment. It is also seen in Table 4.4 that the time recordings for this task do not vary a lot between the electrode measurements.

Task 2, attaching the hub to the measuring tool, is performed often with a bit of difficulty as it is hard for the operator to see the positioning of the spiral both rotation-wise and whether the electrode is inserted all the way toward the copper plate. The time recordings in Table 4.4 can also indicate that this problem exists since the time recordings between the electrodes vary a lot. An observation of this task is that the electrode top is pushed into the copper plate if not rotated correctly during insertion, which sometimes happens since it is hard to see the electrode positioning due to lack of visualization when the electrode is inside the metal cube, seen in Figure 4.2.

Task 3, screwing the measuring cylinder toward the electrode spiral, is generally performed without any issues. Although, there are instances where the task needs to be repeated because the LED indicator fails to light up. This problem is likely to originate from the incorrect insertion of the FSE, although it is challenging to find the exact cause due to the limited visibility of the electrode parts during the test. The problem encountered during task 3 forces the operator to repeat both task 2 and task 3, causing increased measurement time. Additionally, tasks 2 and 3 may need to be redone due to the measurement value obtained during task 3 exceeding the accepted tolerances. Consequently, the placement and measurement are repeated. The second measurement often yields a value within the tolerances, indicating that this issue also is indeed caused by the misplacement of the electrode during task 2. This issue occurred specifically during the time study when measuring electrode E5, causing the time on task 3 and the total time to clearly deviate compared to other electrodes. Another observation done on task 3 is that the LED light does not provide a clear indication. This poses a risk as the operator may not notice the signal and therefore screws the measuring cylinder excessively, thus affecting the spiral height by compression. The insufficient distinction between the LED light indicator turned on and off is visualized in Figure 4.4.

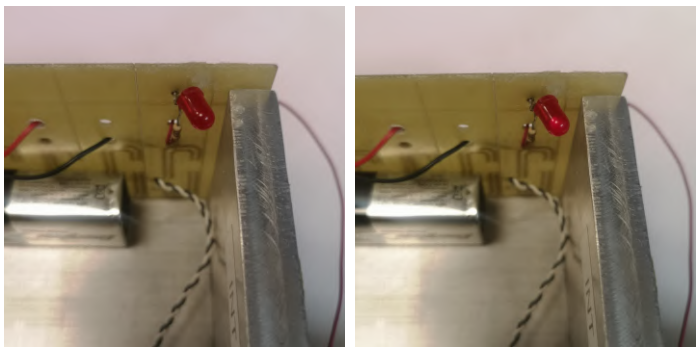

(a) LED light indicator off.

(b) LED light indicator on.

Figure 4.4: The insufficient difference of the LED light indicator.

Task 4, collecting the measurement and detaching the electrode from the tool, is performed without any difficulties both according to observations and the assessment of the operator. The spiral height value is collected and stored by pressing a button and the electrode is easily detached from the tool. This is also supported by the time recordings of task 4 as the values differ a bit but all are very short, indicating a smooth performance of the task. Another important observation in Task 4 is that the operator has to screw out the measuring cylinder before inserting a new electrode. Otherwise, the new electrode may become compressed due to spiral height differences.

The mean values from the time study are also presented in Table 4.4. The task consuming the most amount of time is task 3 with a mean value of 9.8 s, and the mean total time for the measurement quality inspection is 30.6 s.

5

Concept Development

The concept development is performed by first doing an initial brainstorming, deciding on the fundamental concept regarding the system, and then performing the concept developed in an idea generation process. The result of these methods is described in this chapter.

5.1 Initial brainstorming

Information from the initial study is used to understand the parameters that have to be measured. Whereafter the possible camera angles for acquiring these measurements are brainstormed and a decision is made that the camera will be placed in a fixed position during the quality testing. This will be sufficient for retrieving the visual input needed for calculating the two quality parameters.

The electrode has to be put in a fixture to ensure that it is captured correctly in the picture. It is also stated that there is a probability that the electrode needs to remain in the same position, which would require the ability to rotate the electrode within the fixture.

Python 3.11 is chosen as the programming language for this project as it offers the library OpenCV which includes a wide range of features for image processing and computer vision [36].

5.2 Idea generation

The image can be very different depending on the lighting of the electrode. The electrode reflects light if the light is directed directly at it, meaning that the electrode gets very different colors in different lighting conditions. Therefore the conclusion made is that the electrode needs to be placed in a box that has controlled lightning inside of it so that each control will be done as similarly as possible and no external factors will affect it.

The fixture must effectively hold the entire electrode in place during rotation, while ensuring that the hub is properly fixed within the setup. This is crucial for achieving consistent and similar images for all measurements. It is also essential for the images

to capture the complete spiral along with a portion of the hub. To achieve this, the use of a stop is necessary. One approach is to incorporate a thin object into the fixture, positioned opposite the hub, as visualized in Figure 5.1. The spiral can then be placed around the thin object, allowing it to act as a stop for the hub without touching the spiral itself. Thereby avoiding affecting the shape of the spiral.

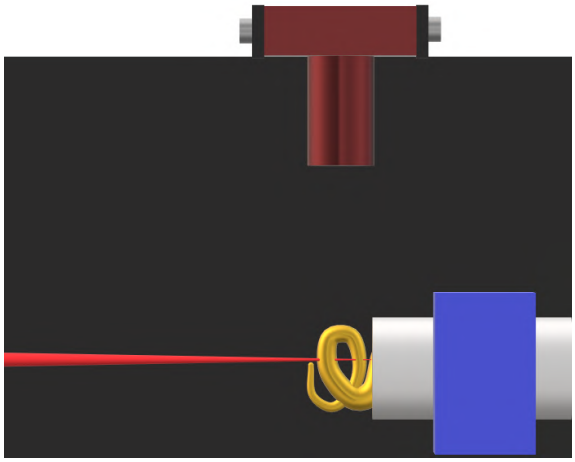

Figure 5.1: A sketch of the setup with a sharp stop pointed at the center of the spiral in order to ensure that the spiral is placed under the camera. The setup is placed within a black box where additional light would be added.

After examination of the color channels of the electrode image, it can be concluded that the spiral contains mainly high values of the red and green color channels. Therefore, it is beneficial to identify the hub using only the blue color channel and for that, a color camera is needed. Considering that the CMOS also has much lower prices and the quality difference between the sensors is quite small, a CMOS sensor is suitable for the system. In addition, since the electrode will not move in a linear path under the camera, a regular area scan camera is most suitable for the task.

The desired accuracy of the height measurement has to be considered when deciding the resolution of the camera. The necessary accuracy is set to ϵ_{height} and that means that the pixel size has to be smaller than the accuracy. The pixel size is dependent on the resolution and field of view as described in Equation 2.6.

If the electrode is positioned far from the camera, the depth of focus will increase, possibly allowing for simultaneous focus on the hub, the front, and the back of the spiral. However, this would result in a larger pixel size, potentially compromising the measurement accuracy if the resolution is not sufficiently high. The decision regarding the FOV and resolution is thus determined by the importance of focusing on both the front and back of the spiral. Since the angle of the tip is to be measured, the tip's position must be consistently located. Consequently, it may not be necessary to focus on all depths of the spiral, but rather prioritize focus mainly on the tip. The approach taken will depend on the system's design and how the angle is accurately determined. However, it can be beneficial having a system capable

of identifying the tip's location even though it is not in the correct position. For instance, a system that can detect the tip and provide guidance on how to rotate the electrode to the correct position.

There are several possibilities to get the tip into position, one way is that the user twists it correctly by looking at the electrode through a graphical user interface that tells when the electrode is positioned correctly. Another way could be to have a stop so that the user rotates the electrode until it hits a stop. In that case, it needs to be properly examined whether the spiral could change shape or take damage in such a system. A final way could be to have a system that can detect the electrode and the angle of the tip in motion. Then it could be enough to rotate the tip over the interval and retrieve the measurement from that.

If there should be a system that detects the spiral tip in motion and determines when it is in position, it is important to consider not only the depth of field but also how well the camera works with a moving object. Therefore, if the detection is intended to be performed while in motion, the camera must have global shutter and a higher FPS to avoid a discontinuous video. However the system and its detection will have to be created first to decide how the measuring should be done, in motion or in still position.

5.3 Setup conclusion and detailed development plan

The setup and detailed plan of the system development are described in the following sections. It is divided into three different sections, one for the software, one for the fixture, and one for the combined plan.

5.3.1 Software setup plan

In Table 5.1 the steps for the software development are presented. The first step will be to program the detection of the Goldtrace FSE spiral and hub which is needed for the height measuring. The second step is to detect the spiral tip point, which is needed to localize the orientation of the electrode during placement in the fixture. The third step is to investigate how well the three detections work in combination with rotational movement with speeds. The purpose of this is to come to more insights on how the complete measuring process can be done by the operators, and how to make certain that the electrode is placed correctly to obtain the needed measurements accurately. This step in the process will also include choosing a camera for the final solution, and it will have an impact on whether a higher FPS or Global shutter is needed. The fourth step will focus on extracting the measurements for the quality check. To measure the distance from the hub to the spiral tip, and to measure the spiral tip angle. The fifth step includes gaining an understanding and defining which rotational interval on the spiral gives a correct measurement of the tip angle. The sixth, and last step of the process consists of deciding and implementing exactly how the software will interact with the hardware. In this step, feedback

from the measuring system to the user will be implemented, the measurements will be stored, and also calibration will be investigated.

Table 5.1: The steps of the software development plan.

Task	Work task
1	Detect FSE spiral and hub
2	Detect FSE spiral tip point
3	Investigate movement and speeds with detection
4	Extract measurements
5	Find positioning-interval for the electrode
6	Define and implement the interaction between hardware and software

5.3.2 Fixture setup plan

The fixture setup will consist of two different prototypes. The first one is used to experiment with the surrounding conditions, mainly the amount of lightning. The second is the final fixture that is more robust and meets the requirements of what surroundings the software needs.

The preliminary fixture will consist of a material that is easy to cut and adjust. It will be equipped with LED strip lighting that can be adjusted both in positioning and illumination. The Dino-Lite camera will be attached to an available camera stand that makes it possible to adjust in height.

The final fixture will be 3D printed and equipped with fixed lightning and a fixed position for the new camera to optimize the settings. This 3D-printed fixture will also include a holder for the electrode to keep it in place.

5.3.3 Combined setup plan

The first two steps in the software development are to create the detection of the spiral, hub, and tip point. In order to do these successfully, a preliminary fixture is needed. This fixture will give the possibility to create a closed surrounding with preset lighting that makes it possible to experiment with the conditions in the detection. The creation of the preliminary fixture is initialized at the same time as the detection software, and it will be continuously developed along with the first two steps of the software development, see Table 5.1. When reaching the sixth step of the software development, the development of the final fixture will be initialized.

6

System Development

This chapter focuses on presenting the result of the whole system development, consisting of the software development, fixture development, and then a summarizing overview of the final design.

6.1 Software development

The development of the software is done in two different stages. First, the detection of the hub and the spiral is created, which is needed to enable the creation of the measuring processes. Secondly, the measurement of the spiral height and spiral angle is created, including how the electrode should be placed for the measurements and how the data from the measurements should be analyzed and processed. The general software system idea is visualized in Figure 6.1, where the first part consists of retrieving a picture frame of the electrode, the second part is the detection of the hub and spiral and the third part is the measurement of the height and angle.

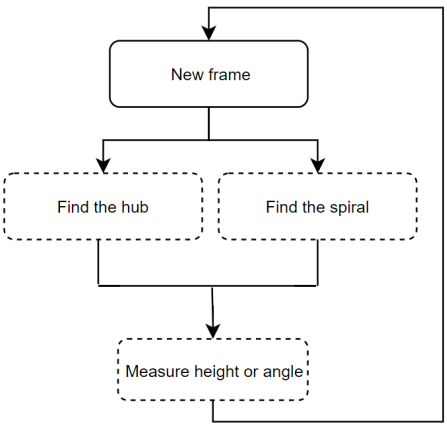

Figure 6.1: A flowchart of the general software system idea.

6.1.1 Hub and spiral detection

The detection of the hub and the spiral is based on a thresholded image where the contours are processed to approximate lines. The choice of the threshold with contour method is based on an evaluation of several image segmentation techniques

namely, Sobel edge detection, Canny edge detection, Laplacian edge detection and the threshold with contours. These methods are provided in OpenCV.

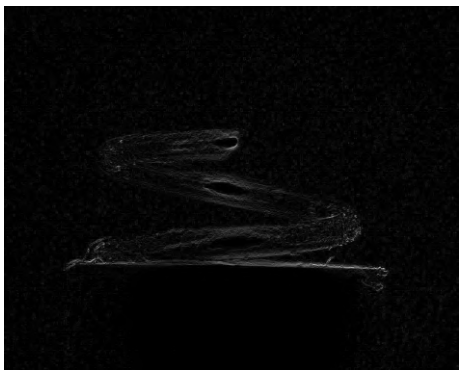

(a) Image processed using sobel edge detection.

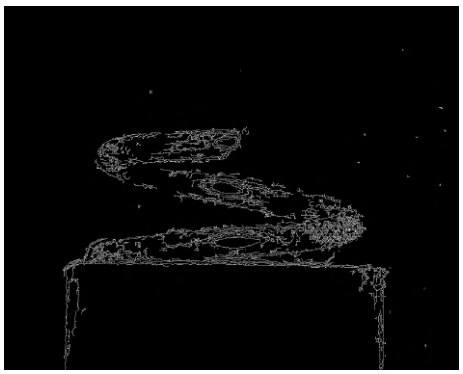

(b) Image processed using canny edge detection.

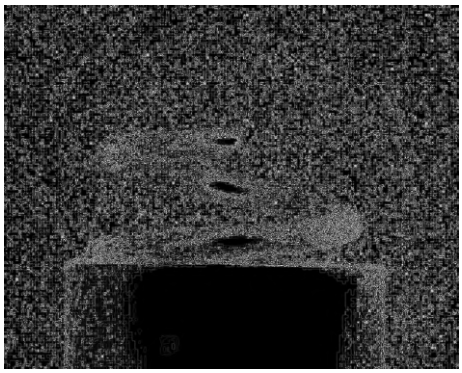

(c) Image processed using laplacian edge detection.

(d) Image processed using threshold segmentation.

Figure 6.2: Images processed by using different edge detection methods to detect the spiral and hub.

It is evaluated that the threshold technique has more variable parameters which makes it more adaptable. Many of the other techniques have more fixed parameters and are depending on filtering that uses a pre-determined kernel size. Therefore, the threshold technique is considered the most promising method in this project. The detection is based on two different thresholds that approximate different lines that later are merged into one final detection. One binarization detects the hub and the spiral together and approximates the spiral and the sides of the hub. The other binarization detects the hub and it approximates the top line of the hub. The detection is described in more detail in Figure 6.3, and the following sections describe each part of the detection software.

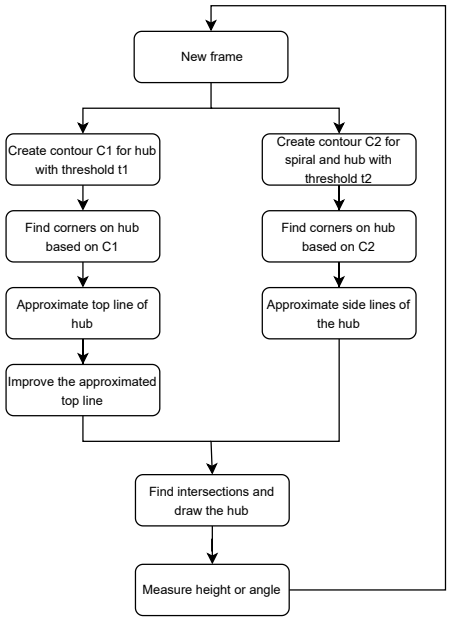

Figure 6.3: A flowchart of the overall system showing the detection of the hub and the spiral in more detail.

6.1.1.1 Create contours

The image of the electrode consists of three different color channels, red, green and blue. Those can be seen in Figure 6.4 and they show that the hub, because of its white color, contains approximately the same amount of each color. The spiral however contains more of the red and green channels than the blue channel. Therefore, the blue channel is a good image to use when distinguishing between the hub and the spiral since the contrast between the two is greater.

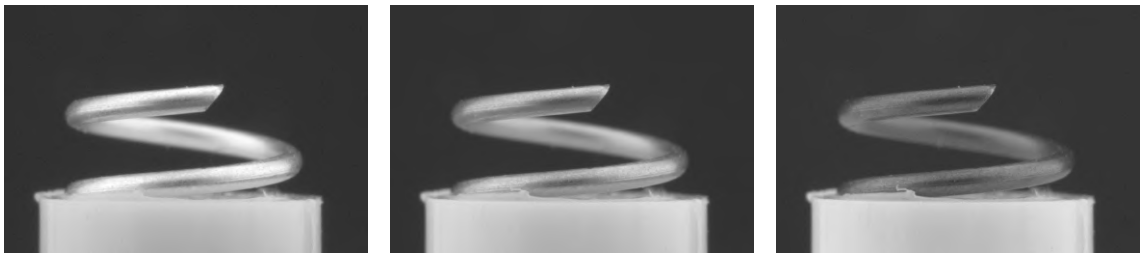

(a) The red color channel of the electrode.

(b) The green color channel of the electrode.

(c) The blue color channel of the electrode.

Figure 6.4: The electrode's three color channels, RGB.

The detection of the hub and spiral is based on a binarization of the images, where two different binarizations are performed. One binarizes the hub, t1, and one binarizes the hub together with the spiral, t2. The binarization is done by thresholding at certain values. The optimal thresholding value is dependent on several external factors, for example, the lightning of the electrode and the f-value of the camera.

These are therefore determined together. To do an evaluation, a trackbar is created that can easily change the threshold value while having a live update. The goal is that the hub and spiral threshold t2 will later lay the foundation for both the hub sides and the spiral and the hub threshold t1 will lay the foundation for the top line of the hub. The decided values are t1=190 for the hub detection and t2=95 for the entire electrode, both hub and spiral. The hub detection is based on the blue color channel and the electrode detection is based on a black-and-white version of the image. The result of the binarization on one electrode is presented in Figure 6.5b and it is clear that the threshold works to find the objects but some parts in the detected area are still detected as dark.

(a) The electrode image is binarized with threshold t2 to filter out all but the spiral and hub.

(b) The electrode image is binarized with threshold t1 to filter out everything but the hub.

Figure 6.5: The two different binarizations of the image, t1 and t2.

The thresholded areas are enclosed with a contour that is seen in Figure 6.6, and these contours are created using methods in OpenCV. It is clear that the contours are found in more places than only at the edges of the electrode. Therefore, the redundant contours are removed by extracting only the largest contour area, remaining only the contours that can lay a foundation for the final lines that will be regarded as the hub.

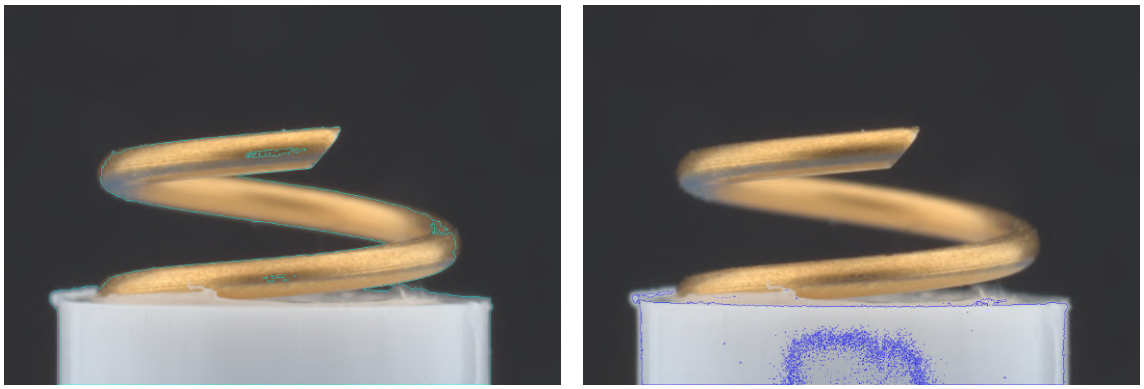

(a) The spiral contours found with t2. **(b)** The hub contours found with t1.

Figure 6.6: All contours found for threshhold t1 and t2.

The extra contours that are not necessary are moved by only keeping the contour that encloses the largest area. The contour remaining, c1 and c2, can be seen in Figure 7.6c. In Figure 7.6d, the same contours can be seen but they are created with a different threshold, the threshold in that case is t1=160 and it is noted that it detects too much of the hub.

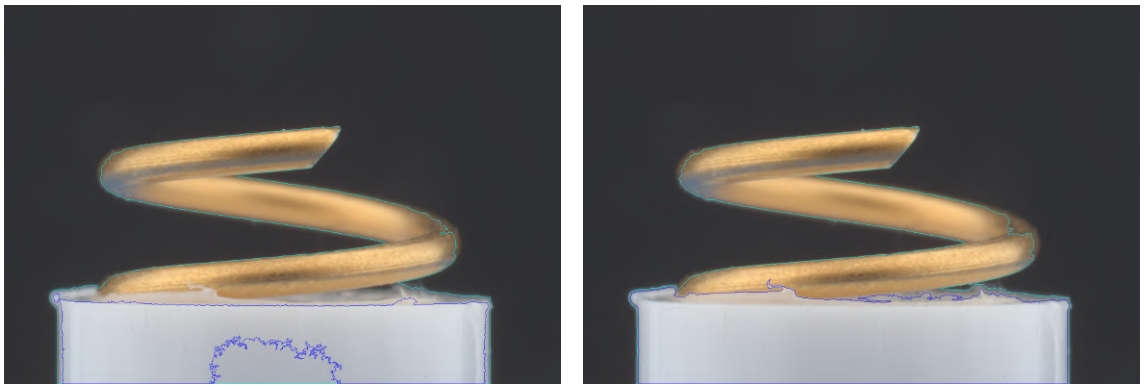

(a) Final contours with chosen thresholds, c1 is the blue contour and c2 the green contour. **(b)** Final contour with incorrect threshold, including too much in the hub edges.

Figure 6.7: The difference between contouring hub with a correct vs. incorrect threshold.

The testing of the system with different electrodes shows that if the external factors, camera settings, and lightning, are consistent, there is no need for different thresholds for different electrodes. The electrodes do not differ in color and therefore, the set threshold is appropriate for every electrode. However, in some unusual cases, the hub or spiral contains some dirt or dust that affects the contour creation and necessitates that the electrode is cleaned before doing a measurement. This case can be seen in Figure 6.8.

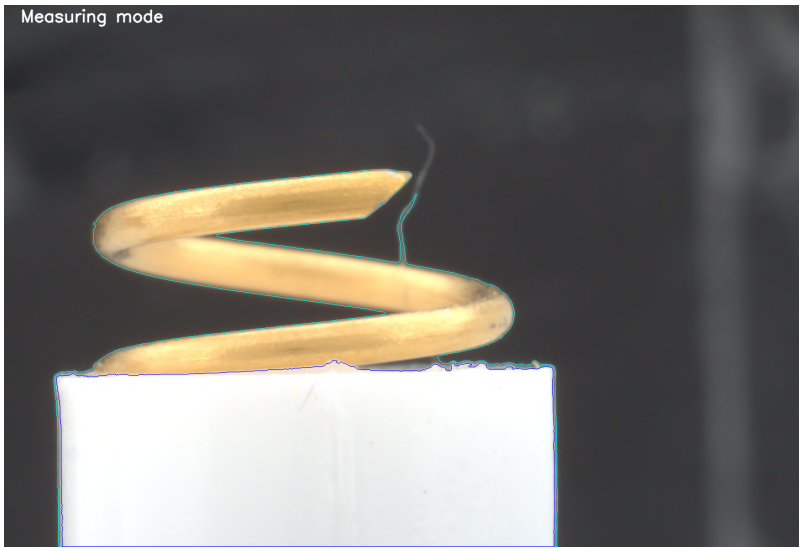

Figure 6.8: An electrode with a contour that also detects the dirt that is attached to the spiral.

6.1.1.2 Detect corner

The contour comprises a large number of points, and the neighboring points on the edge are also positioned consecutively in the array. The starting point of the contour is always positioned at various locations along the contour. In order to approximate the contours into a line, the contours must be trimmed at the corners of the hub. This process leaves three shorter contours that represent the left side of the hub, the right side of the hub, and the top line. To achieve this, the contours are rearranged to begin from the lower left corner of the hub and continue upwards along the hub line towards the upper left corner. The starting point is indicated in Figure 6.9. The rearranging of the contour is done by finding all the contour points with a y-value at the bottom of the image and then taking the point with the lowest x-value as a starting point and making sure that the next point has a y-value higher up in the image. The corners of the contours are detected by examining the derivative $\frac{dx}{dy}$ of the contour. The value of the derivative at the start of the contour is considered a reference value. It is then examined where on the contour the derivative differs. This is evaluated during the testing phase, by trying different values and comparing performances. The number of points is decided to be 60 points as illustrated in Figure 6.9. If there are more points in the reference interval, a risk is that the corner will be included in the interval and if there are fewer points in the interval, a risk is that a protruding piece of the hub will affect the measurement. Starting from the 60th point on the contour, every 20th point is analyzed to determine if there is a difference in the derivative. This involves examining the derivative of points 60-80, then 80-100, and so on. The distance of 20 points is set based on the performance during the development phase and the testing of different values. To be classified as a corner, the value of the derivative must differ by more than 0.5 compared to the reference value. In the case of a straight hub, a difference of 0.5 corresponds to an angular difference of 45°. The value 0.5 is also evaluated and tested during the

development phase to find the most promising.

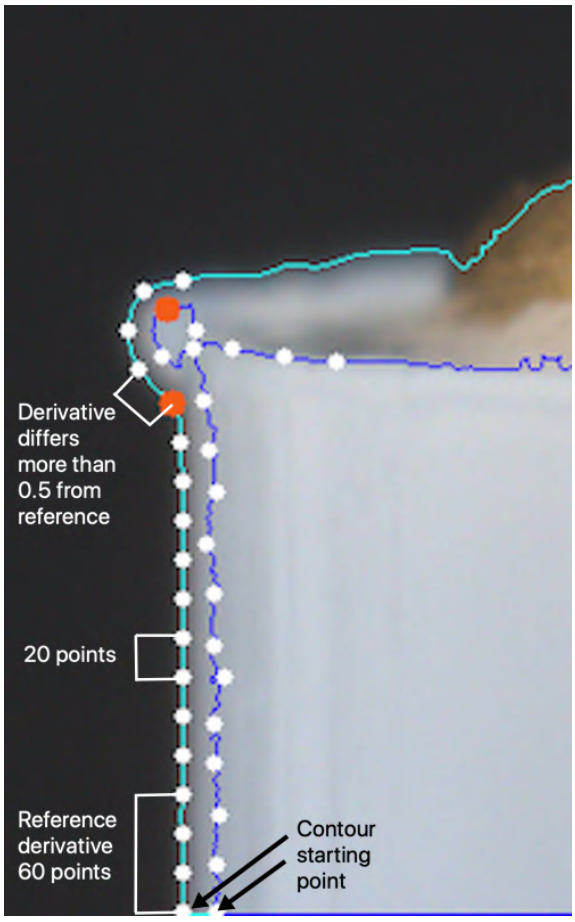

Figure 6.9: Zoomed-in image of the left hub side. The detected corners of the hub are marked with an orange marking. The white dots represent the points that are examined. The distance between the white markings is 20 points. At the bottom, the reference derivative is marked and the contour start is marked. The place where the derivative of the light blue contour starts to differ is also marked.

The light blue contour in Figure 6.9 is the contour surrounding the hub and the spiral. A difference in the derivative of this contour is only considered as a corner if there are at least three consecutive points out of five that exhibit the difference. If setting fewer than three out of five points as a rule, there is a possibility that a protruding piece of the hub might be falsely detected as a corner. On the other hand, if more than three out of five points are set, the contour may extend too far up on some spirals, causing the corner points to fall on the spiral itself. The spiral has a derivative similar to the reference and therefore the corner is detected wrongly in that case. The reason for not using three out of three points is that the hub occasionally extends slightly before flattening at the top, as illustrated in Figure 6.9. In such cases, if only three points were used, the corner would not be detected. It is important that the corner of the light blue contour must not be detected too late. That would mean that some of the top hub lines would be included when

doing the line approximation for the hub side-lines later. Therefore, the index of the corner point is multiplied by 0.8 to certain that the corner is not detected too late. In the dark blue contour, which surrounds only the hub, a corner will be recognized only when five consecutive points exhibit a derivative that deviates from the reference.This criterion is applied because since the hub is flat on top, there should always be five consecutive points that differ from the reference. As the hub contour forms the basis for the top line of the hub, it is preferable for its detection to be slightly delayed rather than occurring too early. Therefore the index of the corner point is multiplied by 1.2 to make certain that the corner is not detected too early. In Figure 6.10, the corner detection is seen for one electrode. To obtain the right corners of the hub the same method is used but the contours are rearranged to start in the lower right corner and go up along the right hub line instead.

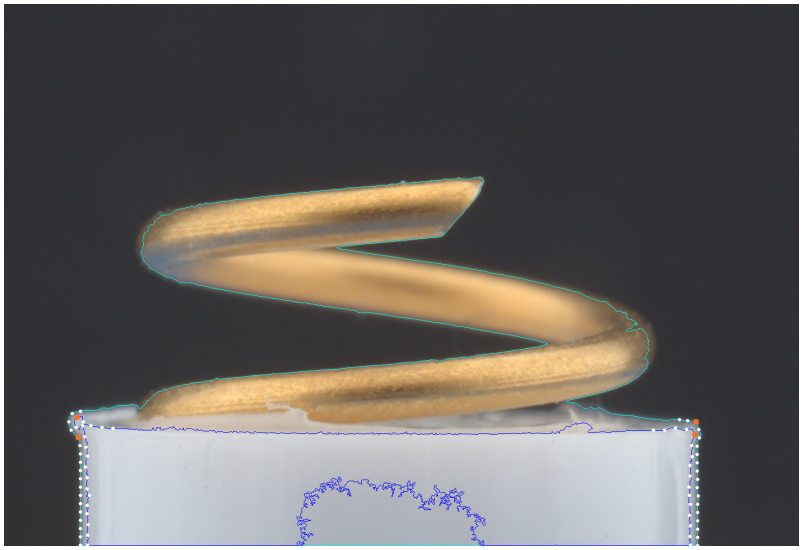

Figure 6.10: The detected corners of the hub are marked with an orange marking. The white dots represent the points that were examined. The interval for the examination of derivative is every 20th point.

6.1.1.3 Approximate hub lines

Lines are approximated from the cut contours by using the least square method described in Equation 2.9 and 2.10. All the lines are approximated over the entire image to make sure that the side lines intersect with the top line. This is done by using trigonometrical identities. The result of the approximation is illustrated in Figure 6.11. The least square method is chosen after evaluating and comparing with the performance of the Hough Transform that can be seen in Figure 6.12b.

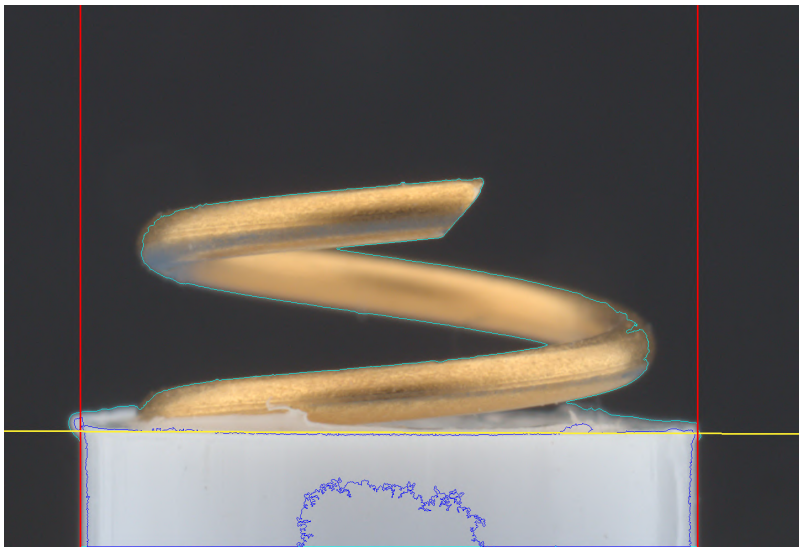

Figure 6.11: The approximated lines acquired by using least square method on the contours.

The implemented Hough transform method uses the built-in Hough line function in OpenCV. The function finds straight lines in the image and the lines found are presented in Figure 6.12b. The length of the lines is set to be shorter compared to the width and height of the hub. The reason for this is that it only finds lines where it already exists straight lines in the image. Since the hub lines are not completely straight, the method does not find them if set to long. The shorter lines are approximated to one top line and two side lines by firstly filter out those that are detected at other places, such as the spiral, and dividing the lines into top lines, left or right lines. Then they are extended over the image to find the coordinates where they cross the sides of the image. The median of the coordinates is taken to approximate three final lines. Since this method requires the presence of straight lines in the image to perform the detection, it does not perform very well if the hub has many irregularities. Therefore, the least square method is chosen as the final approach.

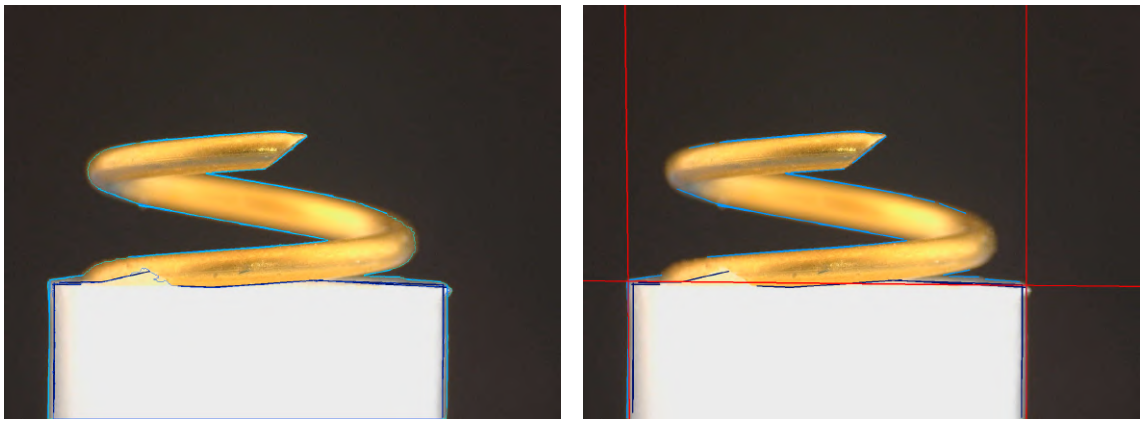

(a) Lines detected using Hough line transform. Blue lines represents lines from the hub contour c2 and light blue lines represents lines from the spiral and hub contour c1.

(b) The blue, short Hough transform lines together with the red, approximated hub lines.

Figure 6.12: Hub line approximation performed with Hough line transform

6.1.1.4 Improve the top line approximation and drawing of the hub

When using the least square method, the top line of the hub sometimes gets an angle that is incorrect due to irregularities in the hub. Therefore, an improvement of the line is done. This is done by comparing the contour of the hub and the approximated line. Everything in the contour that is positioned higher than the approximation is removed and replaced with the approximated line. The part of the top line closest to the side often contains more irregularities and because of this, the contour is cut 15 pixels from the sidelines. This means that those irregularities do not affect the final approximation. The line is thereafter approximated again by doing the least square method on the new contour that contains parts of the old contour and parts of the already approximated line. This line approximation has a better angle but is still sometimes placed too high from the hub line which is considered the optimal placing. Therefore the line is moved down to the lowest point of the contour. Even when moving the contour down, the contour is cut from the sides to not be affected by irregularities, this time with a value of 150 pixels. The determination of the extent to which the contour should be removed is based on evaluating the performance during the development and testing phase. Tests are conducted on hubs with the most significant irregularities, exploring various values to find the optimal solution. Figure 6.13a shows three different approximations, while Figure 6.13b shows the final hub detection.

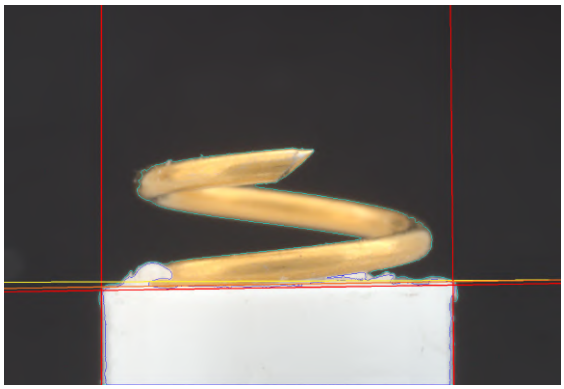

(a) Three different top lines, the yellow is the firstly approximated line as in Figure 6.11, the orange is the improved approximation and the red is the final approximation after moving the orange down to the lowest contour point.

(b) The finalized hub detection.

Figure 6.13: The hub detection using least square method and how it is improved.

6.1.2 Measuring height and angle

The measurement of the spiral tip angle α is calculated through Equation 2.11, from the slope of the two spiral tip lines described in section 6.1.2.2. The measurement of the spiral height h is calculated from the number of pixels between the highest point of the spiral and the hub top line. It is necessary to perform a calibration of the system to convert the height given in a number of pixels into a value given in mm. The two measurements are visualized in Figure 6.14.

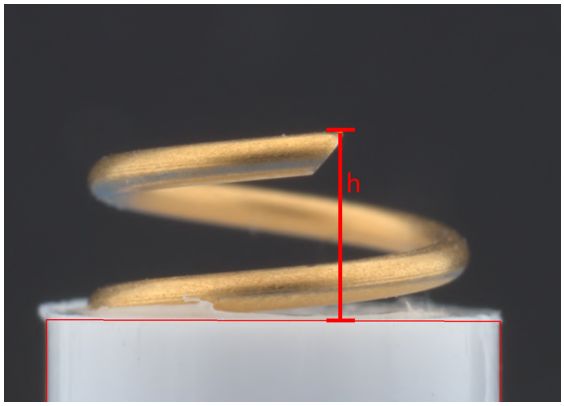

(a) Spiral height h measured from hub top line to spiral highest point.

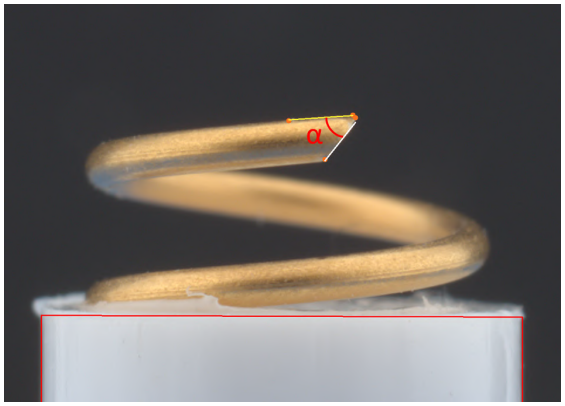

(b) Spiral tip angle α measured between the two tip lines.

Figure 6.14: Calculated spiral height h and angle α.

For both measurements, height and angle, it is important that the electrode is positioned correctly. This is to ensure that the height measurement is done in the

same positioning as where the calibration is performed, and the angle measurement is done when the tip is seen from a view that visualizes the tip angle in a correct way. The positioning intervals are defined as a percentage of the hub width and are measured from the left hub-side as visualized in Figure 6.15. The measurements are performed within the positioning intervals when the spiral's highest point is positioned between D1 and D2 %.

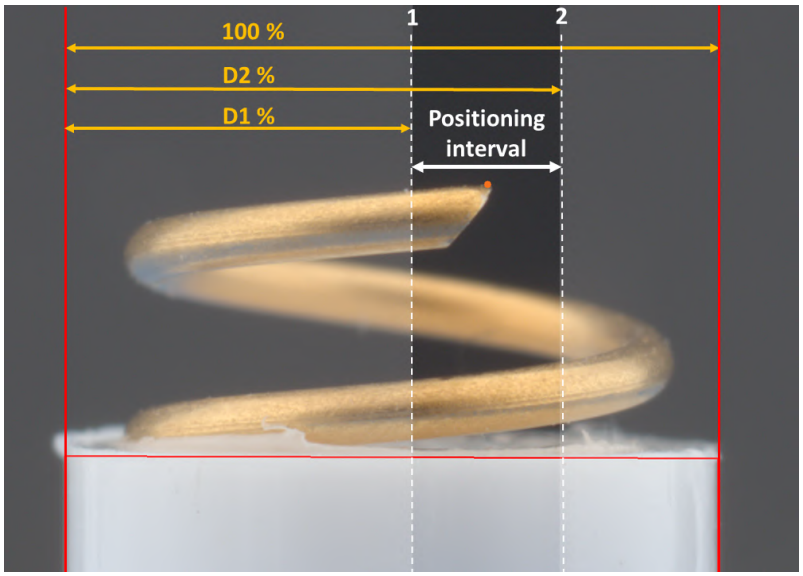

Figure 6.15: Positioning interval showing where the spiral highest point have to be placed to carry through the measuring.

The measuring functions of the software system are presented in Figure 6.16. The last step is that when a height or angle measurement has been done in the system it is added to a height or angle list that will contain all the measurements for the electrode currently being measured. All this stored measurement data that is retrieved from the system has to be analyzed and processed to get a final measurement. In this section, it is described how this is done and which processing method that works best for this system.

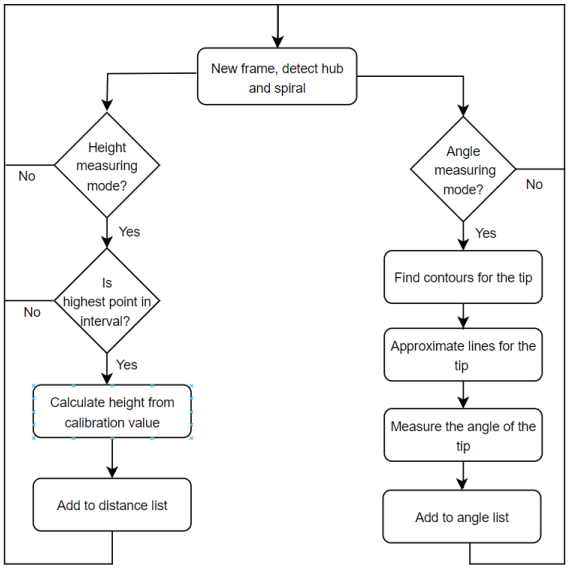

Figure 6.16: Flowchart of the height and angle measuring mode.

6.1.2.1 Height measuring

The height measuring is based on a measurement from the highest point of the spiral to the hub line. Therefore, when the height is to be measured, the highest point of the spiral is found first. After that, the distance is calculated in pixels and then converted into mm, with the help of a calibration. For the height measurement to be possible, the highest point needs to be placed at a certain position and several measurements have to be taken to get a measurement as precise and accurate as possible. These steps are further explained in the following sections.

Finding highest point

The highest point of the FSE spiral needle, i.e. the point furthest away from the hub has to be located in order to determine the height of the spiral, see the point marked in orange in Figure 6.17a. During the examination of the electrode variations it can be stated that approximately one-third of the electrodes have a slight deformation furthest up on the spiral, close to the tip point, which results in the highest point being located a bit to the left of the actual tip point in many of the electrodes, see Figure 6.17b.

The highest point of the spiral is found by iterating through each contour point of the spiral and calculating each point's shortest perpendicular distance to the hub top line. The hub top-line is transformed into the linear line Equation 2.7, and used for calculating the distance through Equation 2.8, which gives the minimum distance between a line and a point. After the distance for each point has been calculated, the point with the largest distance is selected as the highest point.

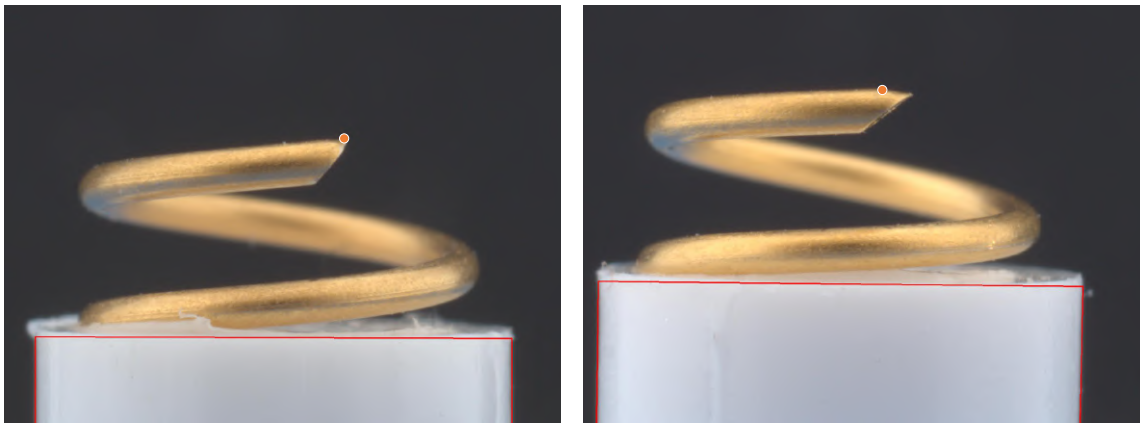

(a) Location of the highest point marked on a normal electrode.

(b) Location of the highest point marked on a flattened electrode.

Figure 6.17: Location of the spiral highest point marked as an orange circle on a normal and a flattened electrode.

Calibration

A calibration mode is created for the system to enable calibration of the system and thereby a conversion of the distance in pixels to mm. The calibration is performed by placing a calibration ruler under the camera lens at the same height as the electrode would be placed, shown from the camera perspective in Figure 6.18a. The user performs the calibration by entering the calibration mode and placing two markings 8 mm apart on the picture appearing when running the system. The distance between the two markings is regarded as a fixed distance of 8 mm and the number of pixels between the markings is calculated by Pythagoras theorem. Therefore the known distance in mm can be divided by the number of pixels to get the size of one single pixel. The reason for not having a smaller distance is that an error of one pixel when placing the markings would cause a larger pixel size error.

Helplines appear after placing the first marker in order to support the user to get the correct placement of the second marker, visualized in Figure 6.18b. These helplines consist of one line appearing between the first marker and the location of the computer's mouse pointer, and the second line perpendicular to the first line, crossing the current mouse position.

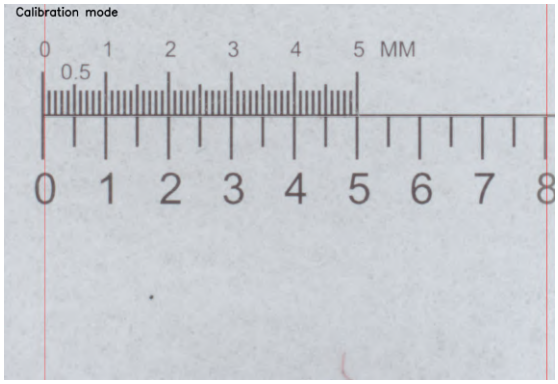

(a) Calibration ruler placed under the camera, calibration mode entered and first marker already placed and helplines are visible.

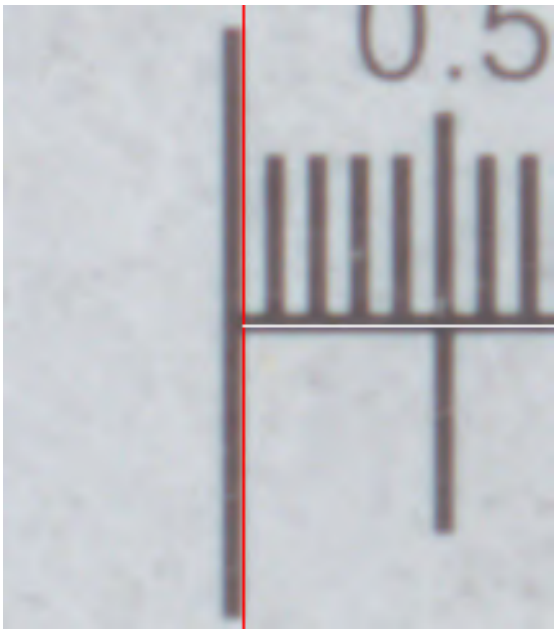

(b) Magnification on the help lines aligning with ruler.

Figure 6.18: Calibration mode, lines appearing for the placement of the second marker.

Height positioning interval

The purpose of using a positioning interval and collecting all the values within it, rather than only collecting one height value at one precise position, is that the height measuring process becomes easier to perform by the user when the electrode does not have to be positioned with high accuracy. Instead, the user can slowly rotate the electrode across the positioning interval. An interval can also work as a way to retrieve measurements in different positions, thus increasing the chance that a measurement that has been affected by an irregularity will not have as significant impact on the final result when several measurements are taken into account. Because increasing the number of measurements can minimize the impact of random errors caused by an unpredictable change [14].

As shown in Figure 6.15, it is checked whether the spiral's highest point is within the positioning interval by measuring the shortest distance from the approximated left hub-line to the highest point of the spiral, i.e. the spiral top, trough Equation 2.8. The middle point of the hub width, 50%, is set as the benchmark for the height positioning interval since the calibration is performed at this height, and it is therefore considered the most accurate place to perform the measurements.

Ten electrodes are examined and the spiral height is determined for different positions of the highest point for each of the electrodes. This is done by letting an

electrode rotate and measuring the height together with the position for each frame. From this result, it is possible to determine a positioning range x mm, equal to a percent unit from the middle point where the height measurement seems to not be affected by the rotation. See a visualization of the spiral top positioned at the hub width middle, r2, minus the positioning range x in Figure 6.19.

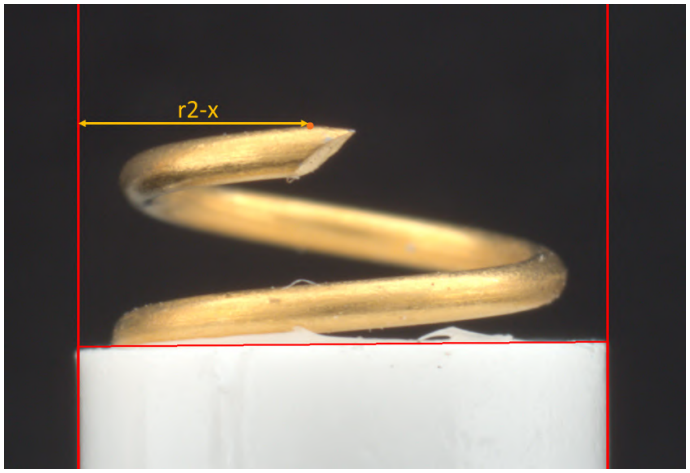

Figure 6.19: The relative distance between the hub sideline and the highest point of the spiral, the top point.

From these 10 tested electrodes, it can be concluded that a height positioning interval can be set to 45-55% of the hub width, i.e. a=5%. From the 10 tests, none of the measurements in the positioning interval 45-55% differs more than the maximum 0.01 mm in height from the reference value that is collected when the highest point is positioned in the middle, at 50%. Three out of 10 electrodes show that there can be a difference of more than 0.02 mm when using a wider measuring range of 40-60% which leads to the conclusion that this would be a too large positioning interval. It varied how many frames that were captured per test on each electrode since this depend on how fast the electrode is rotated, but the minimum amount of frames within the range of 45-55% was 10. Thereby also the minimal number of measurements in the interval 45-55% is also 10. In Table 6.1 it is presented how many of the measurements for each electrode that differed up to 0.01 mm from the reference measurement and also how many measurements that differ 0.00 mm from the reference value. It is a clear majority of the measurements for each electrode differ 0.00 mm, that is, less than 0.005 mm from the reference. This implies that the positioning interval of 45-55% is the correct choice.

Table 6.1: Variation of measurements within the chosen range of 45-55% for 10 separate electrodes E1-E10, where each frame that is captured results in a measurement. The variation is based on a comparison with the height measuring at 50 %.

	Measurements within range 45-55%	**Measurements differing 0.01 from reference**		**Measurements differing 0.00 from reference**	
	Total quantity	**Quantity**	**%**	**Quantity**	**%**
E1	15	1	7	14	93
E2	13	2	15	11	85
E3	11	0	0	11	100
E4	24	0	0	24	100
E5	29	2	7	27	93
E6	14	4	29	10	71
E7	14	3	21	11	79
E8	35	0	0	35	100
E9	27	10	37	17	63
E10	28	2	7	26	93

Height data management

A height measurement is conducted for each frame where the highest point is located in the decided positioning interval, 45-55%, and this height is stored in a height list. All data in this list then has to be processed in order to give one final height measurement for the tested electrode. Taking all the data into consideration can make the system's final result less affected by small variations and errors that could have occurred on some of the frames of the tested electrode.

The electrode variations impact the detection differently depending on very small changes in how the electrode is rotated. To ensure that not only one placement is measured, a programming requirement is implemented, mandating that measurements must be taken when the highest point is detected at both ends of the interval, the interval b in Figure 6.20. This approach minimizes the potential impact of small electrode variations on the measurements.

The size of the end interval b is determined by testing to find an interval large enough to make it relatively easy to meet the requirements when performing the tests. Accordingly, a positioning interval a=5% has been decided and an end interval b=2% is decided, and thereby the measurement has to be done in the range (50-a) to (50-a+b) %, specifically 45-47% and also in the range (50+a-b) to (50+a) %, specifically 53-55%, see Figure 6.20.

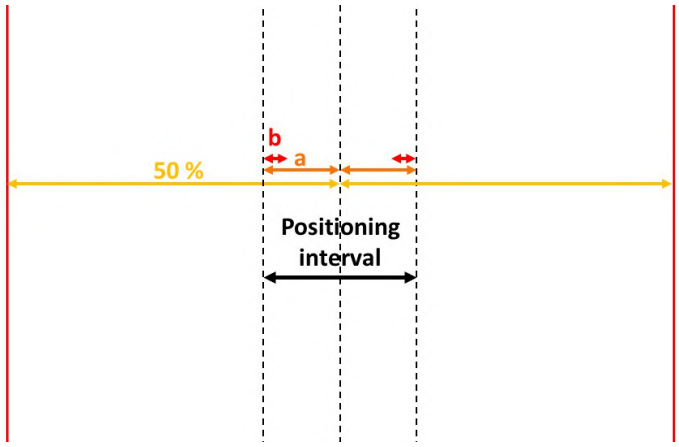

Figure 6.20: The measuring intervals a and b calculated from the hub sidelines.

There also has to be a minimum amount of captured frames where the height measurements have been successfully carried through. Additionally, the best way to determine a final height result from the height calculation of each frame has to be concluded. Both of these decisions are made by testing how large variation that is found between the final height results when measuring the same electrode 10 times. This is performed with a minimum amount of 10 captured frames, and then with a minimum amount of 20 captured frames, and these two alternatives are tested in combination with calculating the final height by taking the mean or median value of all the 10/20 measurements. Table 6.2 indicates that having a minimum of 20 frames is slightly better than having 10 frames per test. After testing both alternatives, it can be concluded that the user experience and the simplicity of performing the test are not affected significantly by the higher requirement of 20 frames. Thus a minimum of 20 frames per height measurement is determined.

Table 6.2: The difference between the maximum and the minimum measured height using four different methods for each electrode E1-E3. The methods are mean of 10 and 20 measured frames and median of 10 and 20 measured frames. The green cells show if it is better to use 10 or 20 frames.

	Mean of 10 (mm)	**Mean of 20 (mm)**	**Median of 10 (mm)**	**Median of 20 (mm)**
E1	0.0418	0.0072	0.0045	0.0200
E2	0.0042	0.0062	0.0474	0.0392
E3	0.0238	0.0037	0.0212	0.0044
Mean	0.0233	0.0057	0.0244	0.0212

After 20 measurements have been determined, the mean method vs median method is examined more thoroughly through a more extensive test performed by two separate users doing tests on 10 additional electrodes, measuring each electrode 10 times per method. The variation for both methods is determined by storing the 10 calculated final heights of the same electrode in a list, and the difference between

the largest and the smallest final height result for each electrode is then determined by extracting the smallest and largest height stored in the list. Table 6.3 displays the variation for each electrode for both methods and both users and furthermore, the mean value for all 10 electrodes of how much difference is obtained for the two separate methods and for the two users. From this result, it is concluded that the mean is the best method to calculate the final height measurement since the result shows that the mean gives a distinctly lower difference for both users.

Table 6.3: The difference between the maximum and the minimum measured height for each electrode and each method for two separate users. The deviation is based on 10 tests on each electrode. The green cells mark if the mean or median method is the best.

	Mean of 20, User A (mm)	**Median of 20, User A (mm)**	**Mean of 20, User B (mm)**	**Median of 20, User B (mm)**
E1	0.0072	0.0200	0.0069	0.0079
E2	0.0062	0.0392	0.0059	0.0183
E3	0.0037	0.0044	0.0033	0.0131
E4	0.0040	0.0045	0.0021	0.0078
E5	0.0055	0.0046	0.0045	0.0168
E6	0.0044	0.0048	0.0046	0.0044
E7	0.0068	0.0073	0.0041	0.0026
E8	0.0074	0.0099	0.0059	0.0075
E9	0.0044	0.0028	0.0033	0.0039
E10	0.0238	0.0328	0.0092	0.0082
Mean	0.0073	0.0130	0.0050	0.0091

6.1.2.2 Angle measuring

The angle measurement relies on two lines that enclose the electrode tip, and the angle is calculated using the slopes of these lines according to Equation 2.11. In addition to accurately measuring the angle, it is crucial to identify the precise placement of the spiral's tip point and determine the optimal number of frames to base the measurement on. These aspects are discussed in detail in the following sections, aiming to enhance the system's effectiveness and efficiency.

Finding the tip

Two approximated lines are needed to perform an angle measurement of the spiral tip. These lines have to distinguish and outline the edges around the FSE spiral tip. To approximate the two lines, it is necessary to identify four points that are determined in accordance with Neoventa, as shown in Figure 6.21a. These points serve as reference points for estimating the angle between the lines. The locating of the four points is performed by examining only the contour surrounding the highest point and therefore the contour is cut where the x-axis value is 150 lower than the x-axis value for the highest point of the spiral, see Figure 6.21b. This value is reached by evaluating multiple electrodes and observing that the contour is consistently cut to exclude unnecessary data, but still ensures that the four points are always included with good margins.

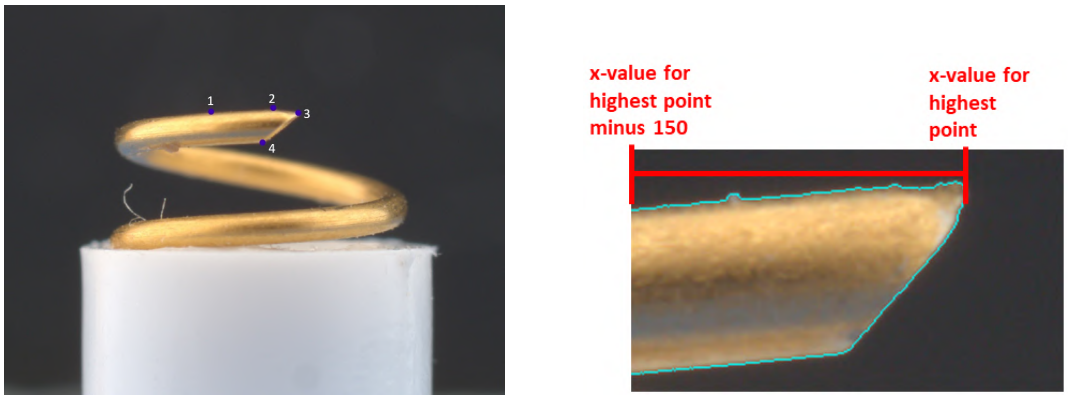

(a) The necessary points for angle measurement: 1-4.

(b) Isolated part of contour used to find point 1, 3 and 4.

Figure 6.21: The points and the contour that are necessary for approximating the angle measuring lines.

Point number 2 is defined as the highest point detection. Point number 1 is defined as the contour point located at the x-axis value of the highest point minus 150 pixels in the x-axis. The location of point number 1 is set to ensure that many contour points are included in the line approximation but at the same time, the spiral rotation is not yet distinguishable, and therefore a linear line can be created. Point number 3 is found by extracting the contour point with the highest X-axis value as this is considered to always be the tip point. Point number 4 is located by using the same method as when locating the corners of the hub, see Section 6.1.1.2. It is found by comparing the change of the derivative between the contour points of each 15th contour point. The results of finding the four points for one normal electrode and for one flattened electrode are visualized in Figure 6.22.

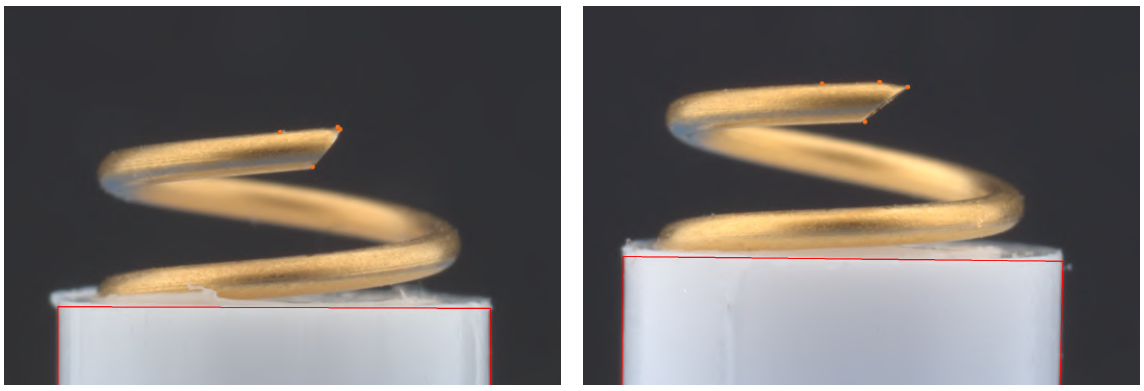

(a) Tip points on a normal electrode.

(b) Tip points on a flattened electrode.

Figure 6.22: Figure illustrating the tip lines necessary for the angle measurement for a normal electrode and a flattened one.

After finding the four points, two arrays with points from the spiral contour array are extracted. One contains the points between point 1 and 2, and one contains

the points between point 3 and 4. The least square method, Equation 2.9 and 2.10, is applied on these two intervals to approximate two lines that outline the spiral tip. The results of approximating the two lines for one normal electrode and for one flattened electrode are visualized in Figure 6.23.

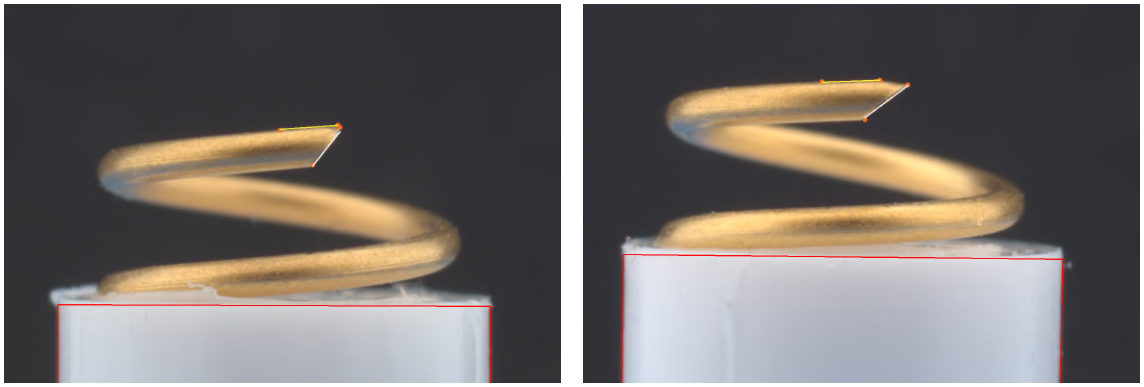

(a) Tip lines for a normal electrode. **(b)** Tip lines for a flattened electrode.

Figure 6.23: Figure illustrating the approximated tip lines for the angle measurement for a normal electrode and a flattened one.

Angle positioning interval

The determination of the positioning interval for angle measurement involves a thorough evaluation process. This evaluation aims to determine if it is possible to establish a specific positioning interval that can yield accurate measurements with a defined level of uncertainty for the system. The investigation focuses on evaluating measurement accuracies of 0.5°, 1°, and 1.5°. To conduct this evaluation, the position placements are collected as a percentage relative to the hub width for each frame during the rotation of one electrode. For the same frame, the angle measurement is also collected. This study is conducted using ten different electrodes. Subsequent investigation revealed a direct correlation between electrode misplacement and an increase in the observed angle, as illustrated in Figure 6.24.

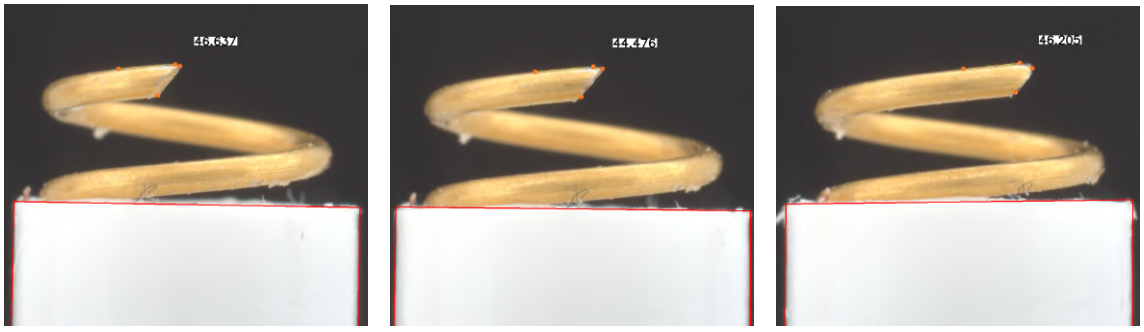

(a) The spiral tip is rotated too far to the left. **(b)** The spiral tip is rotated correctly. **(c)** The spiral tip is rotated too far to the right.

Figure 6.24: Angle measurement for electrodes placed in different positions.

Considering this relation, the minimum angle measured is considered the correct angle. The positioning interval is then examined when the measurements are 0.5°, 1°, and 1.5° larger than the correct angle value. This information is presented in Table 6.4.

Table 6.4: The positioning intervals for each tested electrode with the accuracy 0.5°, 1° and 1.5°.

	Positioning interval for 0.5° accuracy (%)	**Positioning interval for 1° accuracy (%)**	**Positioning interval for 1.5° accuracy (%)**
E1	64-64	62-64	61-68
E2	57-58	54-59	54-60
E3	60-63	57-65	54-65
E4	54-55	54-57	51-58
E5	56-59	56-61	55-61
E6	59-59	56-61	56-62
E7	53-60	52-60	47-62
E8	64-65	64-66	64-66
E9	63-64	63-66	62-67
E10	59-61	57-61	56-64

As can be seen in Table 6.4, the smallest position interval differs much, from electrode E4 with an interval of 54-55% up to electrode E8 with an interval of 64-65%. Based on the given information, Electrode E4 has a range of 51-58% when the accuracy is set at 1.5°, while electrode E8 has a range of 64-66% at the same accuracy level. This implies that if the positioning interval does not include angles that are more than 1.5° off from the correct value, it would not encompass the correct value for either electrode. In other words, in order to capture the correct angle within the positioning interval, it is necessary to include angles that deviate by more than 1.5° from the correct value. These patterns can be seen on several of the electrodes, electrodes E2, E4, and E5 need a positioning interval that is under 61% to achieve less than 1.5° accuracy. However, electrodes E1, E8, and E9 need a percent range that is over 61% to achieve less than 1.5° accuracy.

Given that the observations are derived from only 10 electrodes, it is indeed plausible to expect even greater variations in a larger batch. The irregularities in the cutting of electrode tips have a significant impact on angle measurements. As a result, it becomes challenging to establish a consistent positioning interval that guarantees accurate angle measurements for all electrodes. Given that the observations are derived from only 10 electrodes, it is indeed plausible to expect even greater variations in a larger batch. Consequently, the system is designed to rely on the user's judgment to determine what they consider to be an optimal electrode position for angle measurement.

Angle data management

The number of frames used to measure the angle and the processing method for obtaining a final measurement are both determined through evaluation. However,

since the electrode is placed by the user in a fixed position without rotation over an interval, it becomes more challenging to identify the frames that are correctly positioned and capable of providing accurate data. This study aims to explore the differences in evaluation when using five frames compared to ten frames. Additionally, it investigates two distinct approaches for processing the measurements: using the mean or the median. It is important to note that the accuracy of the measurements is dependent on the correct placement of the electrode, which may lead to variations in the most suitable method of data management among different users. Considering, the evaluation in this study was conducted by four different users, namely User A, User B, User C, and User D. It is done by having the users do the angle measurement 10 times on five different electrodes. The measurements are processed as previously described: mean of the last five frames, mean of the last 10 frames, median of the last five frames, and median of the last ten frames. The largest difference in the angle measurement for each user and electrode using each method is analyzed in the evaluation. This can be visualized in Table 6.5. The mean deviations for all the users are also presented.

Table 6.5: Table showing the deviations of 10 measurements from tests on five different electrodes made by four different users. The green cells mark which method is the best for each user and electrode.

Electrode 1	User A	User B	User C	User D	Mean deviation
Deviation mean 5 (°)	3.792	0.994	1.209	0.517	1.628
Deviation mean 10 (°)	3.585	0.711	1.093	0.380	1.442
Deviation median 5 (°)	3.874	0.866	1.291	0.567	1.650
Deviation median 10 (°)	3.480	0.827	1.431	0.513	1.563
Electrode 2	User A	User B	User C	User D	Mean deviation
Deviation mean 5 (°)	2.646	1.448	2.734	1.553	2.095
Deviation mean 10 (°)	2.446	1.053	2.296	1.274	1.767
Deviation median 5 (°)	2.632	1.335	2.775	1.993	2.184
Deviation median 10 (°)	2.213	1.191	2.465	1.264	1.783
Electrode 3	User A	User B	User C	User D	Mean deviation
Deviation mean 5 (°)	2.058	0.848	1.575	1.807	1.572
Deviation mean 10 (°)	2.144	0.909	1.346	1.892	1.573
Deviation median 5 (°)	2.235	1.398	1.700	1.955	1.822
Deviation median 10 (°)	2.168	1.270	1.386	2.125	1.737
Electrode 4	User A	User B	User C	User D	Mean deviation
Deviation mean 5 (°)	1.750	1.125	0.622	0.969	1.116
Deviation mean 10 (°)	1.688	1.443	0.911	0.963	1.251
Deviation median 5 (°)	1.839	1.550	0.775	0.988	1.288
Deviation median 10 (°)	1.694	1.463	0.652	0.988	1.199
Electrode 5	User A	User B	User C	User D	Mean deviation
Deviation mean 5 (°)	1.393	2.702	0.882	2.357	1.834
Deviation mean 10 (°)	1.348	2.063	0.964	2.398	1.693
Deviation median 5 (°)	1.550	2.840	1.164	2.373	1.982
Deviation median 10 (°)	1.201	2.155	1.153	2.474	1.746

Table 6.5 reveals that different data-gathering methods yield varying results for different users and electrodes. Specifically, it is observed that Person A consistently exhibits lower variations when utilizing the median of 10 frames. This discrepancy may be attributed to the fact that during the tests it was observed that Person A tended to have a shorter waiting time when the spiral was in position compared to the other users. Consequently, some of the last 10 frames could potentially capture incorrect positions and thereby measure incorrect angles. In this scenario, employing the median method would effectively eliminate such outliers compared to using the mean method. Conversely, for Person B and Person C, the mean of 10 frames proves to be the optimal approach, as three measurements yield the best values using the mean of 10 frames. User D demonstrates that the mean approach

is the most effective, but not specifically the mean of five or mean of 10 frames. By calculating the mean deviation for the four users in the right column, it becomes evident that the mean of 10 frames method yields the best results in three out of five electrode cases, while the mean of five frames method is optimal in two out of five electrode cases. As a result, it is recommended to utilize the mean of the last 10 measured frames for each electrode. However, it is crucial to inform the user to hold the electrode steady for a brief period before storing the value. This precaution ensures that no measurements are taken when the spiral is in the wrong position, thereby improving the accuracy of the data.

6.2 Fixture development

In the subsequent sections, the development of the resulting fixture is presented. Initially, a preliminary fixture is created and subsequently refined to produce the final fixture, culminating in the final design. Additionally, the selection of the camera is discussed in this section.

6.2.1 Fixture

The first fixture, see Figure C.27, consists of an adjustable camera stand and a foam cube to hold the electrode in place. A cardboard box is placed over the spiral to remove external lightning. Instead LED lists are attached to the cardboard walls to control the lighting in the box. To control the lightning even further, the LED list is connected to a dimmer, and diffusion filters are placed in the box, surrounding the spiral. To ensure proper positioning of the electrode under the camera, a stop is created by cutting a guide tube to a specific length. The test electrode is inserted into the shortened guide tube, with its drive tube mounted. The guide tube comes to a halt upon insertion as it does not fit into the hole in the foam, which is designed to match the size of only the drive tube and hub. Finally, the drive tube grip is stopped at the end of the guide tube, effectively placing the electrode in the desired position for camera observation.

This preliminary fixture works well for testing the system and testing different parameters to find the optimal conditions, but it is lacking in robustness and is sensitive to disturbances and movements.

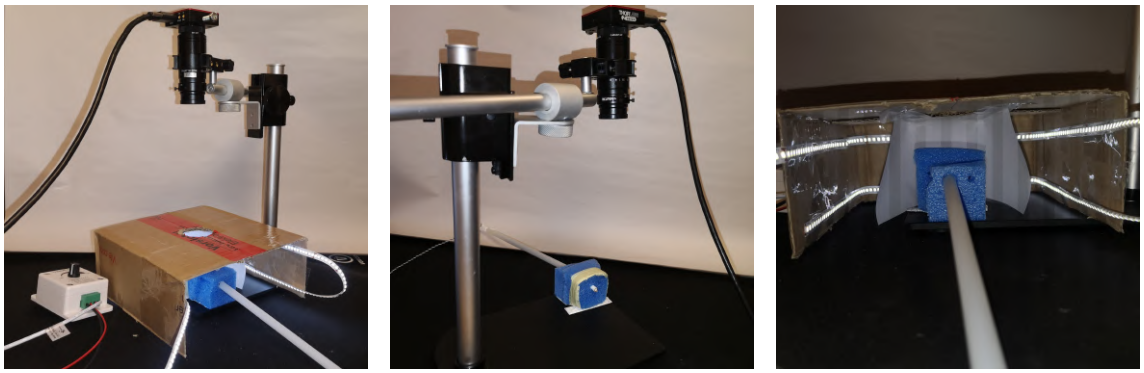

(a) The complete preliminary fixture.

(b) The preliminary fixture without the controlled lightning.

(c) The box and LED list in the preliminary fixture.

Figure 6.25: Figures showing different parts of the preliminary fixture.

A final fixture can be seen in Figure 6.26. It provides the system with fixity to ensure that the software will have the same conditions each time a measurement is done. Hence this fixture has a fixated distance between the electrode placement and the camera sensor, as well as it is being constructed in more durable materials such as metal as can be seen in Figure 6.26c. The camera is fastened with screws into the fixture so that it cannot move and not be affected by external factors. The box in the final fixture is made out of a black plastic box as seen in Figure 6.26a. Therefore, a white surface is placed inside the box so that the box will not devour light, this can be seen in Figure 6.26f. In the same figure, it can also be seen how the diffusion filters are added, which purpose is to diffuse the light. Compared to the first box there is an additional lightning LED in the box and one additional LED list is placed on the bottom in front of the electrode that is not included in the first fixture. The stand is inserted into the box by sliding the aluminum plate into the box until it stops. It is seen in Figure 6.26b how the plate is inserted.

In order to make the insertion of the electrode as easy as possible and ensure that the electrode stops in the camera's field of view, a stop is added. It is not the same stop as originally thought in Figure 5.1. Instead, a shortened guide tube is cut in the right length and is fastened in the fixture in the same way as in the preliminary fixture. This means that the drive tube grip on the electrode will act as a stop and prevent the electrode from being inserted too far. The reason for using an external stop instead of relying on a physical obstruction within the box to halt the insertion of the electrode, is to eliminate any factors that could potentially disrupt the camera image and thereby the detection process. Additionally, the usage of an external stop lowers the risk off affecting the integrity of the electrode through for instance compression, or something sharp damages the hub or spiral.

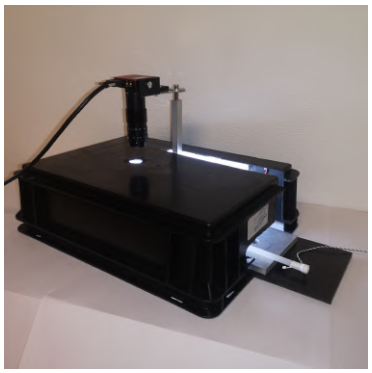

(a) An overlook of the final fixture.

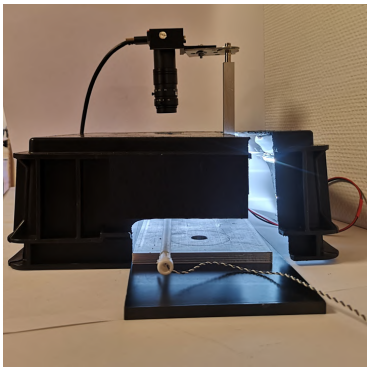

(b) Final fixture showing how the camera stand and fixture is sliding into the box.

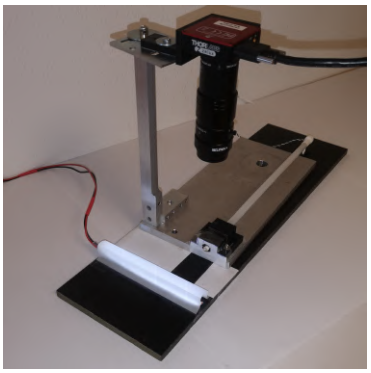

(c) Final fixture showing how the camera is attached to the fixture.

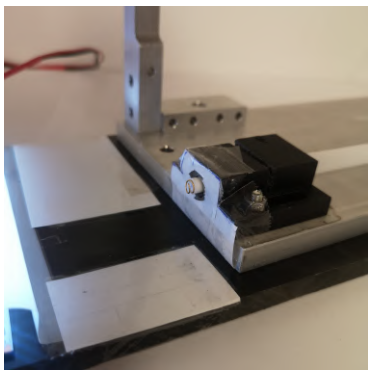

(d) Close-up picture of a correctly placed electrode in the fixture.

(e) The final lightning box showing how the LED stripes are placed.

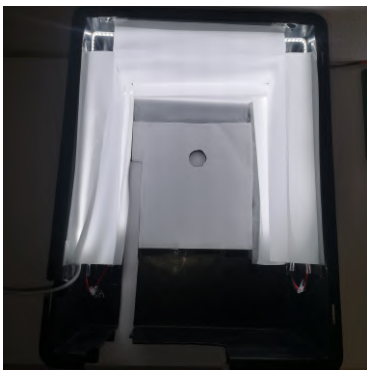

(f) The final lightning box with diffusion filter covering the light.

Figure 6.26: Figures showing different parts of the final fixture.

6.2.2 Camera selection

The software developed with the Dino-Lite camera that focuses on the detection of the spiral and hub shows that the Dino-Lite camera works well when the electrode is still and placed correctly in front of the camera. It is beneficial that the camera can adjust its focus and zoom in and out on the electrode to find the right FOV. That also means that the camera's settings can be adjusted to the final, more fixed fixture. However, since the Dino-Lite has a rolling shutter instead of a global it does not detect the electrode in motion as well as wanted if the measuring should be done in motion. It is also hard to place the electrode in the correct position since the image gets blurry when the electrode moves. The Dino-Lite is not possible to control from Python to the extent that is wanted. The focus is often changed when the program is opened and some frames are much darker than the others. Thorlabs camera *Zelux 1.6 MP CMOS Compact Scientific Camera CS165CU1(/M)* fulfills many of the requirements. A suitable lens for the camera is the Thorlabs lens MVL50M23 in regards to FOV and focal distance. The specifications of the Zelux

camera with the lens can be seen in table 6.6 together with the specifications of the Dino-Lite camera.

Table 6.6: Specifications for the two cameras.

Component	Dino Lite	Zelux
Resolution	1.3 Megapixel (1280x1024)	1.6 Megapixel (1440 x 1080)
Monochrome or color camera	Monochrome	Monochrome
Maximum frame rate at highest resolution (FPS)	15	34.8
Sensor Shutter Type	Rolling Shutter	Global Shutter
Programming Interfaces Provide for Python	No	Yes
Field of view (mm)	(39x31)mm-(2.2x2.8) mm	14x18 mm
Aperture	Not stated	f/2.8-f/22

As can be seen, the Zelux camera performs better or the same as the Dino-Lite camera in every aspect except the possibility to adjust the FOV. The FOV can however be adjusted by adding an extra distance between the camera and the lens [37]. The Zelux camera also has an adjustable aperture which is desirable when using a threshold technique that is dependent on the brightness of the image. The necessary distance for the tube is decided by adding different cylinders between the lens and camera and deciding when the FOV is the wanted field. The extension needed is 25 mm, which gives the desired FOV. The final camera used in the final system is therefore the *Zelux 1.6 MP CMOS Compact Scientific Camera CS165CU1(/M)* with a 50 mm focal lens, MVL50M23, and a 25 mm extension tube.

6.3 Final design

The final system consists of one fixture and one software. The fixture provides a holder for the electrode, a box with lightning, and a camera stand. The software measures the needle spiral height and the angle of the spiral tip and stores the measurements. When doing a measurement the user has to insert the electrode with the drive tube into a guide tube that is fastened in the fixture. The software answers to the user's keyboard command. A press on the m-key means that the system should measure, a press on c means calibration and r means remeasuring the last electrode, and these commands are described in the graphical user interface illustrated in Figure 6.27.

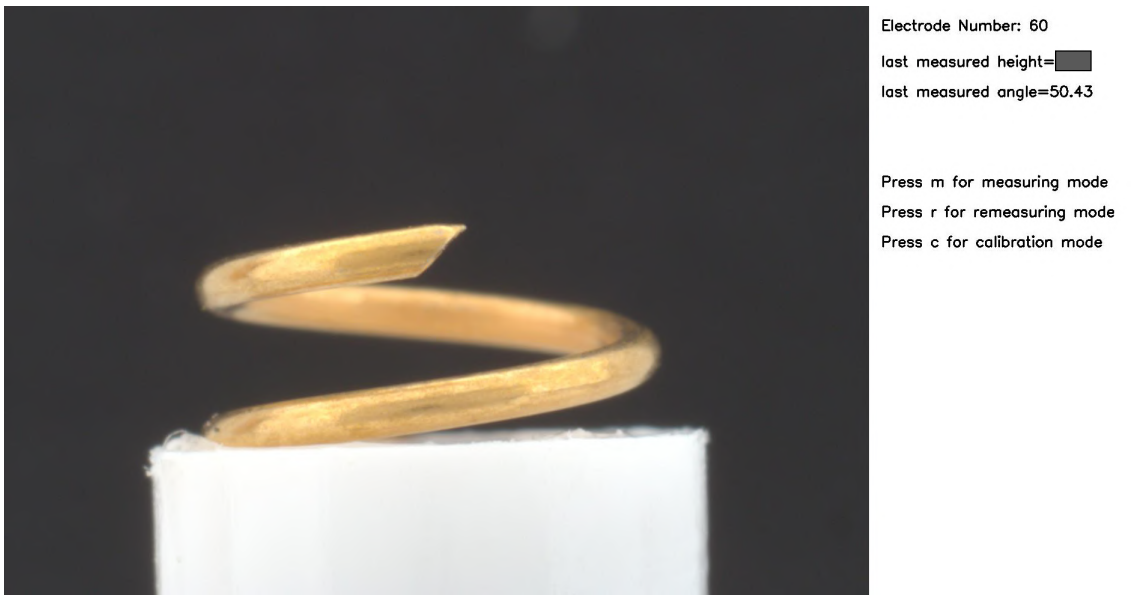

Figure 6.27: User interface when launching the system. Presenting which keyboard commands that are available, and also presenting the previously measured angle- and height values.

During the electrode measurement process, the height is initially measured. To ensure accurate positioning, the electrode is rotated over the middle of the screen, aligning it between two helplines that indicate the desired position interval. When the top of the electrode is placed within interval b, as shown in Figure 6.20, the helplines transition from red to green. Figure 6.28 illustrates when an electrode is rotated over the left b-interval.

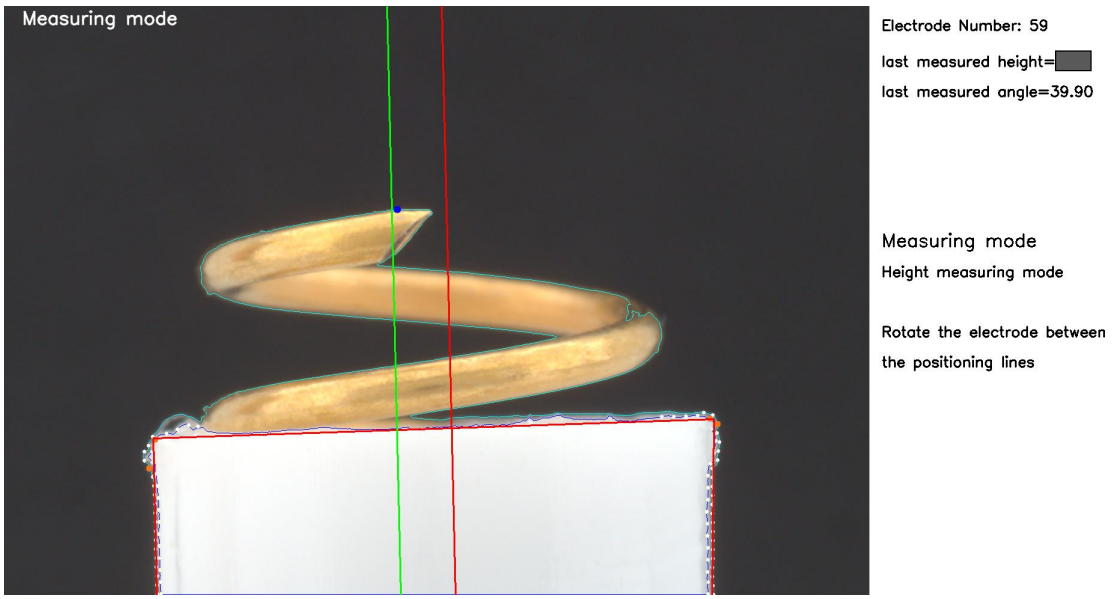

Figure 6.28: User interface when the system has entered height measuring mode. Helplines showing the positioning interval for where the user should rotate the spiral tip to measure.

Once the height measurement is complete, it is in angle measuring mode and the electrode needs to be positioned in an angle measuring position, as indicated by the interface in Figure 6.29. The user is prompted to press the enter key when the electrode is correctly positioned, and then they must hold the electrode still until the measurement process is complete, as indicated on the screen. The measurements obtained are saved in an Excel file, allowing the user to extract the data as needed.

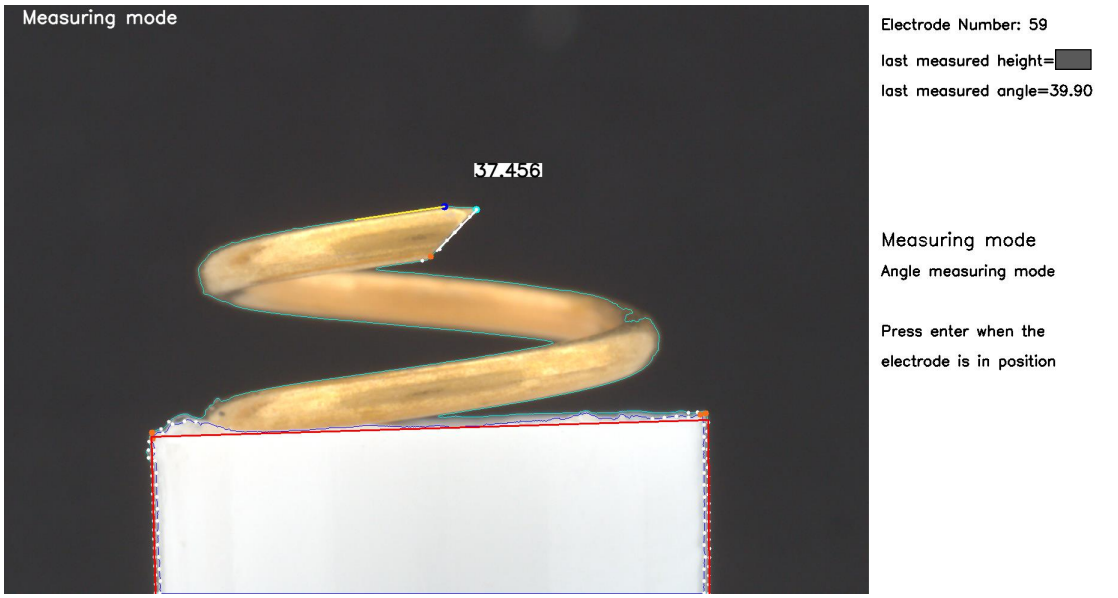

Figure 6.29: User interface when the system has entered angle measuring mode.

7

Evaluation of the system

The result of the evaluation is presented in this chapter. It is divided into a precision- and accuracy evaluation and a time efficiency evaluation, comparing with the current solution. The precision and accuracy performance is evaluated for both the angle measurement and the height measurement. Finally, the performance is compared with the preferable system requirements.

7.1 Effectiveness performance

During the testing phase involving all 140 available electrodes, the system successfully detects the angle lines of each electrode in the correct position. This indicates that the lines on the tip of the electrodes are consistently aligned in a manner that matches the expected placement as determined by the tester. Regarding the detection of hubs, it has been observed that irregularities in the hub structure can occasionally lead to a top hub line that deviates from the actual hub angle. This discrepancy has been noticed in approximately 6% of the electrodes, specifically on nine out of the total 140 electrodes tested. Figure 7.1 illustrates examples of four out of the nine hubs that were misdetected.

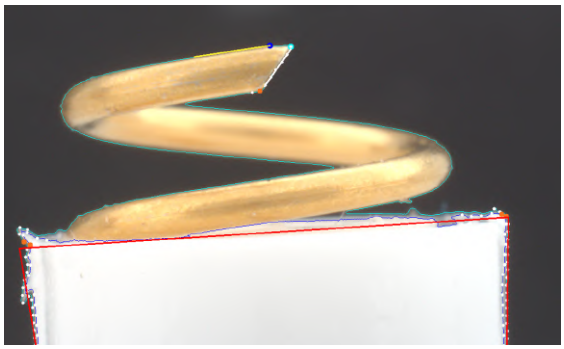

(a) The placement of the top hub line is placed skewed.

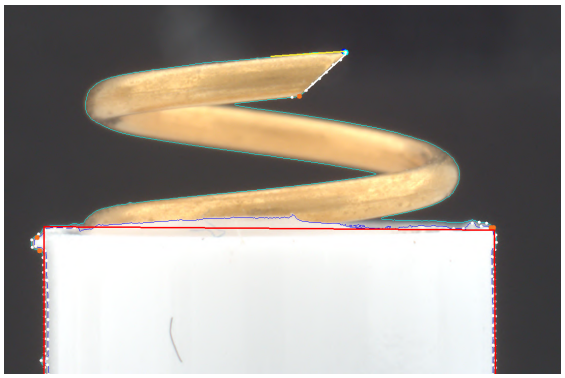

(b) The top hub line is placed too high compared to the hub.

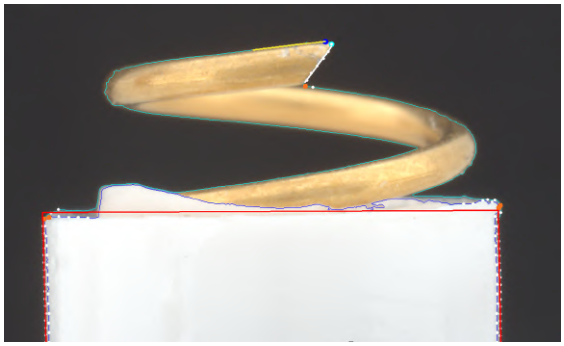

(c) The placement of the top hub line is skewed cause of one large irregularity.

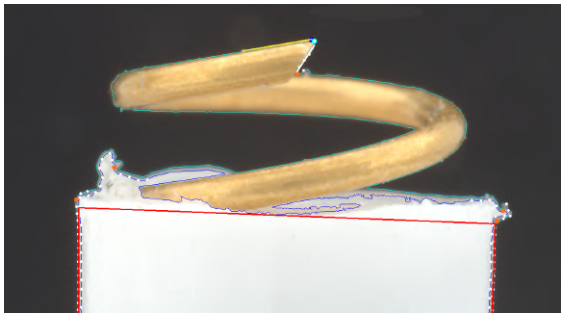

(d) Major irregularities on the hub places the top hub line too far down in the right corner.

Figure 7.1: Examples of detections where the hub detection is placed wrongly.

It is also noted during the detection evaluation that the detection works well despite irregularities of the hub on many electrodes. This can be seen in Figure 7.2.

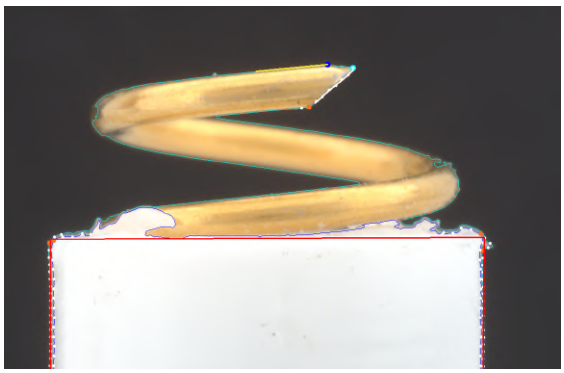

(a) The placement of the hub lines are good despite irregularities on the hub.

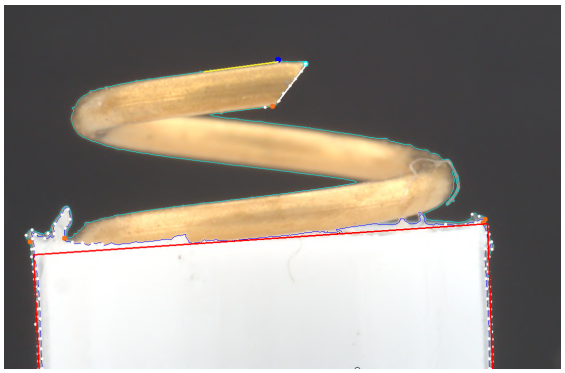

(b) The placement of the hub lines are good despite irregularities on the hub.

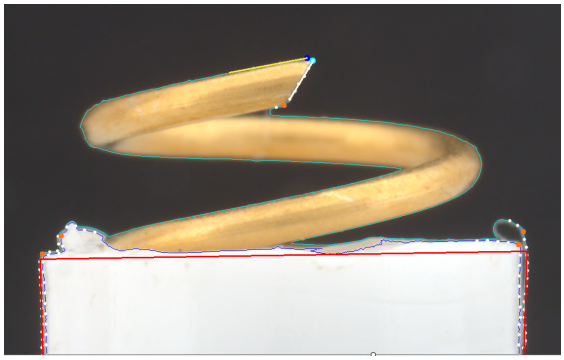

(c) The placement of the hub lines are good despite irregularities on the hub.

Figure 7.2: Examples of detection were the hub lines are detected well despite detecting a hub that contains irregularities.

7.1.1 Calibration system

In this test it is found that the result is not significantly affected by the possible variation of how a person performs the calibration. Neither is it significantly affected by changing who performs the test. This is concluded from analyzing the result presented in Table 7.1 where it is shown that the result varied very little between the 10 tests of the calibration. The smallest number of pixels marked as the 8 mm distance in the 20 tests is 1317.74. and the biggest number is 1319.74. This means that the difference is only 2 pixels, which corresponds to approximately 12.133 μm and the pixel size variance is 0.009 μm.

Table 7.1: Calibration system verification

Test	A: Pixel value (μm)	A: No. of pixels	B: Pixel value (μm)	B: No. of pixels
1	6.062	1319.68	6.067	1318.68
2	6.067	1318.65	6.067	1318.68
3	6.067	1318.68	6.062	1319.68
4	6.062	1319.68	6.067	1318.68
5	6.066	1318.74	6.062	1319.68
6	6.067	1318.61	6.067	1318.68
7	6.067	1318.61	6.067	1318.68
8	6.067	1318.61	6.067	1318.68
9	6.067	1318.68	6.071	1317.74
10	6.062	1319.74	6.066	1318.74

7.1.2 Height measurement

The precision of the developed system and the currently used system at Neoventa is compared by analyzing the calculated maximum differences between 10 tests on each electrode and user, presented in Tables 7.2 and 7.3. The developed system shows a distinctly lower variance and thereby a higher precision for all three users on all three electrodes. The developed system shows only a variance of a maximum 0.007 mm for the height measurements of one electrode, and a minimum of 0.004 mm. The current system shows a maximum variance of 0.289 mm of one electrode and 0.023 mm as a minimum.

Table 7.2: Height difference in between 10 measurements for electrode E1-E3 using the current system. Performed by User A-C

CURRENT SYSTEM			
	User A (mm)	**User B (mm)**	**User C (mm)**
E1 difference	0.078	0.095	0.289
E2 difference	0.059	0.023	0.055
E3 difference	0.107	0.076	0.119

Table 7.3: Height difference in between 10 measurements for electrode E1-E3 using the developed system. Performed by User A, B and D.

DEVELOPED SYSTEM			
	User A (mm)	**User B (mm)**	**User D (mm)**
E1 difference	0.004	0.004	0.004
E2 difference	0.004	0.007	0.004
E3 difference	0.006	0.007	0.007

To continue the evaluation of the height measurement, 25 electrodes are measured in the developed system. User A performs the measurements two times, and User B performs the measurement two times. For both users, the two results for each electrode are compared and a difference is obtained for each electrode for both user's measurements. So, for each electrode, there are four measurements carried through. Also, the difference between the minimum and maximum values among these four is calculated for each electrode. Appendix B includes the difference for all 25 electrodes between the two measurements for User A, between the two measurements for User B, and the maximum difference between all four tests presented in three different tables, Table B.1, B.3 and B.4.

The data presented in Table 7.4 shows the calculated mean, minimum and maximum

value of the 25 calculated differences for User A, User B, and for the four tests. The data shows that the mean value of differences between the tests for one user is a bit lower compared to the mean difference between all four tests, 0.004 mm and 0.005 mm compared with 0.010 mm. Although, the maximum difference for one user compared to the maximum difference between the four tests is almost exactly the same, 0.017 mm and 0.015 mm compared with 0.017 mm. The difference between the four tests for each electrode varies from 0.002 mm up to 0.017 mm, and the differences vary evenly between 0.002-0.017 mm. This can be seen in the data in Appendix B.2 where the maximum differences between the four tests for all 25 electrodes are presented in the order of magnitude. Assuming from the data that 0.017 mm is the largest difference acquired when repeating measurements on an electrode, the system has an estimated approximate uncertainty of ± 0.009 mm.

Table 7.4: Height measurement mean, minimum and maximum difference within the developed system. Tests performed two times on the 25 electrodes by User A, tests performed two times on the 25 electrodes by User B.

	User A test 1-test 2 (mm)	**User B test 3-test 4 (mm)**	**Maximum difference between all four tests (mm)**
Mean	0.004	0.005	0.010
Min	0.000	0.000	0.002
Max	0.017	0.015	0.017

The height measurement is also evaluated by comparing the four tests performed with the developed system with measurements done by User A in the Dino-Capture software, and also with measurements done on the current system by an experienced user from Neoventa. In Figure 7.3 all the six measurements for each of the 25 electrodes are presented in a diagram. It is visualized that all four tests of the current system align very well. The four tests are also aligning well with the measurements from the Dino-Capture, with only small differences between the two systems. Although, the green line presenting the current system, clearly shows that smaller values are obtained for 24 out of 25 electrodes and that the current system generally differs evidently from the five other tests. The developed system aligns much better with the third, independent system, Dino-Capture, compared with how well the current system aligns with Dino-Capture. This indicates that the developed system and Dino-Capture are more accurate systems than the current system.

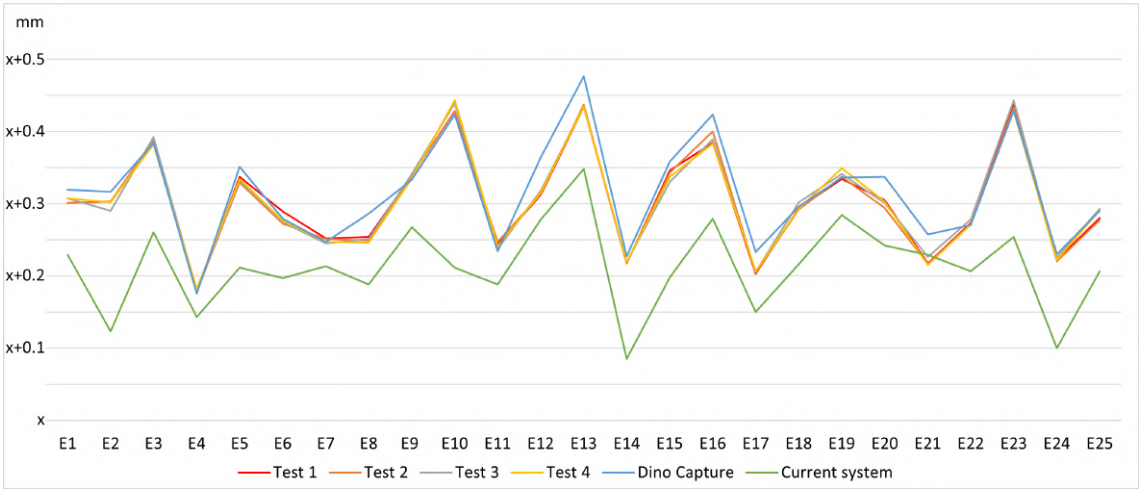

Figure 7.3: A diagram showing the relation between the four tests of the current system, the test with the Dino-Capture software and the test performed with the current system. Test 1-4 are performed with the developed system.

The difference between the developed system is compared further to the Dino-Capture and the current system by calculating the difference between all four tests performed with the developed system and the test performed with the Dino-Capture, as well as the test performed with the current system. The differences between the developed system and the Dino-Capture for all 25 electrodes are presented in Appendix B.3. The differences between the developed system and the current system is presented in Appendix B.4. As the data presents in the appendices, the values taken with the Dino-Capture software are very close to all the measurements from the developed system for all 25 electrodes. Meanwhile, there are evidently larger differences between the developed system and the current system, as also visualized in previous Figure 7.3. The appendices also show that both the average difference and the maximum difference are evidently larger between the developed system and the current system, comparing to the maximum and mean difference between the developed system and the Dino-Capture system. Also, as seen in Appendix B, the differences between the developed system and the values from Dino-Capture vary both ways, so sometimes the developed system acquires smaller values than Dino-Capture and sometimes Dino-Capture acquires smaller values than the developed system. On the contrary, as stated, the values acquired from the current system are clearly smaller than the values from the developed system for 24 out of 25 electrodes.

To conclude the evaluation of the developed height measurement, the result of the evaluation indicates that the developed system is both more accurate and more precise than the currently used system. The result also provides a roughly estimated uncertainty of ± 0.009 mm. However, it is important to note that this uncertainty estimation does not account for incorrectly detected electrodes or the uncertainty associated with calibration.

7.1.3 Angle measurement

Table 7.5 displays the results conducted from test on five different electrodes, with each test being performed ten times by four users. The table presents the largest differences observed among the ten tests and highlights the variations. Notably, User C and User D are the developers of the system and therefore possess experience and familiarity with its operation. In contrast to User C and User D, it is important to note that Person A and Person B lack experience with the system. Furthermore, the instructions provided to them did not include specific details on how to place the electrode. Nevertheless, when considering the average mean of the deviation across all users, it amounts to 1.5 °.

Table 7.5: Evaluation of four different users testing the system. Each user remeasures one electrode 10 times and the largest deviation is presented in the table.

Electrode	Variation User A (°)	Variation User B (°)	Variation User C (°)	Variation User D (°)	Mean for the electrode (°)
E1	3.6	0.7	1.1	0.4	1.4
E2	2.4	1.1	2.3	1.3	1.8
E3	2.1	0.9	1.3	1.9	1.6
E4	1.7	1.4	0.9	1.0	1.3
E5	1.3	2.1	1.0	2.4	1.7
Mean for the user	2.2	1.2	1.3	1.4	1.5

Based on the evaluation of this test, it is evident that the system exhibits varying levels of precision depending on the user. This finding indicates that the system does not meet the system requirements outlined in Table 4.2, which specify that the measurement results should be independent of the person conducting the test.

Figure 7.4 illustrates the outcomes of testing 25 distinct electrodes, with each electrode being assessed twice by two different experienced users. Test 1 and Test 2 were performed by the same user, whereas Test 3 and Test 4 were carried out by a different user. The exact measurements together with the largest variation for each electrode's measurement is presented in Appendix B. The mean of the variations, and thereby the mean difference between the tests, is 1.5 °. The differences between the tests conducted by the same user show a slightly lower variation. The average difference between Test 1 and Test 2 is 0.7 °, and the same applies to Test 3 and Test 4. However, the mean average between Test 1 and Test 3, as well as between Test 1 and Test 4, is only slightly higher at 0.8 °.

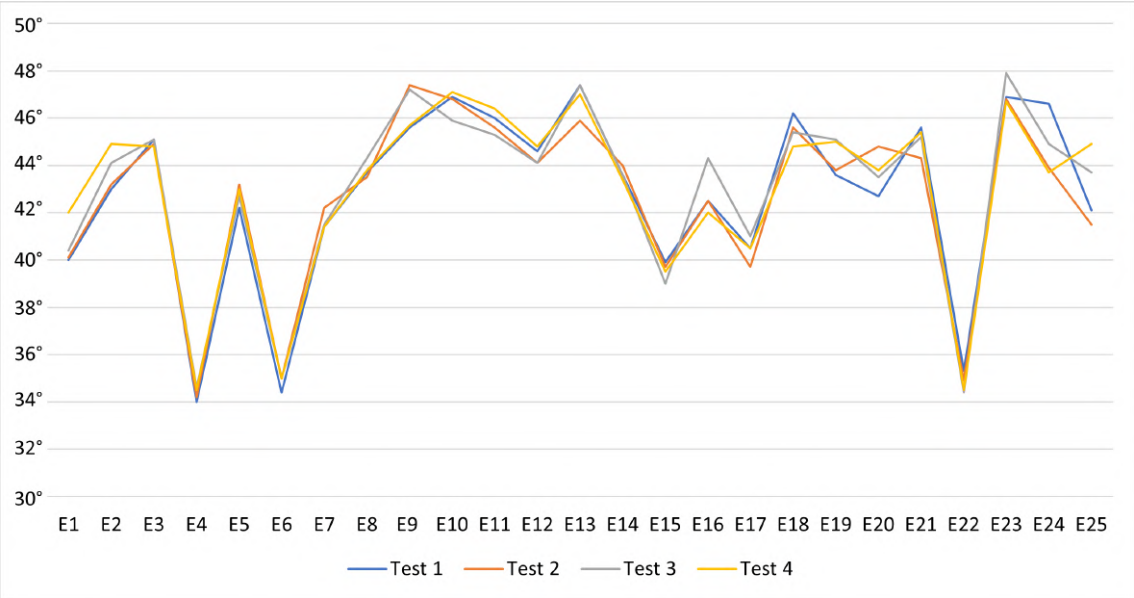

Figure 7.4: A diagram showing the angle measurements on 25 electrodes performed by two different users, User A and B. User A has performed Test 1 and Test 2 while User B has performed Test 3 and Test 4.

Figure 7.5 and Figure 7.6 demonstrate differences in positioning for electrode 24 and electrode 25, which lead to large variations in the measurements, as can be seen in Figure 7.4. While the differences in positioning may not seem significant in the images, and the alignment of the tip lines may also not appear noticeable, these small variances still lead to several degrees of variation in the obtained angle measurements.

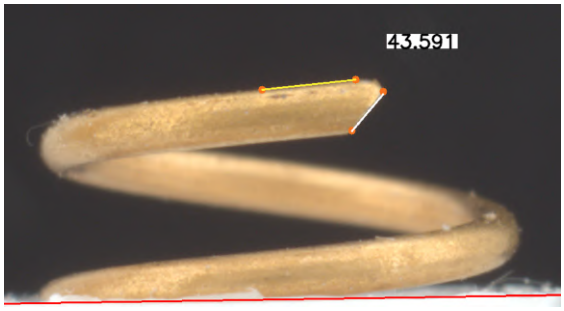

(a) The angle measurement on electrode 24, measuring an angle of 43.6°.

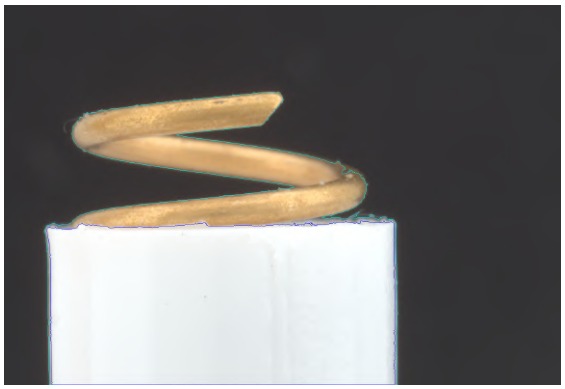

(b) The placement of electrode 24, when measuring an angle of 43.6°

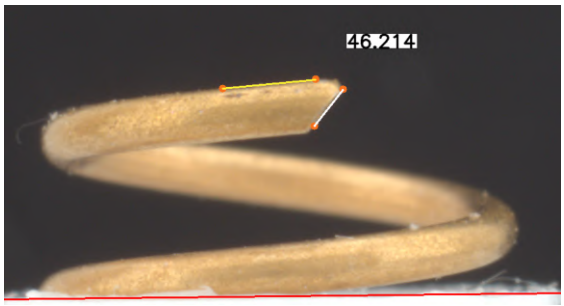

(c) The angle measurement on electrode 24, measuring an angle of 46.2°.

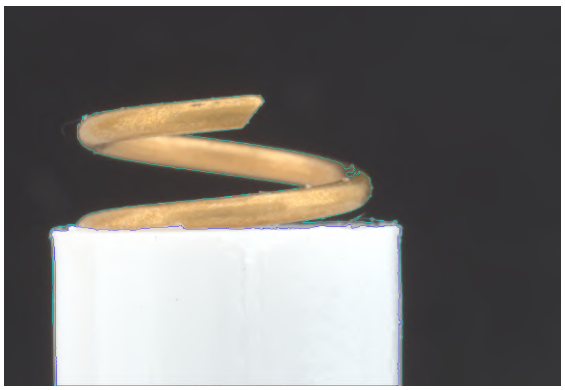

(d) The placement of electrode 24, when measuring an angle of 46.2°

Figure 7.5: The difference in angle measurements on electrode 24, depending on small position changes.

(a) The angle measurement on electrode 25, measuring an angle of 41.8°.

(b) The placement of electrode 25, when measuring an angle of 41.8°

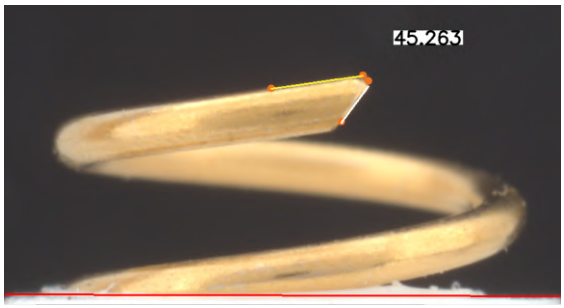

(c) The angle measurement on electrode 25, measuring an angle of 45.3°.

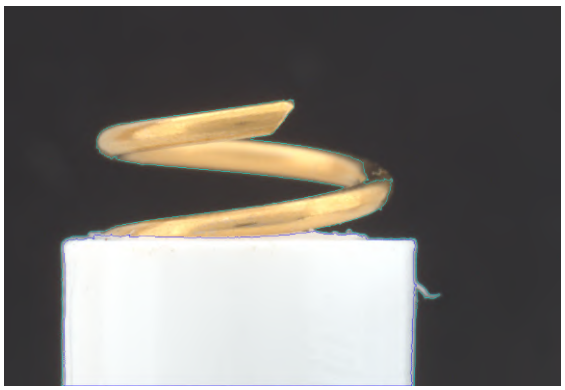

(d) The placement of electrode 25, when measuring an angle of 45.3°

Figure 7.6: The difference in angle measurements on electrode 25, depending on small position changes.

The final evaluation of the angle measuring is presented in Table 7.6. This shows the angle measuring performed with two different measuring systems. One is by manually drawing lines on an image in the Dino-Capture software used in the height evaluation. The second method is the developed system. The average difference between the measurements is 1°. It is important to mention that the tests were conducted on two separate occasions, which introduces the possibility of variations in electrode placement between the measurements. In Appendix C, photos are provided illustrating both methods. It is worth noting that the images of the developed system only display one frame, whereas the results in Table 7.6 are based on 10 frames.

Table 7.6: A comparison between the developed system and a measurement method where the electrode is positioned in front of a camera and the lines forming the angle are manually drawn.

Electrode	Manually drawn lines (°)	Developed system (°)	Difference
E1	43.1	41.7	1.4
E2	37.5	35.3	2.3
E3	42.1	43.3	-1.2
E4	43.1	41.3	1.8
E5	34.6	33.8	0.8
E6	42.9	43.8	-0.9
E7	38.6	38.9	-0.3
E8	37.4	34.7	2.7
E9	43.2	42.7	0.5
E10	47.0	46.1	0.9
E11	45.9	47.3	-1.4
E12	44.8	43.3	1.5
E13	36.2	36.2	0.1
E14	43.2	43.9	-0.7
E15	44.1	43.8	0.3
E16	46.3	46.9	-0.6
E17	45.1	41.1	4.0
E18	40.2	41.3	-1.1
E19	42.3	42.6	-0.3
E20	35.9	35.2	0.7
E21	35.0	35.5	-0.5
E22	35.7	35.2	0.5
E23	44.3	43.0	1.3
E24	44.1	42.6	1.5
E25	34.3	35.5	-1.2
E26	44.5	44.0	0.6
E27	42.2	42.5	-0.3

The assessment indicates that the system demonstrates a similar performance to the manually measured images. The average difference is comparable to the variance observed when testing 25 electrodes between two different users. Notably, Electrode 17 shows a large difference between the two systems, as evidenced in Appendix C, where the electrode placement during the tests differs. Consequently, it can be concluded that both systems perform with a similar level of accuracy. Additionally, the mean difference across four tests for the developed system is approximately 1.5°, this is seen in both the evaluation with four users and the one with two users. When the electrode is hard to place is the deviation larger. It is uncommon that the angle measuring differs more than 3°. Therefore, the concluded measuring uncertainty is ±1.5° which does not fulfill the system requirement of ϵ_{height}. Nevertheless, it provides a reasonable approximation of the angle's magnitude and remains within the tolerances specified by Neoventa for the angle.

7.2 Efficiency performance and observations

Comparison with observation and time study on current system

Observations and time recordings are conducted on the developed system, following the same methodology employed in the observation and time study of the current system, as described in Section 4.2.

The developed system consists of four work tasks containing several smaller work elements each. These are presented in Table 7.7. Observations noted on these tasks were that the user has to be a bit careful when inserting the electrode in Task 1 so that it is not bumped into the edges of the tube guiding the electrode into the fixture, since this can compress the spiral. Also, the wires on the electrode can sometimes be in the way when positioning the electrode in Task 1 or when rotating the electrode during Task 2. This problem is apparent in the time recordings, shown in Table 7.8, for electrode E8 when the wires disturbed the positioning in Task 1, resulting in a much higher time consumption than for the rest of the electrodes. Task 3 can sometimes consume a bit more time when the electrodes do not have one position evidently best fit for the angle measurement. Therefore, the time consumption of Task 3 can vary a bit depending on the electrode appearance.

Table 7.7: Work tasks in the developed system.

Task	Work task	Comment
1	Insert and position electrode in measuring fixture	Wires sometimes complicates positioning in the fixture
2	Start height measurement and rotate electrode until finished	Wires sometimes in the way when rotating in the fixture
3	Place electrode for angle measurement and start measurement. Wait until finished	Some electrodes more difficult to decide where to measure
4	Store measurements and take out electrode	

Table 7.8: Time study on the developed system.

	Task 1 (s)	Task 2 (s)	Task 3 (s)	Task 4 (s)	Total time (s)	Comment/deviation
E1	5.1	3.4	3.1	2.3	13.9	
E2	5.0	5.3	3.5	2.2	16.1	
E3	5.3	4.7	4.3	2.4	16.8	
E4	4.7	2.9	4.0	2.5	14.1	
E5	5.0	3.0	3.4	1.6	13.0	
E6	5.5	3.2	3.3	1.6	13.6	
E7	4.5	3.3	3.2	2.1	13.1	
E8	8.2	4.6	3.4	2.3	18.5	Wires disturbing the rotation in task 1
E9	5.1	3.0	3.7	2.9	14.7	
E10	5.5	3.1	3.7	1.9	14.1	
Mean	**5.4**	**3.7**	**3.6**	**2.2**	**14.8**	

A comparison of the developed system's and the currently used system's mean times for the tasks and the total time for the measuring process are accounted for in Table

7.9, where it is presented that the developed system consumes around half the time as the current system.

Table 7.9: Mean times for the tasks of both systems.

	Current system	Developed system
Mean Task 1 (s)	8.2	5.4
Mean Task 2 (s)	8.3	3.7
Mean Task 3 (s)	9.8	3.6
Mean Task 4 (s)	4.3	2.2
Mean Total time (s)	30.6	14.8

In Table 7.10 it is shown which tasks contain equal work elements. Both Task 2 in the current system and Task 1 in the developed system only consists of grabbing a new electrode and placing it in the fixture, ready for measuring. Task 3 in current system and Task 2 in the developed system both contain the work elements that include performing the height measurement of the electrode. Task 4 of both the current system and developed system contains only collecting the measurements and detaching the electrode from the measuring tool/system. In Table 7.10 the times for these pairs can be compared and it shows that all three tasks are performed faster in the developed system.

Table 7.10: Tasks from the current and the developed system with equal work elements.

Comparable tasks between systems			
Current system		**Developed system**	
Task 2	8.3 s	Task 1	5.4 s
Task 3	9.8 s	Task 2	3.7 s
Task 4	4.3 s	Task 4	2.2 s

Task 1 in the current system, which involves separating the electrode from the drive tube, cannot be directly compared to any work task in the developed system. This is because in the developed system, the test is performed with the electrode already within the drive tube, eliminating the need for this separate task. Similarly, Task 3 in the developed system, which entails measuring the tip angle, cannot be compared to any previous task from the current system. This is because measuring the tip angle is a new addition and has not been performed before in the quality control of the FSE.

7.3 Evaluation of system performance compared to system requirements

According to Table 4.2, the system requirements specify that the system should be capable of measuring both the angle and height of the electrode accurately while being robust against human and external factors, as well as being efficient. The height measurement is achieved by determining the distance between the hub and

the highest point of the spiral, as outlined in the requirements. In 6% of the measurements, the hub detection is placed a little wrong which affects the measuring. According to the system requirements, the evaluation of the height measuring shows that different users perform the same accuracy and precision. The estimated uncertainty, which is below 0.009 mm, indicates that the system requirement is fulfilled in regards to the preferred uncertainty ϵ_{height}.

The angle measuring component accurately measures the angle of the spiral tip, but its precision of $\pm 1.5°$ falls short of the desired accuracy threshold, denoted as ϵ_{angle}. Nevertheless, the system's accuracy is still within the tolerance range for the angle, allowing it to effectively indicate whether the angle falls within the acceptable interval. When used by two different experienced users, the system performs with consistent accuracy. However, if an inexperienced person operates the system, the accuracy may decrease.

Currently, no angle measuring is performed and the system can therefore not compare the efficiency with today's system. It takes however approximately three extra seconds to do the angle measuring and the developed height measuring system takes almost half the time to perform as the developed, making it more efficient as stated in the system requirements.

The requirement that the system should measure the same even if it is moved, is achieved. Very little external light affects the electrode and the fixture is built robustly. However, the positioning of the camera might change a little if the system is moved. Therefore, a built-in calibration system in the software is created that makes it possible to adjust the calibration when the system is moved.

8

Discussion

8.1 Knowledge acquisition

The knowledge acquisition leads to the desired measurement uncertainties of the system, specifically the ϵ_{height}. This uncertainty arises from the concern that electrodes might be mistakenly approved when they are actually outside the acceptable range. At present, the measurement tolerance is determined by the current measuring system, which is prone to human errors. Consequently, there is a possibility that electrodes outside the acceptable range are being approved. Since this tolerance is currently in use, it is likely that ϵ_{height} could be higher and still assure good quality. Instead, an achievable objective could be to design a system that is more accurate and precise compared to the existing one. Currently, there is no quality control in place for angle measurement. This implies that even if a newly developed measuring system has a higher measuring uncertainty, it would still enhance the quality of the electrodes. Hence, it can be concluded that the angle measuring system is considered successful, even if it fails to attain the desired uncertainty, ϵ_{angle}.

During the observation study, the testing conducted in Gothenburg was observed. However, the testing was solely performed by a single user who primarily conducts the tests. To obtain a comprehensive understanding of the current system, it would be beneficial to observe the challenges and issues encountered by different users. It is possible that individuals testing the spiral height in the production site face different problems and difficulties compared to the testing person at Neoventa.

Given that the system under development in the study is new, users lack the same level of experience as the testing person at Neoventa had with the current system during the observation study. Consequently, it would be advantageous to compare the two systems when users possess an equal degree of familiarity with both. This approach would facilitate a more meaningful and comprehensive evaluation.

8.2 Concept development

During the concept development phase, a camera was available and used to gain a basic understanding of the software's requirements and the overall system. This early access to the camera allowed for the prompt initiation of system development,

including both the software and fixture. However, it also carries the risk that not enough background theory was gathered before the development started. For instance, only four different image processing methods were examined, and further studies could have been conducted on their potential implementation. As a result, there is a possibility that a more suitable method for the software or an entirely different approach to constructing the fixture exists, which could yield better results. The idea of placing a camera over the electrode, as described in section 5.2, was primarily derived from being the first setup attempted. Nonetheless, if more time had been allocated solely to conceptual decision-making without testing different techniques, likely the project would not have been completed within the specified timeframe. Thus, a balance was struck between the need for thorough concept evaluation and the imperative to meet project deadlines.

8.3 System design and performance

During the concept development discussions, it was noted that limited literature was reviewed prior to commencing the development phase. Consequently, the method of thresholding was decided very early on in the project through trial and error, without thoroughly investigating and trying to implement other image processing methods. Section 6.1.1 provides an overview of the methods that were tested and it is described that the threshold technique was chosen early in the process. It could have been beneficial to explore alternative image processing methods in more detail. However, the results of the detection in section 6.1.1.3 shows that the detection works and the detection evaluation in section 7.1 shows that 94% are detected correctly using this method.

As outlined in section 6.3, the user interface of the final system offers users feedback on measurement results and indicates the current state of the system, including calibration mode and measuring mode. Additionally, it provides continuous information about the available buttons for user interaction. Consequently, users receive both feedback on their actions and support throughout the process. However, there are still areas where potential improvements could be made to enhance the user experience. For example, the signals indicating the system's state changes, such as starting to measure the angle, could be further developed to make it clearer for the user. Additionally, there is no signal when a measured electrode dimension is outside the tolerances, nor is there a signal when a measurement has been performed incorrectly. In the developed system, this issue is instead up to the user to notice and solve. Due to these flaws, there is a risk that a user might perform the measurements incorrectly and fail to remeasure the electrode. If this goes unnoticed, the results of the quality inspections could indicate an incorrect quality trend.

The final fixture in this prototype, described in chapter 6.2.1, is not optimal. The construction allowed most of the observed problems with the current system to be avoided, but some other problems appeared. Through the observation study of the current system, it became evident that there is a significant risk of electrode compression during both insertions into the measuring tool and during the mea-

surement process. The fixture is designed to remove the risk of compressing the electrode inside the fixture and during the measurement, ensuring more reliable measuring results. Although, during the electrode insertion, the user has to be accurate to not compress the spiral against the edge of the tube. The distinction between these compression risks lies in the visibility and user control of the two systems. In the developed system, it is easy to detect and avoid compression issues owing to better visibility. The real-time picture visualization of the electrode on the computer ensures constant visualization despite the placement within a closed box. This enhances the user's comprehension and understanding of whether the test has been performed correctly. In contrast, the observation study of the current system showed that the lack of visibility in the system makes it challenging for the user to identify whether the spiral is being compressed during the test. In the current system, there are occasions where an electrode is remeasured when the user obtains significantly different measurement values, and due to the lack of visibility, it is often impossible to determine the cause of the difference between the obtained results.

Overall, the observation studies on the current and the developed system show that the new setup reduces the risk of measurements being affected by human errors. The new system provides more cognitive support, guiding the user on how to perform the test and visualize whether the test is executed correctly and if the detection works as it should. For example, unlike the current system, the effectiveness of the developed system is not either dependent on the user preparing for the next electrode, such as manually unscrewing the measuring cylinder to avoid compression of the spiral. There is still a risk that the software can perform the detection with a bit of variation, but the risks of human errors are reduced owing to the autonomous detection and measuring as well as the fixture not allowing different positioning. The one evident risk of human error that remains in the developed system is the risk of incorrect rotational placement of the electrode for the angle measurement, which is a result of lacking cognitive support telling the user what is more or less accurate in this measurement.

The developed computer vision system is more efficient when comparing the time studies. However, the observation study shows one issue in the developed system that can potentially cause the time consumption for a test to increase. That is the wires of the electrode hinder its rotation and placement. This issue could probably be addressed by constructing a fixture with more space around the drive tube grip. Despite this potential delay, the developed system consistently proves to be more efficient than the current manual system. In the current system, the first task is to separate the electrode from the drive tube, which is not required in the developed system. Therefore it may be relevant to compare the time study without including this task. Nevertheless, if subtracting the time for Task 1 from the total time for the current system, the developed system remains more efficient in all cases when comparing the time for each electrode. Additionally, the developed system also has an added time consumption due to the angle measurement that has not been included in the quality control before, and despite this additional task, the developed computer vision system is still more efficient as a measuring quality inspection system to implement in the production.

The height measurement evaluation indicates that the uncertainty is below the acceptable threshold, ϵ_{height}. However, this number is solely based on the precision of the system and the detected variations regarding the measured height. It fails to account for instances when the system incorrectly detects the hub. The evaluation reveals that the hub is detected incorrectly approximately 6% of the measurements. It is necessary to examine the extent of the detection errors to achieve a more accurate measurement uncertainty. The perception of misplacement arises from a human interpretation of the correct positioning. Since this interpretation can differ among users, the percentage may vary from what is stated in the evaluation. A more objective approach would involve multiple users testing the detection instead of relying on the evaluation and interpretation of a single user.

The uncertainty also fails to consider the possibility of incorrect calibration placement. The calibration process involves positioning the calibration ruler vertically at the same height as the top spiral. If the vertical position is incorrect, the calibration result will be inaccurate, rendering all subsequent measurements erroneous. Therefore, it is essential to evaluate the correct vertical positioning of the calibration ruler before determining the measurement uncertainty as is currently stated. Furthermore, since the accuracy of the system relies on evaluating the detection of the hub and the calibration positioning, it is challenging to determine the exact accuracy. However, the evaluation indicates that the precision is lower compared to the current system. Considering the measurements obtained from the Dino Camera, it can be inferred that the system is potentially more accurate than the current system. This means that the height measurement overall is more effective than the system used currently, both regarding accuracy and precision.

The angle measurement evaluation reveals that the uncertainty of the system exceeds the acceptable level, ϵ_{angle}. Considering that there today is no way to measure the angle, the system is still a good tool to use even though the requirements are not fulfilled. It provides a reasonably accurate estimation of the angle's magnitude and whether it falls outside or is close to the tolerance range. As shown in Figures 7.5 and 7.6, the uncertainty is influenced by variations in electrode placement among different users, as well as inconsistencies in measurements even when placed similarly by the same user. Notably in the evaluation, experienced users exhibit smaller differences compared to inexperienced users. Since the system is primarily intended for repeated use by an individual, the performance of experienced users becomes more relevant.

Overall, the angle measurement functionality falls short of meeting the required uncertainty level, ϵ_{angle}, as well as the expectation of precision and accuracy being unaffected by different users. However, the system successfully detects and measures the correct angle, demonstrating minimal susceptibility to external factors such as light interference. This makes the angle measuring an effective system that can be beneficial to use even though there are some effectiveness improvements that can be done.

Dust and particles have the potential to disrupt the detection process and lead to

inaccurate measurements as seen in Figure 6.8. It is assumed that this issue will not arise during production as the quality inspections are conducted in a clean environment. However, it should be noted that the quality tests in Gothenburg are not conducted in a dedicated clean room, increasing the risk of measurement disturbances. Consequently, the effectiveness of the system may be compromised, resulting in lower accuracy and precision of the measurements performed in Gothenburg. However, the electrodes are tested rather close in time to the unpacking, and therefore the risk of dust and particle disturbances decreased compared to the testing environment during the development of the system, which took place over several months.

8.4 Future work and improvements

As stated in the aim of the study, the developed product is a prototype that will require additional improvements before it can be introduced into production. One area for improvement is the camera stand. The current stand is composed of multiple smaller parts that are assembled using screws and bricks. Ideally, a single component would securely hold the camera without any movable parts. Presently, there is a possibility that the camera may experience slight movement if the stand is pushed or relocated, necessitating recalibration after any external impact on the stand. Furthermore, the insertion of the camera stand and electrode holder can be enhanced to mitigate the risk of it becoming stuck in the diffusion filters. One potential solution is to position the stand farther away from the filters or design a stand that is attached outside of the lightning box, eliminating the need for sliding it into place as is currently done. Finally, another improvement that can be made to the fixture is the use of a lighting box with a different color. It has been observed that the current black box tends to absorb a significant amount of light, resulting in variations in lighting intensity across the electrode. While a white surface has been added to mitigate this issue, it would be more effective to have a different color for the lighting box from the outset. By using a lighting box with a more suitable color, the distribution of light would be more uniform, ensuring consistent brightness of the electrode throughout the imaging process. To minimize the risk of users inadvertently compressing the spiral against the edge of the guide tube while inserting the electrode, an enhancement can be implemented for the opening of the guide tube. One possible solution is to incorporate a funnel-like object at the opening to eliminate sharp edges. However, it is important to consider that this modification may affect the functionality of the current stop mechanism provided by the guide tube. Careful evaluation is necessary to ensure that any changes made to the opening of the guide tube do not compromise its stop mechanism.

One way to improve the angle and height measuring would be to have an automatic rotation done when the electrode is placed. This would remove the need of having a human doing it and thereby diminish the human factor. It would therefore mean that the height measuring will be done more smoothly and that all placements in the positioning interval could be just as accounted for. However, before this, the software needs to be improved so that it can find and tell when the electrode is in

the correct position for the angle measuring. An additional, improvement for the software would be that the user could manually position the hub lines on the image in those cases when the hub is detected inaccurately. This would mean that the share of 6% inaccurate hub detection could still get a height measurement that is correct as long as the user notices the wrong detection and replaces it.

An additional improvement for the software would be to allow users to manually adjust the position of the hub lines on the image in cases where the automatic hub detection is inaccurate. This feature would enable users to correct any erroneous hub detection, ensuring that the height measurement remains accurate. Even if the system initially detects the hub incorrectly, the user's ability to manually intervene and replace the erroneous detection would significantly improve the measurement accuracy. With this capability, the 6% share of inaccurate hub detection could be mitigated, as long as users identify and rectify any wrongly detected hubs.

A potential future improvement for better detection accuracy would involve enhancing the detection of hub corners. Some electrodes exhibit irregularities and outward protrusions from the hub, which can lead to corners detected too early or too late. Enhancing the robustness of the corner detection algorithm would equip the system with improved capabilities to accurately identify and locate the corners of the hub. This improvement would result in fewer instances of inaccurate hub detection, enhancing the overall reliability and precision of the measurement process.

As previously mentioned, the calibration process can be enhanced by ensuring a stable and accurate vertical level. One approach is to develop a secure holder specifically designed for the ruler that guarantees the correct height. Alternatively, a new product could be created, mimicking the cylindrical shape of the drive tube. This new product could be marked with ruler lines or predetermined distances, and inserted into the fixture. The software could then be trained to detect these lines, enabling automated more accurate calibration.

A final improvement for the system would involve enhancing the user interface to make it more intuitive and user-friendly, as previously discussed. This would require conducting further evaluations to determine the necessary features and functionalities. One approach to achieve this improvement would be to provide clear and informative feedback to the user. Additionally, implementing multiple windows and incorporating the use of different colors could enhance the user experience and facilitate ease of use.

8.5 Ethics

The establishment of this quality test, along with the determination of tolerances governing the number of scrapped electrodes, is giving rise to an ethical dilemma concerning the choice between ensuring safer deliveries to fewer people or risking less safe deliveries to a larger number of individuals. The measuring system has to be very accurate to ensure that electrodes with wrong dimensions are not approved,

since these electrodes can create wounds on the fetuses' heads. The measuring system also has to be very precise to ensure that not too many electrodes are scrapped due to high measurement uncertainty, since if many electrodes are scrapped, then all women in labor may not be able to retrieve an electrode although they are considered to need one. The lack of electrodes can directly risk the health of both the pregnant woman and the fetus. If the accurate and precise system would indicate that many electrodes have dimensions outside the tolerances, it is an ethical decision to decide whether it is better to risk fetuses getting a wound and possibly an infection, or if it is better to risk that some women will not get an electrode, causing the ECG to not be monitored properly, risking serious health hazards and in worst case death.

9

Conclusion

The main objective of this study was to develop a prototype computer vision system for the quality control of Neoventa's Goldtrace FSE. The system aimed to measure the angle of the spiral tip and the height of the needle spiral. In addition to the development of the prototype, the study also focused on evaluating its efficiency and effectiveness.

The prototype consists of software designed to detect and measure the electrode, along with a fixture that provides stability and minimizes the impact of external factors on the measurements. The evaluation of effectiveness revealed that the developed prototype surpassed Neoventa's current height measurement system in terms of accuracy and precision. The height measurement was not significantly influenced by human factors, as different users achieved consistent results.

However, angle measurement is not currently performed in Neoventa's system due to the absence of a reliable measurement method. The developed prototype addresses this limitation by providing an approximation of the angle size. Nonetheless, the precision of the angle measurement varies among users, mainly due to the nature of the electrode tips, making it challenging to consistently place the electrode in the same position. Consequently, the interpretation of the correct electrode placement still requires human intervention. The evaluation indicates an accuracy of approximately $\pm 1.5°$, suggesting a relatively accurate measurement by the system.

Considering the lack of an angle measurement system in Neoventa's current practices, the developed prototype offers a more effective solution. The height measurement system demonstrated improved precision and accuracy compared to the existing system, making the developed system a preferable choice for Neoventa. Additionally, the evaluation indicates that the system's efficiency is enhanced by measuring both angle and height, it is even more efficient than the current system that solely measures height. Nonetheless, as the system remains in the prototype stage, further enhancements can be made to improve its robustness and effectiveness.

Bibliography

[1] W. R. Cohen, S. Ommani, S. Hassan, *et al.*, "Accuracy and reliability of fetal heart rate monitoring using maternal abdominal surface electrodes," *Acta Obstetricia et Gynecologica Scandinavica*, Nov. 2012. DOI: 10.1111/j.1600-0412.2012.01533.x.

[2] S. Allarakha, *What is a scalp electrode?* [Online]. Available: https://www.medicinenet.com/what_is_a_scalp_electrode/article.htm (visited on Mar. 15, 2023).

[3] Neoventa, *Goldtrace*. [Online]. Available: https://www.neoventa.com/products/goldtrace/ (visited on Mar. 15, 2023).

[4] M. Andersson. "Spädbarn får sår av skalpelektroder - flera har behövt antibiotika," Vårdfokus. (Oct. 2021), [Online]. Available: https://www.vardfokus.se/nyheter/spadbarn-far-sar-av-skalpelektroder-flera-har-behovt-antibiotika/ (visited on Jan. 17, 2023).

[5] M. Andersson. "Troligt tillverkningsfel bakom skalpsåren," Vårdfokus. (Oct. 2021), [Online]. Available: https://www.vardfokus.se/nyheter/troligen-tillverkningsfel-bakom-skalpsaren/ (visited on Jan. 17, 2023).

[6] R. Anjoran, *What is the "aql" (acceptance quality limit) in simple terms?* Aug. 2018. [Online]. Available: https://qualityinspection.org/what-is-the-aql/ (visited on May 25, 2023).

[7] S. Anand and P. Loganathan, *A Guide for Machine Vision in Quality Control*. Dec. 2019, ISBN: 9781003002826. DOI: 10.1201/9781003002826.

[8] . Z. Technologies, *What is the difference between machine vision and computer vision?* [Online]. Available: https://www.zebra.com/us/en/resource-library/faq/general-technology/what-is-the-difference-between-machine-vision-computer-vision.html (visited on Feb. 21, 2023).

[9] M. Javaid, A. Haleem, R. P. Singh, S. Rab, and R. Suman, "Exploring impact and features of machine vision for progressive industry 4.0 culture," *Sensors International*, Mar. 2022. DOI: 10.1016/j.sintl.2021.100132.

[10] Swedish medical products agency, *Regulatory frameworks for medical devices*, Jan. 2021. [Online]. Available: https://www.lakemedelsverket.se/en/medical-devices/manufacture/regulatory%20frameworks (visited on Apr. 5, 2023).

[11] Regulation (EU) 2017/745 of the European Parliament and of the Council of 5 April 2017 on medical devices, amending Directive 2001/83/EC, Regulation

(EC) No 178/2002 and Regulation (EC) No 1223/2009 and repealing Council Directives 90/385/EEC and 93/42/EEC.

[12] J. Katta, *Medical device regulation (eu 2017/745) – conformity assessment routes*, 2019. [Online]. Available: https://www.bsigroup.com/globalassets/localfiles/fr-fr/dispositifs-medicaux/ressources/bsi-md-mdr-conformity-assessment-routes-webinar-presentation-16-july-2019-fren.pdf (visited on Apr. 5, 2023).

[13] L. Jinze, L. Zhihong, L. Guofang, *et al.*, "Study of temperature automatic verification system based on computer vision measuring," in *2010 International Conference on Computer and Communication Technologies in Agriculture Engineering*, vol. 1, 2010, pp. 312–315. DOI: 10.1109/CCTAE.2010.5544529.

[14] R. G. Lins, R. E. d. Santos, and R. Gaspar, "Vision-based measurement for quality control inspection in the context of industry 4.0: A comprehensive review and design challenges," *Journal of the Brazilian Society of Mechanical Sciences and Engineering*, vol. 45, no. 4, 2023. DOI: 10.1007/s40430-023-04050-y.

[15] S. Kim, "Applications of convolution in image processing with matlab," M.S. thesis, University of Washington, Aug. 2013.

[16] R. Fisher, S. Perkins, A. Walker, and E. Wolfart, *Laplacian laplacian of gaussian*. [Online]. Available: https://homepages.inf.ed.ac.uk/rbf/HIPR2/log.htm (visited on May 17, 2023).

[17] S. Jaiswal, *Concept of edge detection*. [Online]. Available: https://www.javatpoint.com/dip-concept-of-edge-detection (visited on May 17, 2023).

[18] S. Safir, "Canny edge detection step by step in python - computer vision," *Towards Data Science*, 2019.

[19] B. R.Yogamangalam, "Segmentation techniques comparison in image processing," *International Journal of Engineering and Technology*, 2004.

[20] O. S. C. Vision, *Hough line transform*. [Online]. Available: https://docs.opencv.org/3.4/d9/db0/tutorial_hough_lines.html (visited on May 18, 2023).

[21] G. Holtzer, *How does a camera work? (photography basics explained)*. [Online]. Available: https://expertphotography.com/how-does-a-camera-work/ (visited on Apr. 3, 2023).

[22] G. ALPER, *Ccd vs. cmos image sensors in machine vision cameras?* [Online]. Available: https://mediakurser.se/framerate-vad-ar-det-och-vilken-ska-jag-valja/ (visited on Mar. 2, 2023).

[23] NextScan, *Line scan cameras vs. area scan cameras – microfilm scanning*. [Online]. Available: https://www.nextscan.com/line-scan-cameras-vs-area-scan-cameras-microfilm-scanning/ (visited on Mar. 2, 2023).

[24] B. Fan, Y. Dai, and H. Li, "Rolling shutter inversion: Bring rolling shutter images to high framerate global shutter video," *IEEE Transactions on Pattern Analysis and Machine Intelligence*, pp. 1–16, 2022. DOI: 10.1109/TPAMI.2022.3212912.

[25] Mediakurser, *Framerate – vad är det och vilken ska jag välja?* [Online]. Available: https://mediakurser.se/framerate-vad-ar-det-och-vilken-ska-jag-valja/ (visited on Mar. 2, 2023).

[26] Machine Vision Basics, *Selecting the correct camera.* [Online]. Available: https://www.keyence.com/ss/products/vision/visionbasics/tips/primer1/ (visited on Mar. 1, 2023).

[27] N. Mansutov, *Understanding aperture in photography.* [Online]. Available: https://photographylife.com/what-is-aperture-in-photography (visited on May 19, 2023).

[28] H. Pao, R. Gallotta, A. Daigavane, C. Boo, A. Chattopadhyay, and N. Khanderia, *Distance between point and line.* [Online]. Available: https://brilliant.org/wiki/distance-between-point-and-line/ (visited on May 19, 2023).

[29] C. E. Robert A. Adams, *Calculus: A complete course*, 9th ed. Pearson Canada Inc., 2018, pp. 785–786, 978-0-13-415436-7.

[30] Cuemath, *Angle between two lines.* [Online]. Available: https://www.cuemath.com/geometry/angle-between-two-lines/ (visited on May 19, 2023).

[31] H. S. Jennifer Preece Yvonne Rogers, "Interaction design: Beyong the human-computer interaction," in P. C. Gaynor Redvers-Muttonl, Ed., 5th ed. John Wiley & Sons, 2018, ch. 13, Asking users and experts, pp. 390–398.

[32] H. B. Maynard, K. B. Zandin, L. A. Martin-Vega, *et al.*, *Maynard's industrial engineering handbook* (McGraw-Hill's AccessEngineering). McGraw-Hill, 2001, ch. 124, ISBN: 0071449272. [Online]. Available: https://search.ebscohost.com/login.aspx?direct=true&db=cat07472a&AN=clec.MHAEccn00213928&site=eds-live&scope=site&authtype=guest&custid=s3911979&groupid=main&profile=eds.

[33] C. A. Mattson and C. D. Sorensen, "Product development, Principles and tools for creating desirable and transferable designs," in Springer Cham, Nov. 2019, ch. 3,11, ISBN: 978-3-030-14899-7. DOI: https://doi.org/10.1007/978-3-030-14899-7.

[34] Dino-Lite, *Am4815ztl - edge.* [Online]. Available: https://www.dino-lite.eu/sv/component/eshop/am4815ztl-edge?Itemid=0 (visited on Feb. 28, 2023).

[35] S. Lee, M. Jeong, C.-S. Cho, J. Park, and S. Kwon, "Deep learning-based pc member crack detection and quality inspection support technology for the precise construction of osc projects," *Applied Sciences (2076-3417)*, vol. 12, p. 9810, Oct. 2022. DOI: 10.3390/app12199810.

[36] OpenCV team, *About.* [Online]. Available: https://opencv.org/about/ (visited on Mar. 2, 2023).

[37] Thorlabs, *C-mount extension tubes and spacer rings.* [Online]. Available: https://www.thorlabs.com/newgrouppage9.cfm?objectgroup_id=8284 (visited on May 10, 2023).

A

Appendix 1

A.1 Interview with Neoventa February 1st, 2023

- How and when is the Goldtrace FSE used?
- What parameters of the electrode should be controlled in the new system?
- How is the height measured currently, what problems are there?
- What tolerances are there for the height and angle?
- When and where are tests performed and how many?
- What could happen if the Goldtrace FSE has the wrong dimensions?

A.2 Interview with Neoventa March 23rd, 2023

- Should the height measuring be from the highest point or from the tip point?
- How should the angle measurement be done, from the tip or from the highest point?
- How much time is spent on one quality control using the current system?
- Should the control be with the drive tube attached or without it?
- Is the angle of the tip examined in any way currently?

B

Appendix 2

The three tables in this appendix show the differences between measurements done on 25 electrodes. Measurements were done four times on the developed system, done by two users, two times each. These measurements are compared in Table B.1, where the difference for User A, the difference for User B and the maximum difference between all four tests are presented. In Table B.3, the four measurements done with the developed system are compared with reference measurements done with the Dino-Light camera and the software Dino-Capture. In Table B.4, the four measurements done with the developed system are compared with measurements done with the measuring system currently used by Neoventa. The minimum and maximum differences are presented in all three tables to show how much the difference vary.

Table B.1: Height measurement difference between measurements done with the developed system.

	User A test 1-test 2 (s)	**User B test 3-test 4 (s)**	**Developed system maximum difference of four tests (s)**
E1	0.000	0.000	0.006
E2	0.000	-0.012	0.013
E3	-0.004	0.010	0.010
E4	0.000	-0.002	0.004
E5	0.008	-0.002	0.008
E6	0.017	-0.002	0.017
E7	0.001	-0.002	0.007
E8	0.005	0.005	0.008
E9	0.000	0.006	0.006
E10	0.000	-0.004	0.015
E11	-0.003	-0.004	0.010
E12	-0.001	0.003	0.006
E13	-0.003	0.000	0.003
E14	0.000	0.000	0.002
E15	0.003	-0.007	0.016
E16	-0.016	0.006	0.017
E17	-0.001	-0.001	0.003
E18	0.002	0.009	0.010
E19	-0.003	-0.008	0.015
E20	0.011	-0.002	0.011
E21	0.001	0.011	0.011
E22	0.002	0.007	0.007
E23	0.004	0.015	0.015
E24	0.002	0.003	0.005
E25	0.003	0.002	0.016
Min:	**-0.016**	**-0.012**	**0.002**
Max:	**0.017**	**0.015**	**0.017**

Table B.2: Maximum difference between the four measurements for each electrode done with the developed system. Presented in order of magnitude

	Developed system maximum difference of four tests (mm)
E14	0.002
E13	0.003
E17	0.003
E4	0.004
E24	0.005
E1	0.006
E9	0.006
E12	0.006
E7	0.007
E22	0.007
E5	0.008
E8	0.008
E3	0.010
E11	0.010
E18	0.010
E20	0.011
E21	0.011
E2	0.013
E10	0.015
E19	0.015
E23	0.015
E15	0.016
E25	0.016
E6	0.017
E16	0.017

Table B.3: Height measurement difference between developed system used by User A and B and measurements from the Dino-Capture software. The minimum and maximum difference presented, and the calculated mean value of the differences' absolute values

	User A test 1 -Dino-Capture (s)	**User A test 2 -Dino-Capture (s)**	**User B test 3 -Dino-Capture (s)**	**User B test 4 -Dino-Capture (s)**
E1	-0.018	-0.018	-0.012	-0.012
E2	-0.013	-0.013	-0.026	-0.014
E3	0.000	0.004	0.008	-0.002
E4	0.003	0.003	0.005	0.007
E5	-0.014	-0.022	-0.019	-0.017
E6	0.010	-0.007	-0.005	-0.003
E7	0.005	0.004	-0.002	0.000
E8	-0.032	-0.037	-0.035	-0.040
E9	0.006	0.006	0.008	0.002
E10	0.005	0.005	0.016	0.020
E11	0.010	0.013	0.003	0.007
E12	-0.052	-0.051	-0.046	-0.049
E13	-0.042	-0.039	-0.042	-0.042
E14	-0.010	-0.010	-0.008	-0.008
E15	-0.012	-0.015	-0.028	-0.021
E16	-0.039	-0.023	-0.034	-0.040
E17	-0.030	-0.029	-0.028	-0.027
E18	-0.002	-0.004	0.006	-0.003
E19	-0.002	0.001	0.005	0.013
E20	-0.032	-0.043	-0.036	-0.034
E21	-0.040	-0.041	-0.031	-0.042
E22	0.003	0.001	0.008	0.001
E23	0.008	0.004	0.014	-0.001
E24	-0.008	-0.010	-0.005	-0.008
E25	-0.010	-0.013	0.003	0.001
Min:	**-0.012**	**-0.013**	**-0.011**	**-0.012**
Max:	**-0.052**	**-0.051**	**-0.046**	**-0.049**
Mean of the absolute values of the differences:	**0.016**	**0.017**	**0.017**	**0.017**

Table B.4: Height measurement difference between developed system used by User A and B and measurements from the current system. The minimum and maximum difference presented, and the calculated mean value of the differences' absolute values

	User A test 1 -current system (s)	**User A test 2 -current system (s)**	**User B test 3 -current system (s)**	**User B test 4 -current system (s)**
E1	0.072	0.072	0.078	0.078
E2	0.180	0.180	0.167	0.179
E3	0.124	0.128	0.132	0.122
E4	0.035	0.035	0.037	0.039
E5	0.126	0.118	0.121	0.123
E6	0.092	0.075	0.077	0.079
E7	0.039	0.038	0.032	0.034
E8	0.066	0.061	0.063	0.058
E9	0.072	0.072	0.074	0.068
E10	0.217	0.217	0.228	0.232
E11	0.056	0.059	0.049	0.053
E12	0.034	0.035	0.040	0.037
E13	0.086	0.089	0.086	0.086
E14	0.132	0.132	0.134	0.134
E15	0.148	0.145	0.132	0.139
E16	0.105	0.121	0.110	0.104
E17	0.053	0.054	0.055	0.056
E18	0.078	0.076	0.086	0.077
E19	0.050	0.053	0.057	0.065
E20	0.063	0.052	0.059	0.061
E21	-0.012	-0.013	-0.003	-0.014
E22	0.067	0.065	0.072	0.065
E23	0.183	0.179	0.189	0.174
E24	0.122	0.120	0.125	0.122
E25	0.074	0.071	0.087	0.085
Min:	**-0.012**	**-0.013**	**-0.003**	**-0.014**
Max:	**0.217**	**0.217**	**0.228**	**0.232**
Mean of the absolute values of the differences:	**0.091**	**0.090**	**0.092**	**0.091**

Table B.5: Evaluation of having two different experienced users remeasure 25 electrodes two times each.

Electrode	Test 1 User A (°)	Test 2 User A (°)	Test 3 User B (°)	Test 4 User B (°)	Maximum Difference (°)
E1	40.0	40.1	40.4	42.0	2.0
E2	43.0	43.2	44.1	44.9	2.0
E3	45.1	44.9	45.1	44.8	0.3
E4	34.0	34.2	34.6	34.5	0.6
E5	42.2	43.2	42.7	43.0	1.0
E6	34.4	35.0	35.0	35.0	0.6
E7	41.4	42.2	41.5	41.4	0.8
E8	43.7	43.5	44.3	43.8	0.8
E9	45.6	47.4	47.2	45.7	1.8
E10	46.9	46.8	45.9	47.1	1.2
E11	46.0	45.6	45.3	46.4	1.1
E12	44.6	44.1	44.1	44.8	0.7
E13	47.4	45.9	47.4	47.0	1.5
E14	43.6	44.0	43.6	43.4	0.7
E15	39.9	39.7	39.0	39.5	0.9
E16	42.5	42.5	44.3	42.0	2.3
E17	40.5	39.7	41.0	40.5	1.3
E18	46.2	45.6	45.4	44.8	1.4
E19	43.6	43.8	45.1	45.0	1.4
E20	42.7	44.8	43.5	43.8	2.1
E21	45.6	44.3	45.2	45.4	1.2
E22	35.3	34.9	34.4	34.5	0.9
E23	46.9	46.8	47.9	46.7	1.2
E24	46.6	43.9	44.9	43.7	2.8
E25	42.1	41.5	43.7	44.9	3.4

C

Appendix 3

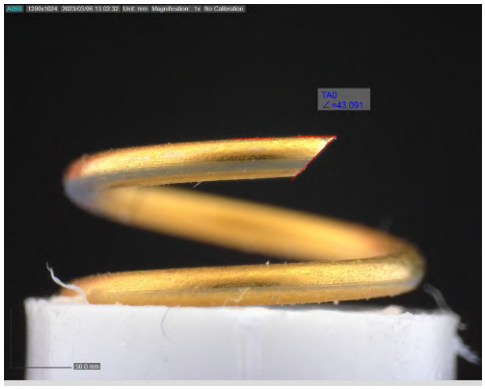

(a) Measurements done by manually drawing lines in Dino-Capture.

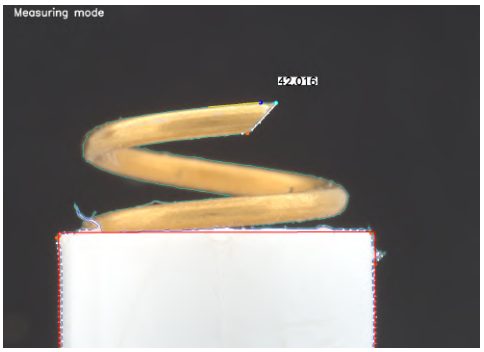

(b) Measurement detected with the developed system.

Figure C.1: Angle measurements of electrode number 1.

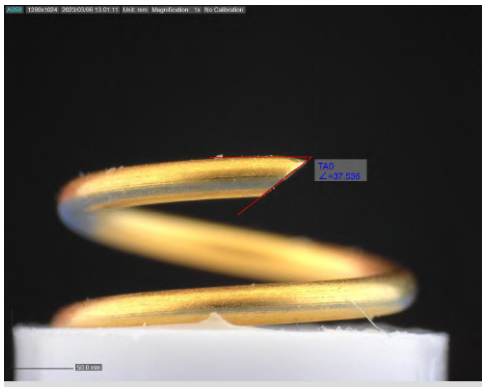

(a) Measurements done by manually drawing lines in Dino-Capture.

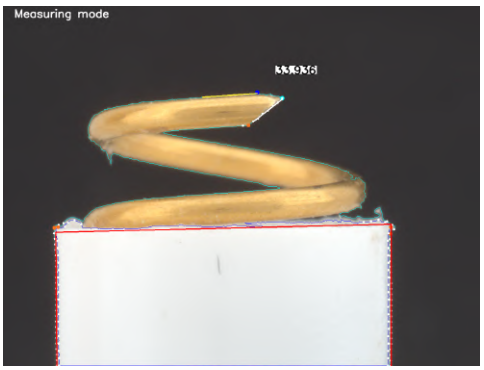

(b) Measurement detected with the developed system.

Figure C.2: Angle measurements of electrode number 2.

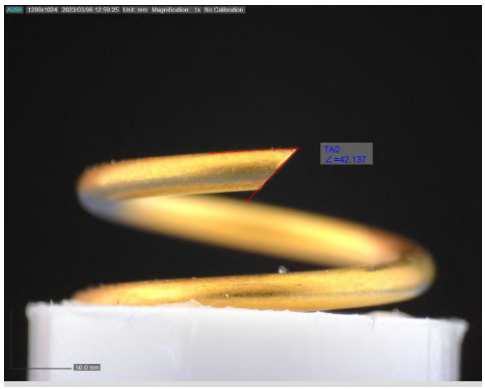

(a) Measurements done by manually drawing lines in Dino-Capture.

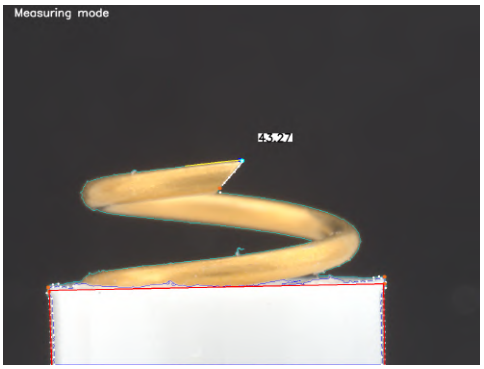

(b) Measurement detected with the developed system.

Figure C.3: Angle measurements of electrode number 3.

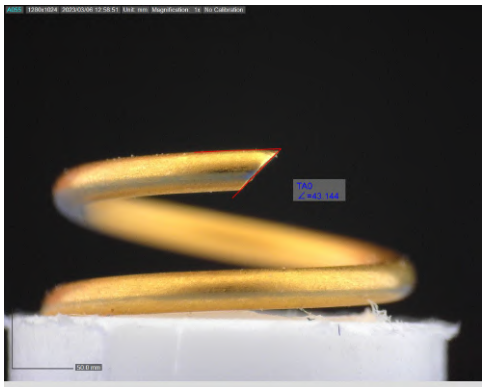

(a) Measurements done by manually drawing lines in Dino-Capture.

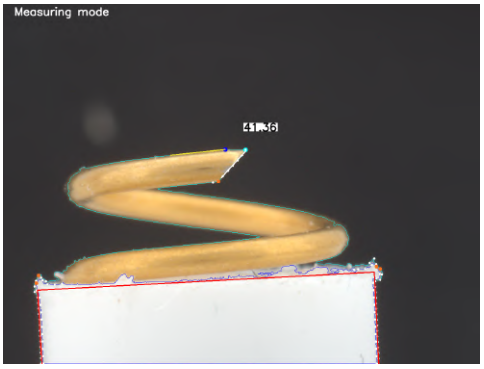

(b) Measurement detected with the developed system.

Figure C.4: Angle measurements of electrode number 4.

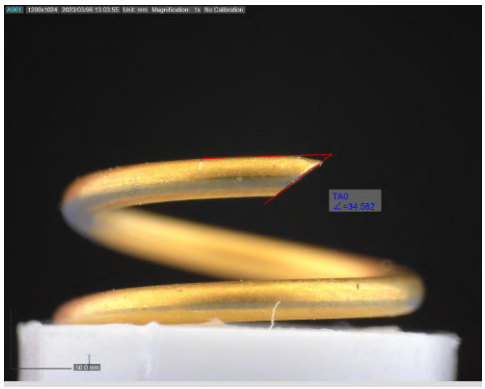

(a) Measurements done by manually drawing lines in Dino-Capture.

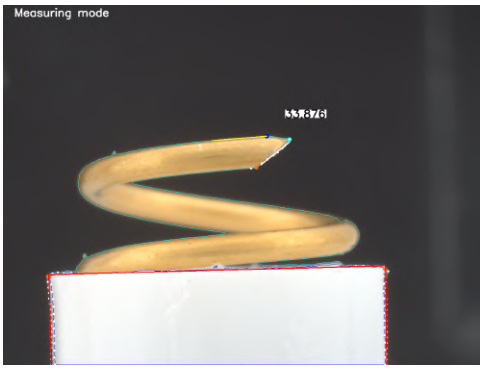

(b) Measurement detected with the developed system.

Figure C.5: Angle measurements of electrode number 5.

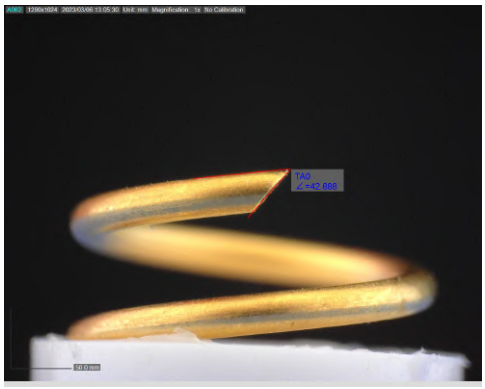

(a) Measurements done by manually drawing lines in Dino-Capture.

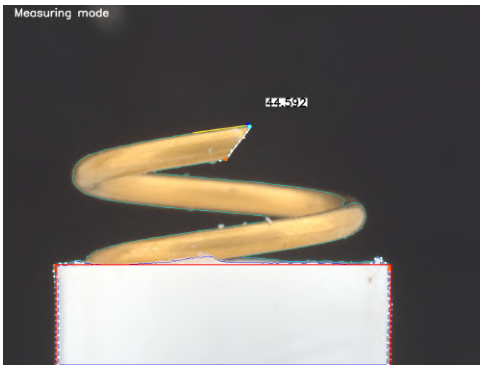

(b) Measurement detected with the developed system.

Figure C.6: Angle measurements of electrode number 6.

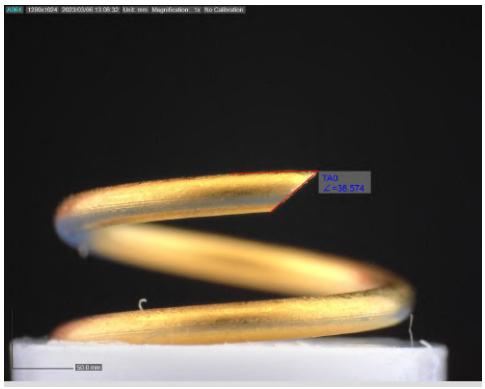

(a) Measurements done by manually drawing lines in Dino-Capture.

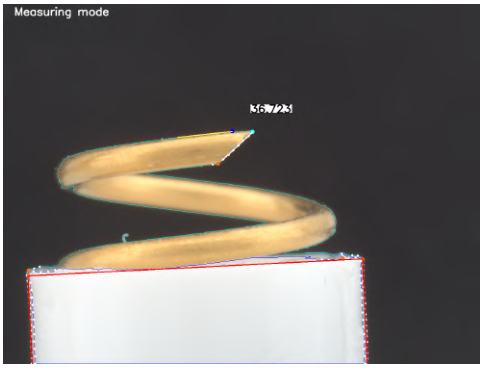

(b) Measurement detected with the developed system.

Figure C.7: Angle measurements of electrode number 7.

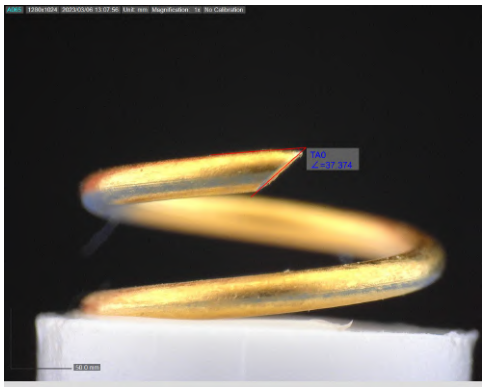

(a) Measurements done by manually drawing lines in Dino-Capture.

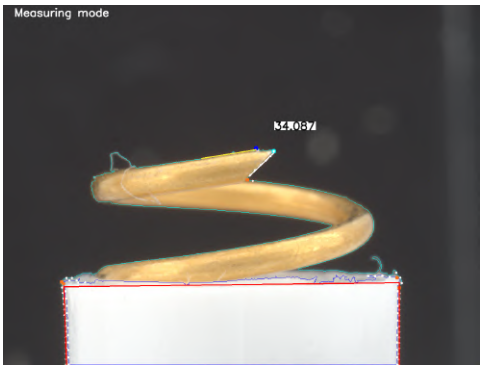

(b) Measurement detected with the developed system.

Figure C.8: Angle measurements of electrode number 8.

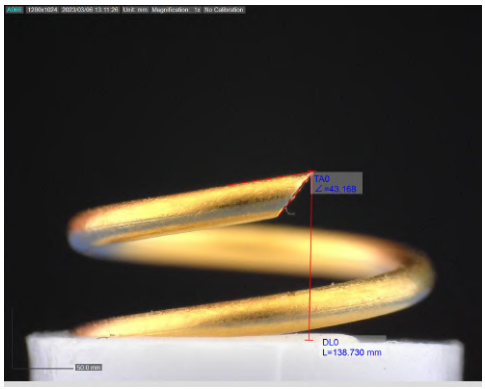

(a) Measurements done by manually drawing lines in Dino-Capture.

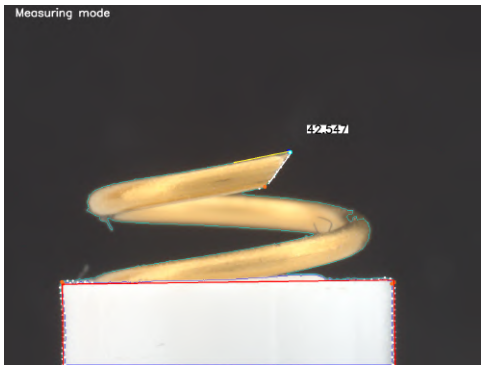

(b) Measurement detected with the developed system.

Figure C.9: Angle measurements of electrode number 9.

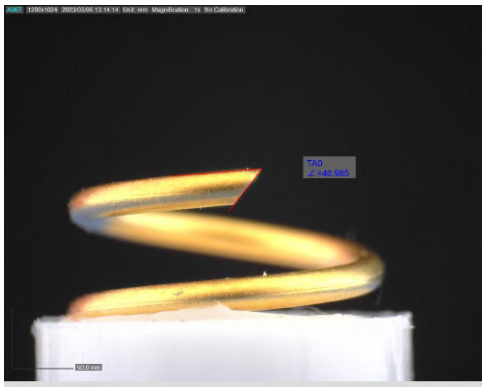

(a) Measurements done by manually drawing lines in Dino-Capture.

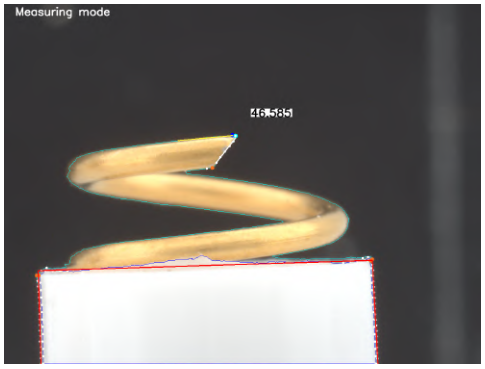

(b) Measurement detected with the developed system.

Figure C.10: Angle measurements of electrode number 10.

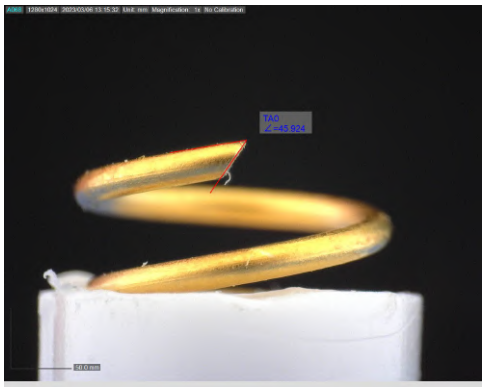

(a) Measurements done by manually drawing lines in Dino-Capture.

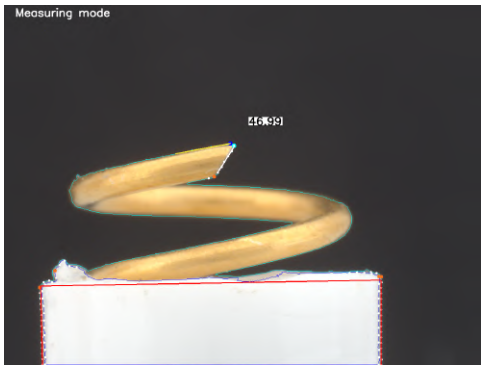

(b) Measurement detected with the developed system.

Figure C.11: Angle measurements of electrode number 11.

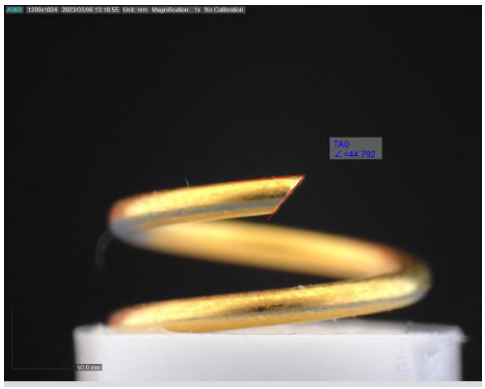

(a) Measurements done by manually drawing lines in Dino-Capture.

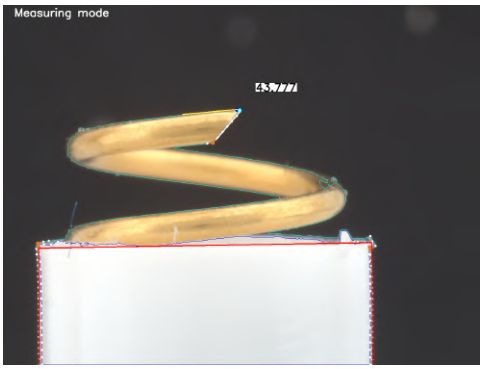

(b) Measurement detected with the developed system.

Figure C.12: Angle measurements of electrode number 12.

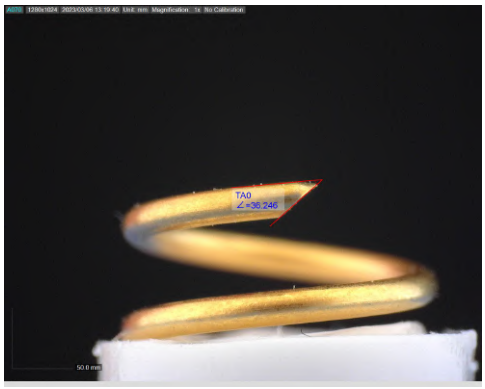

(a) Measurements done by manually drawing lines in Dino-Capture.

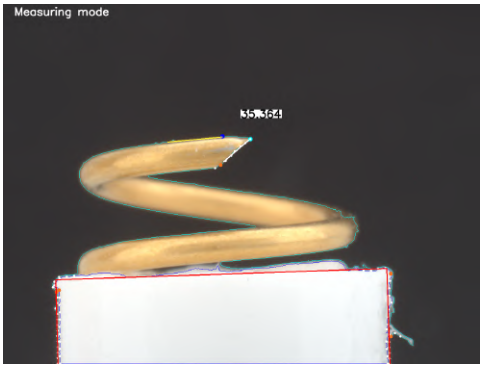

(b) Measurement detected with the developed system.

Figure C.13: Angle measurements of electrode number 13.

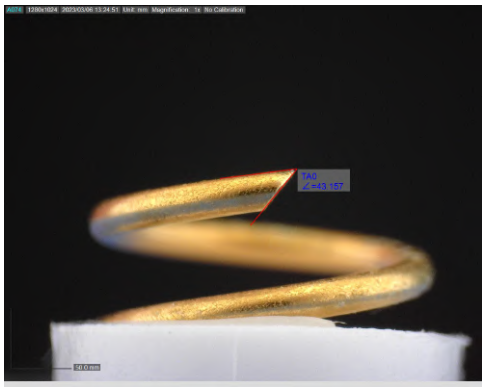

(a) Measurements done by manually drawing lines in Dino-Capture.

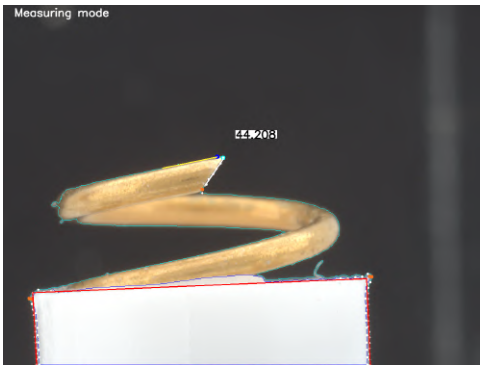

(b) Measurement detected with the developed system.

Figure C.14: Angle measurements of electrode number 14.

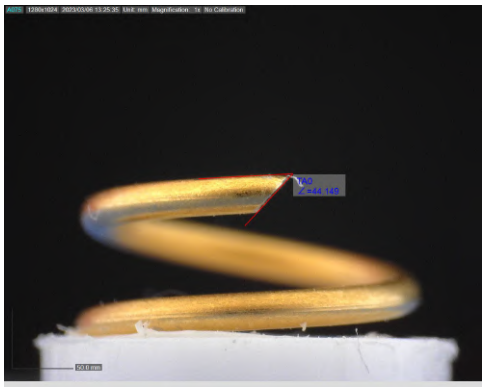

(a) Measurements done by manually drawing lines in Dino-Capture.

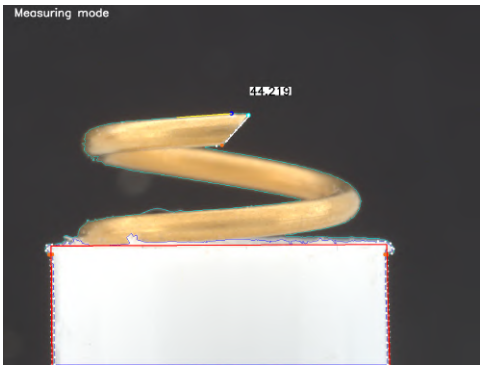

(b) Measurement detected with the developed system.

Figure C.15: Angle measurements of electrode number 15.

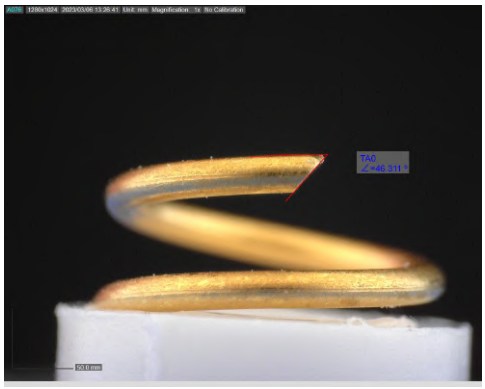

(a) Measurements done by manually drawing lines in Dino-Capture.

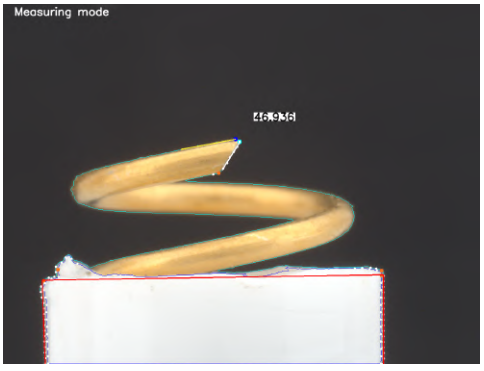

(b) Measurement detected with the developed system.

Figure C.16: Angle measurements of electrode number 16.

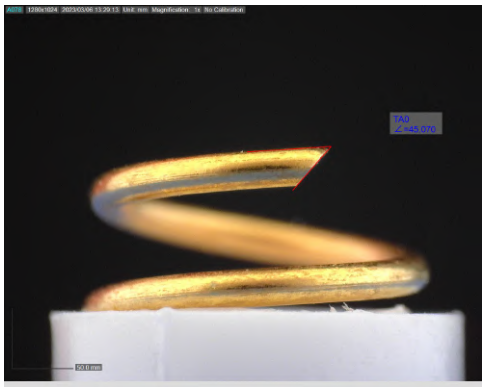

(a) Measurements done by manually drawing lines in Dino-Capture.

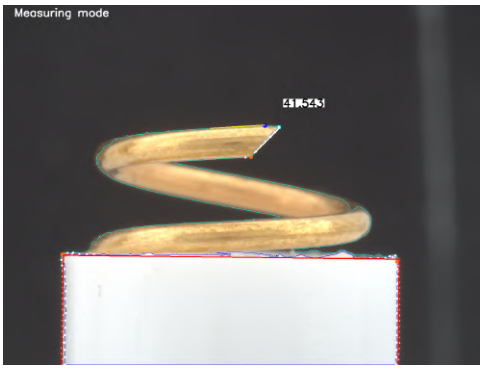

(b) Measurement detected with the developed system.

Figure C.17: Angle measurements of electrode number 17.

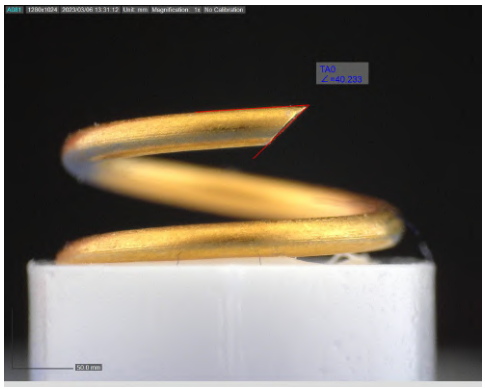

(a) Measurements done by manually drawing lines in Dino-Capture.

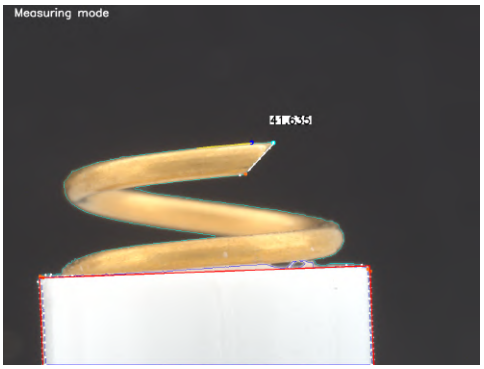

(b) Measurement detected with the developed system.

Figure C.18: Angle measurements of electrode number 18.

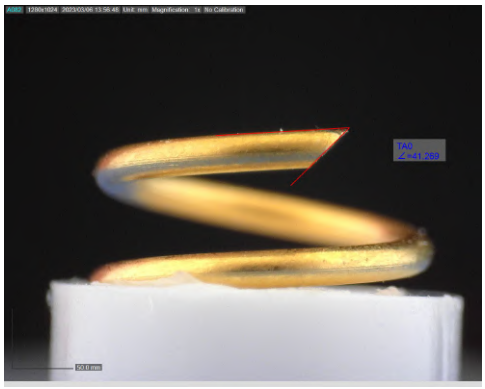

(a) Measurements done by manually drawing lines in Dino-Capture.

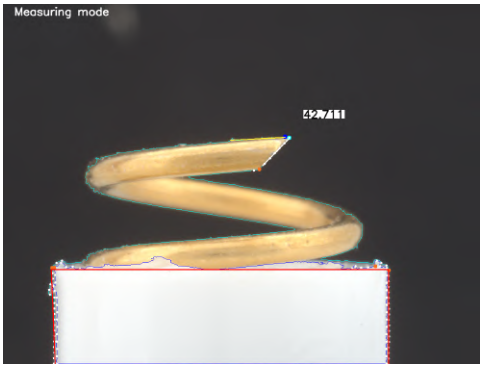

(b) Measurement detected with the developed system.

Figure C.19: Angle measurements of electrode number 19.

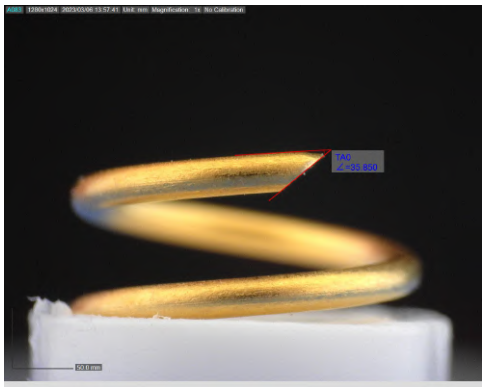

(a) Measurements done by manually drawing lines in Dino-Capture.

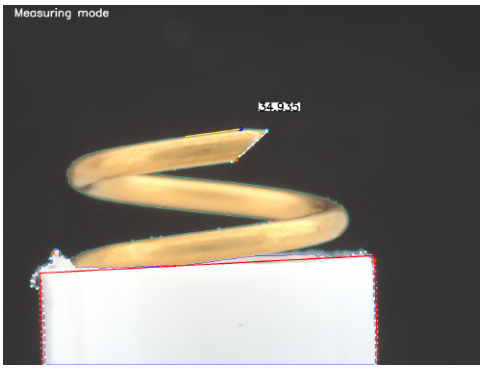

(b) Measurement detected with the developed system.

Figure C.20: Angle measurements of electrode number 20.

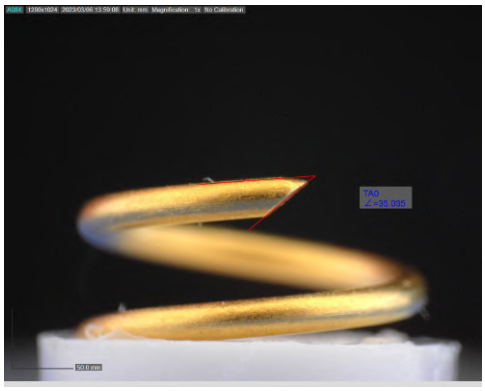

(a) Measurements done by manually drawing lines in Dino-Capture.

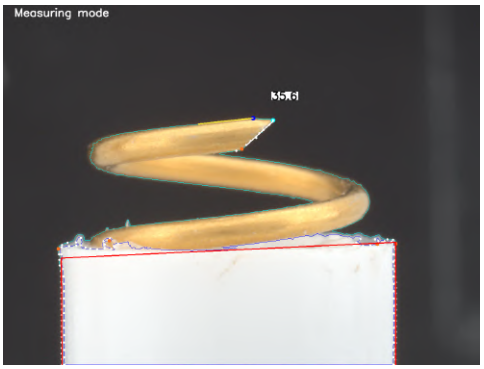

(b) Measurement detected with the developed system.

Figure C.21: Angle measurements of electrode number 21.

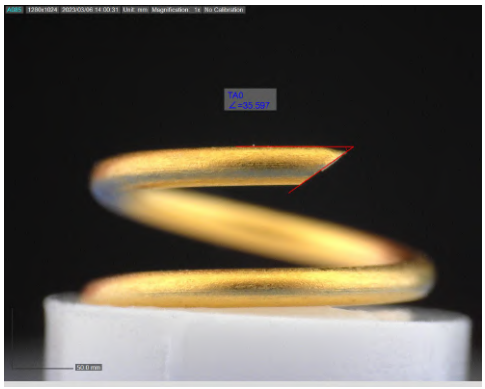

(a) Measurements done by manually drawing lines in Dino-Capture.

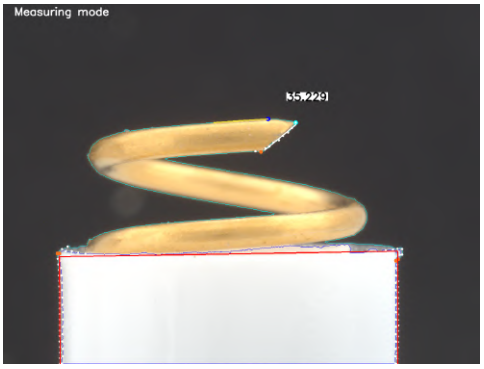

(b) Measurement detected with the developed system.

Figure C.22: Angle measurements of electrode number 22.

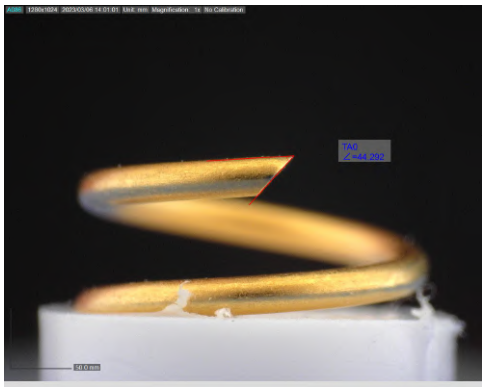

(a) Measurements done by manually drawing lines in Dino-Capture.

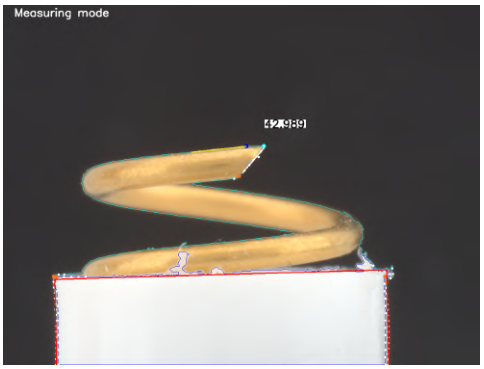

(b) Measurement detected with the developed system.

Figure C.23: Angle measurements of electrode number 23.

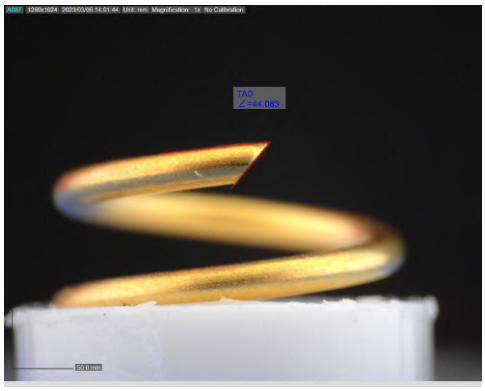

(a) Measurements done by manually drawing lines in Dino-Capture.

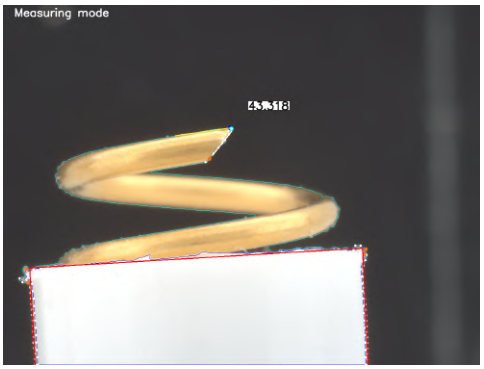

(b) Measurement detected with the developed system.

Figure C.24: Angle measurements of electrode number 24.

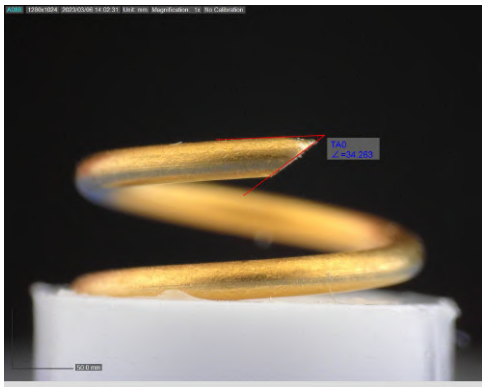

(a) Measurements done by manually drawing lines in Dino-Capture.

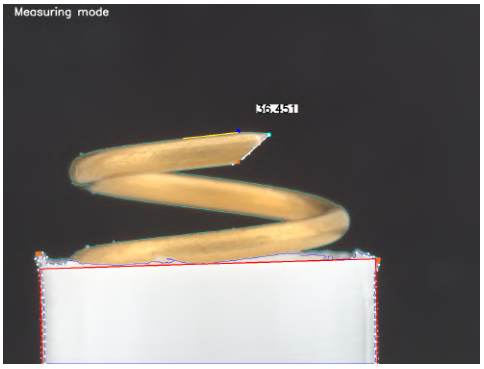

(b) Measurement detected with the developed system.

Figure C.25: Angle measurements of electrode number 25.

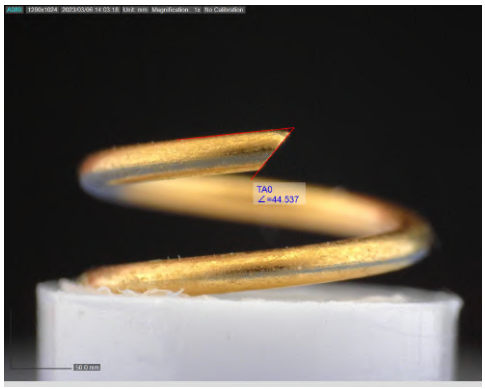

(a) Measurements done by manually drawing lines in Dino-Capture.

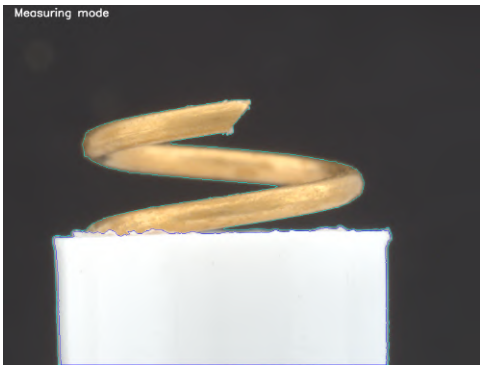

(b) Measurement detected with the developed system.

Figure C.26: Angle measurements of electrode number 26.

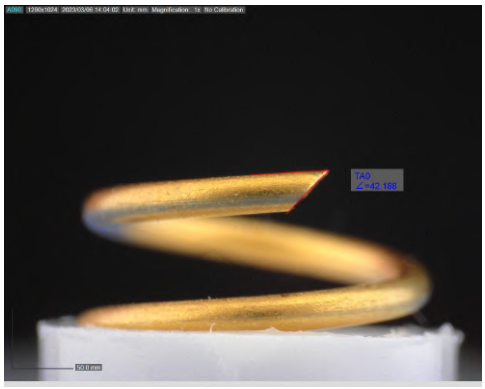

(a) Measurements done by manually drawing lines in Dino-Capture.

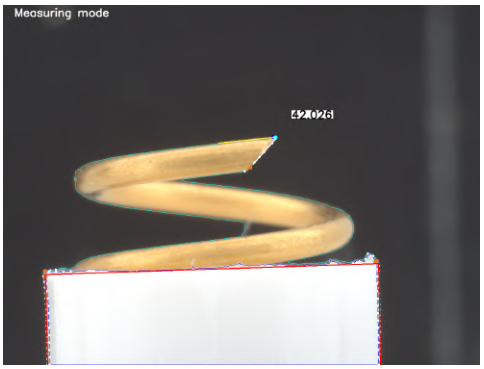

(b) Measurement detected with the developed system.

Figure C.27: Angle measurements of electrode number 27.

DEPARTMENT OF INDUSTRIAL AND MATERIALS SCIENCE
CHALMERS UNIVERSITY OF TECHNOLOGY
Gothenburg, Sweden
www.chalmers.se

CHALMERS
UNIVERSITY OF TECHNOLOGY